Dynamic control of *Escherichia coli* central metabolism for improvement of glucaric acid production

by

Irene Marie Brockman

B.S.E. Chemical Engineering
University of Michigan, Ann Arbor, 2008

Submitted to the Department of Chemical Engineering
in partial fulfillment of the requirements for the degree of

Doctor of Philosophy in Chemical Engineering
at the
MASSACHUSETTS INSTITUTE OF TECHNOLOGY

May 2015 [June 2015]

Signature of Author . . . .

Signature redacted

Irene M. Brockman
Department of Chemical Engineering
May 7, 2015

Certified by . . . .

Signature redacted

Kristala L. Jones Prather
Associate Professor of Chemical Engineering
Thesis Supervisor

Accepted by . . . .

Signature redacted

Richard D. Braatz
Professor of Chemical Engineering
Chairman, Committee for Graduate Students

Dynamic control of *Escherichia coli* central metabolism for improvement of glucaric acid production

by

Irene Marie Brockman

Submitted to the Department of Chemical Engineering on May 7, 2015 in Partial Fulfillment of the Requirements for the Degree of Doctor of Philosophy in Chemical Engineering.

Abstract

Metabolic engineering strategies have enabled improvements in yield and titer for a variety of valuable small molecules produced in microorganisms. Past approaches have been focused on up- and downregulation of genes to redistribute steady-state pathway fluxes, but more recently strategies have been developed for dynamic regulation. Dynamic gene expression profiles allow trade-offs between growth and production to be better managed and can help avoid build-up of undesired intermediates. One pathway that could benefit from better management of growth versus production is the pathway for D-glucaric acid production from glucose developed in the Prather Lab (Moon et al., 2009). Previous work with the glucaric acid pathway has indicated that competition with endogenous metabolism for glucose-6-phosphate (G6P) may limit carbon flux into the pathway. This thesis presents strategies for dynamic control of enzyme in levels in *Escherichia coli* central metabolism, which can be applied for increasing the G6P pool and increasing fluxes into glucaric acid production.

Initially, a strategy for dynamically modulating the abundance of a key glycolytic enzyme, phosphofructokinase-I (Pfk-I), via controlled protein degradation was developed. Through tuning Pfk-I levels, an *E. coli* strain was developed with a growth mode close to wild type and a production mode showing an increased G6P pool available for conversion into heterologous products. A two-phase fermentation with dynamic switching between growth and production modes led to a two-fold improvement in yield and titers of *myo*-inositol, a precursor of glucaric acid, as well as up to a 42% improvement in titers of glucaric acid directly. The system initially developed relied on addition of a small molecule inducer to the culture medium in order to trigger changes in enzyme level. To eliminate the need for timed intervention during fermentation, additional switching systems based on both nutrient starvation (phosphate starvation) and quorum sensing (*esa* system) were developed for autonomous control of Pfk-I levels. With implementation of these systems, Pfk activity automatically declines upon reaching a critical cell density and growth is arrested, without any addition of inducer.

This work represents the first application of a metabolic switching concept to glucaric acid production and illustrates the general usefulness of this strategy for redirecting metabolic fluxes. The protein degradation strategy utilized can be adapted for response to a variety of inputs, opening future routes for development of autonomous response to changes in fermentation conditions.

Thesis supervisor: Kristala L.J. Prather

Title: Associate Professor of Chemical Engineering

Acknowledgments

Table of Contents

List of Figures

List of Tables

List of Abbreviations

Abbreviation	Complete name
3OC6HSL	3-oxohexanoyl-homoserine lactone
AHL	acyl homoserine lactone
aTc	anhydrotetracycline
ATP	adenosine triphosphate
Bis-Tris	2,2-Bis(hydroxymethyl)-2,2',2"-nitrilotriethanol
bp	base pairs
CoA	coenzyme A
CPEC	circular polymerase extension cloning
DAS+4	protein degradation tag AADENYSENYADAS
dFBA	dynamic flux balance analysis
E. coli	*Escherichia coli*
EDTA	ethylenediaminetetraacetic acid
F6P	fructose-6-phosphate
FBA	flux balance analysis
G6P	glucose-6-phosphate
GA	glucaric acid
gDCW	gram dry cell weight
GFP	green fluorescent protein
HPLC	high pressure liquid chromatography
IPTG	β-D-1-thiogalactopyranoside
LAA	protein degradation tag AADENYALAA
LB	Luria-Bertani medium
MI	*myo*-inositol
M1P	*myo*-inositol-1-phosphate
MOPS	3-(N-morpholino) propansulfonic acid
NADH	nicotinamide adenine dinucleotide
NADPH	nicotinamide adenine dinucleotide phosphate
OD_{600}	optical density at 600 nm wavelength

P. stewartii	*Pantoea stewartii*
P. syringae	*Pseudomonas syringae*
PAGE	polyacrylamide gel electrophoresis
PCR	polymerase chain reaction
PEP	phosphoenolpyruvate
Pfk	phosphofructokinase
PTS	phosphotransferase system
RBS	ribosome binding site
RFP	red fluorescent protein
S. cerevisiae	*Saccharomyces cerevisiae*
SD	standard deviation
SDS	sodium dodecyl sulfate
TBS	tris-buffered saline
Tris	*tris*(hydroxymethyl)aminomethane
UTR	untranslated region
YFP	yellow fluorescent protein

Chapter 1: Introduction

Abstract

Metabolic engineering strategies have enabled improvements in yield and titer for a variety of valuable small molecules produced naturally in microorganisms, as well as those produced via heterologous pathways. Typically, the approaches have been focused on up- and downregulation of genes to redistribute steady-state pathway fluxes, but more recently strategies have been developed for dynamic regulation, which allows rebalancing of fluxes according to changing conditions in the cell or the fermentation medium. Dynamic gene expression profiles allow trade-offs between growth and production to be better managed and can help avoid build-up of undesired intermediates. One system which can benefit from better management of growth versus production is the pathway for glucaric acid production developed in the Prather Lab. In this dissertation, strategies were developed for dynamic control of enzyme in levels in *E. coli* central metabolism, which could be applied for increasing the glucose-6-phophate pool and increasing fluxes into glucaric acid production.

1.1 Motivation: improvement of glucaric acid production in *E. coli*

A large number of industrially useful compounds are currently produced through microbial synthesis, from high-value products like antibiotics to commodity chemicals. The microbial synthesis of compounds can offer a number of advantages, especially for pharmaceutical and fine chemical production, where the use of selective enzymes can simplify otherwise complex derivatizations and allow for the production of stereochemically pure compounds. Microbial conversions can also be competitive in the production of bulk chemicals and biofuels, especially when cheaper feedstocks like lignocellulose are utilized. Microbial fermentations generally take place under mild conditions, and that, in combination with the use of renewable feedstocks, provides a green alternative to traditional chemical processes. Notable success stories in this area are the engineering of *E. coli* for the production of 1,3-propanediol from glucose by DuPont / Genencor (Nakamura and Whited, 2003), and the engineering of yeast for production of artemisinic acid by Amyris (Ro et al., 2006).

Among potential microbial synthesis pathways, the production of glucaric acid from glucose was identified as a target in the Prather lab. Glucaric acid has been cited as a "top value added chemical from biomass" in a report from the National Renewable Energy Laboratory and the Pacific Northwest National Laboratory, and glucaric acid and its derivatives can be employed in biopolymer production, as a chelating agent in detergents, and in health research applications (Lee et al., 2011; Walaszek, 1990; Werpy and Petersen, 2004).

A pathway for the production of D-glucaric acid from glucose was successfully developed in the Prather lab. This pathway utilizes three enzymes which are not native to *E. coli*: *myo*-inositol-1-phosphate synthase (INO1) from *Saccharomyces cerevisiae*, mammalian (mouse) *myo*-inositol oxygenase (MIOX), and uronate dehydrogenase (Udh) from *Pseudomonas syringae*. The preferred production mode for glucaric acid would be growth on defined medium with glucose as a sole carbon source. While high expression levels of all enzymes resulted in the production of measurable amounts of glucaric acid on LB medium supplemented with glucose, no production was observed on M9 minimal medium ote>($^{\perp}$‼ HYPERLINK \l "_ENREF_20" \o "Cameron, 2014 #592" ¶Cameron and Collins, 2014)$^{\perp}$¶‼. NO1 and an endogenous phosphatase, were also poorer in M9 supplemented with glucose than in LB. Since it is known that *myo*-inositol is required for activation of MIOX, it was postulated that increasing flux through INO1 might improve pathway yields (Moon et al., 2009).

The substrate for INO1, glucose-6-phosphate, is utilized by the cell in both glycolysis and the pentose phosphate pathway, as well as in biomass formation, as shown in Fig. 1.1. In glycolysis, glucose-6-phosphate is converted to fructose-6-phosphate by phosphoglucose isomerase (Pgi) and then further to fructose-1,6-diphosphate by phosphofructokinase (Pfk). The pentose phosphate pathway begins with the conversion of glucose-6-phosphate to 6-phospho-glucono-1,5-lactone by glucose-6-phosphate dehydrogenase (Zwf). A small amount of glucose-6-phosphate is converted by phosphoglucomutase (Pgm) to glucose-1-phosphate, where it can be used in glycogen biosynthesis. Intracellular glucose-6-phosphate concentrations in *E. coli* have been measured under various conditions, with 1.7 mM given for cells grown in LB medium containing 1% glucose (Morita et al., 2003). The K_M of INO1 for glucose-6-phosphate has been estimated *in vitro* at 1.18 mM, indicating that increases in substrate concentration could still be expected to result in increased conversion rate (Majumder et al., 1997).

Glucose

PTS

Glucose-1-phosphate ← Pgm → Glucose-6-phosphate — Zwf → 6-phospho-glucono-1,5-lactone

Biomass

Pgi

Fructose-6-phosphate

Pentose Phosphate Pathway

Pfk

Fructose-1,6-bisphosphate

Remainder of glycolysis
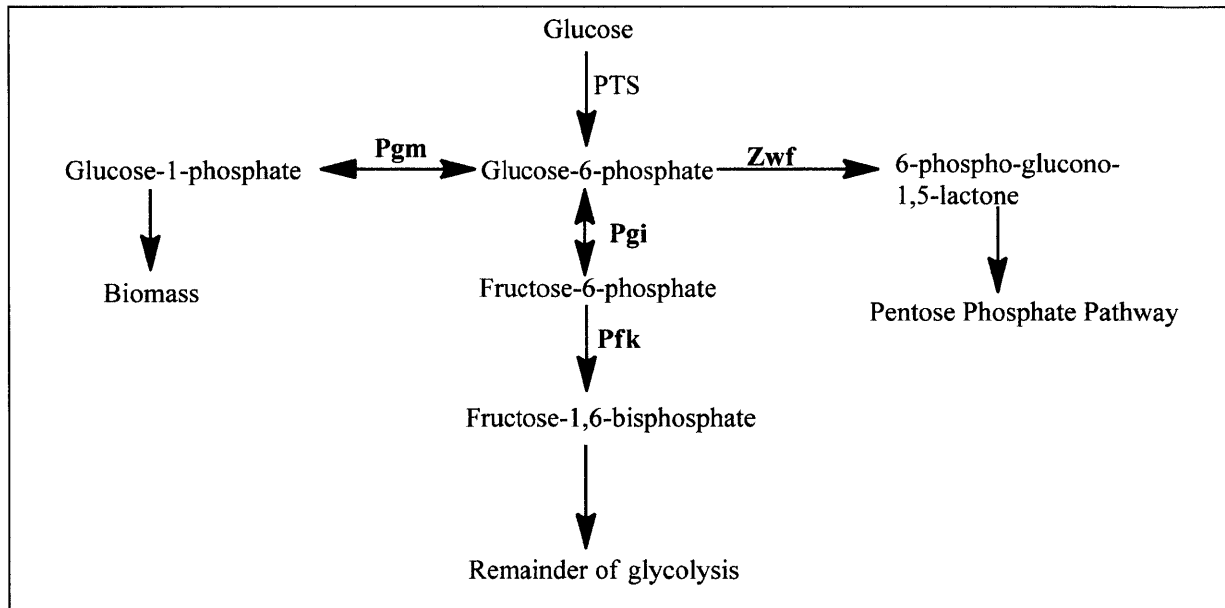
Fig. 1.1 | Principal routes of glucose-6-phosphate utilization in *E. coli*.

One way to increase the glucose-6-phosphate pool is through selective gene knockouts. Aside from *pgm*, which is only responsible for a minor amount of glucose-6-phosphate consumption, *pgi* and *zwf* would be potential targets. The growth characteristics of both *pgi* and *zwf* knockout strains have been studied. Zhao *et.al.* reported that a *zwf* knockout exhibited near wild-type growth rates on glucose, as glycolytic intermediates can still be used to synthesize compounds normally produced through the pentose phosphate pathway (Zhao et al., 2004). However, studies by Canonaco *et. al.* indicate the

reverse does not hold true for a *pgi* knockout, which shows reduced growth on glucose compared to the wild type. High flux through the pentose phosphate pathway is thought to lead to an imbalance in reducing equivalents due to excessive production of NADPH (Canonaco et al., 2001). As ^{13}C labeling studies indicate that the majority of carbon flux proceeds through glycolysis rather than the pentose phosphate pathway, the *pgi* knockout would potentially increase the glucose-6-phosphate pool the most (Fischer and Sauer, 2003; Holms, 1996; Hua et al., 2003; Zhao et al., 2004). However, in order to avoid the undesired side-effect of reduced growth rate on glucose, other strategies need to be considered that would allow for switching between "growth" and "production" modes. This might be possible through dynamically controlling the activity of enzymes involved in consumption of glucose-6-phosphate.

1.2 Strategies and tools for dynamic control of metabolism

Metabolic engineering focuses on the manipulation of cellular metabolism in order to maximize production of valuable products such as biofuels, biochemicals, and proteins. Much of the work in this field has focused on gaining an in-depth understanding of flux distributions in core metabolic pathways and how these distributions can be altered to direct metabolite fluxes toward a particular product of interest. The desired flux distributions are typically in conflict with natural regulatory patterns in the cell, meaning the outcome cannot be achieved by process changes alone, but requires genetic manipulation of the host organism. Aided by both computational and experimental tools, metabolic engineers have been very successful in altering steady-state flux distributions in the cell through the use of gene knockouts, promoter replacements, and introduction of heterologous genes (Alper et al., 2005; Biggs et al., 2014).

As interest has grown in production of a wider variety of products, especially ones involving more complex pathways, interest has also grown in dynamic approaches to cellular engineering (Holtz and Keasling, 2010). Metabolic engineering exists in interplay with the complex regulatory networks of the cell and the native physiology. Native pathway fluxes may differ depending on nutrient availability and growth rate, resulting in changes in the ideal metabolic engineering strategy throughout the course of the fermentation. Additionally, exploiting the capacity of the cell to sense and respond to changing conditions could provide an advantage at large scale, where significant heterogeneity exists within fermenters with respect to nutrient availability, dissolved oxygen, and pH (Neubauer and Junne, 2010).

These types of strategies could also form the basis for switching between growth and production phenotypes, as desired for optimization of glucaric acid production.

1.2.1 Model-based support of dynamic control

Although there are many examples of the successful implementation of static changes to metabolism in order to increase product yields, it is clear that reducing expression of key metabolic enzymes often results in decreased cellular growth rate. While the capacity exists in such knockout strains to produce high levels of product, the productivity is limited by lack of biomass formation. Computational models that integrate an ability to switch flux distributions in the cell between biomass formation and product formation have been used to explore the potential benefits of dynamic control.

In case studies on glycerol and ethanol production, Gadkar *et. al.* demonstrated the theoretical improvements in productivity that could be achieved via dynamic control of enzyme levels in contrast to static knockout or upregulation (Gadkar et al., 2005). By allowing a phase of biomass production before diverting flux through glycerol kinase, their model predicted that production of glycerol could be improved by over 30% in a fixed 6 hour batch time. Similarly, it was shown that dynamically manipulating *ackA* expression in the case of ethanol production could be expected to improve productivity. Subsequent studies have examined how a similar model framework based on dynamic flux balance analysis (dFBA) could be used to predict optimal switching strategies for improved production of succinic acid and serine (Anesiadis et al., 2008; Anesiadis et al., 2013).

In addition to managing trade-offs between growth and production, dynamic control of enzymes in heterologous pathways might offer a way to balance fluxes and minimize protein expression burden. A number of studies have examined how temporal control of enzyme expression within a production pathway could be used to achieve maximum formation of product with the minimal cost of enzyme production (Klipp et al., 2002; Wessely et al., 2011; Zaslaver et al., 2004). For a simple, two-step pathway converting substrate to product, Klipp *et. al.* showed that the fastest conversion of substrate into product was expected to occur when all available protein was first allotted to the initial pathway enzyme, with later switching to more balanced expression of both enzymes (Klipp et al., 2002). Not surprisingly, similar dynamic controls also appear to have developed in natural systems. Zaslaver *et. al.* examined amino acid biosynthesis pathways in *E. coli* and found that promoters for enzymes closer to

the beginning of the amino acid synthesis pathways showed both a shorter response time and higher maximal promoter activity in response to amino acid starvation, in agreement with a mathematical model for maximizing product formation while minimizing enzyme production (Zaslaver et al., 2004). Oscillatory patterns of enzyme expression are another potential route to minimize protein expression burden or to match expression with systems showing a natural oscillatory cycle, such as the cyanobacterial Kai proteins (Nakajima et al., 2005). A kinetic model incorporating oscillatory expression of sets of glycolytic proteins showed that this strategy could be used to increase phosphoenolpyruvate pools by 1.86-fold (Sowa et al., 2014). Aside from protein expression burden, a number of pathway-specific constraints also make temporal control of enzyme expression favorable, including instability of downstream enzymes, toxic pathway intermediates, and product inhibition of upstream enzymes.

1.2.2 Experimental progress in dynamic control

Farmer and Liao (Farmer and Liao, 2000) demonstrated an early example of engineering dynamic controls into central metabolism for improvement of pathway productivity. In lycopene production, phosphoenolpyruvate synthase (*pps*), controls the balance between the precursors glyceraldehyde-3-phosphate and pyruvate, but overexpression of this enzyme causes growth inhibition during glycolytic growth. Recognizing that acetyl-phosphate (AcP) buildup was a signal of excess metabolic capacity, a strain was constructed capable of sensing acetyl-phosphate levels via a transcriptional regulator from the native Ntr regulon in *E. coli*. By controlling expression of *pps* and isopentenyl diphosphate isomerase (*idi*) from the AcP responsive promoter, those enzymes were expressed only when excess glycolytic flux toward acetate occurred. In the strain utilizing this system, yields of lycopene were improved 18-fold over a strain with constitutive expression of all pathway genes. In addition to showing improved lycopene yields, the strain utilizing the AcP responsive promoter instead of the Tac promoter for *pps* expression also showed a growth profile more comparable to the host control, which could help contribute to the final improvement in observed lycopene titers.

More recently, several successful examples of dynamic control have appeared, focusing both on knockdown of native enzymes and balancing of heterologous pathways. An overview of the typical implementations of these types of dynamic control is shown in Fig. 1.2. The studies focusing on control of native enzyme levels have generally been concerned with pathway redirection, splitting carbon flux between pathways critical to cellular growth and heterologous pathways for production of valuable small molecules. This focus on essential genes makes sense, as these pathways offer the most direct

ability to benefit from a controlled tradeoff between biomass formation and product. Areas recently investigated in *E. coli* include both direct transcriptional control of the metabolic enzyme of interest, and controlled degradation of the enzyme. In the area of direct transcriptional control, Solomon *et. al.* modulated glucokinase (Glk) levels via a genetic inverter in order to redirect glucose into gluconate production, improving titers by 30% (Solomon et al., 2012b). Another recent study focused on control of citrate synthase (*gltA*) to redirect acetyl CoA into isopropanol production (Soma et al., 2014). As with *glk*, deletion of *gltA* results in no growth on glucose minimal medium (Patrick et al., 2007), making it a poor target for knockout. Using a genetic toggle switch from Gardner *et. al.* (Gardner et al., 2000), a strain was developed capable of shutting off citrate synthase expression in response to IPTG. Leaky expression of *gltA* still allowed growth and isopropanol production even in the "off" state, but dynamically shutting off expression at 9 hours still resulted in a 10% increase in yields and titers of isopropanol relative to downregulation from the start of the fermentation and more than a two-fold improvement over expression of *gltA* from the native promoter.

Similar results have been achieved via controlled degradation of essential enzymes, relying on addition of a modified SsrA degradation tag to the coding sequence of the gene and expression of an additional adaptor protein, SspB, to increase the rate of proteolysis (McGinness et al., 2006). For example, induced degradation of FabB was used to stop elongation of fatty acids and improve production of octanoate (Torella et al., 2013). While the ssrA/SspB system is designed to function in *E. coli*, it was recently shown that the Lon protease from *Mesoplasma florum* can function as a host-independent system, with expression of the protease resulting in degradation of proteins containing the cognate ssrA tag in *Lactococcus lactis* as well as in *E. coli* (Cameron and Collins, 2014). Protein degradation strategies still require control at the transcriptional level to induce expression of the protease or adaptor protein required for degradation of the target to occur. However, compared to transcriptional switching, they offer the advantage of very rapid depletion of the protein of interest even under conditions of slow growth, when removal via dilution is slow, and the possibility to add degradation tags to genes in their native context, without requiring adjustment of transcription from an inducible promoter to native levels.

These recent studies have focused on dynamic knockdown of essential genes, which represent the clearest benefit of this strategy, because the corresponding gene knockouts are lethal. As the ability to design dynamic systems increases, exploration will likely also expand to genes that are not essential, but

could still benefit from time-dependent control of expression. For example, global regulatory proteins could be placed under defined dynamic control, allowing native regulatory pathways to be rewired to generate a response to a metabolite of interest in lieu of their natural control.
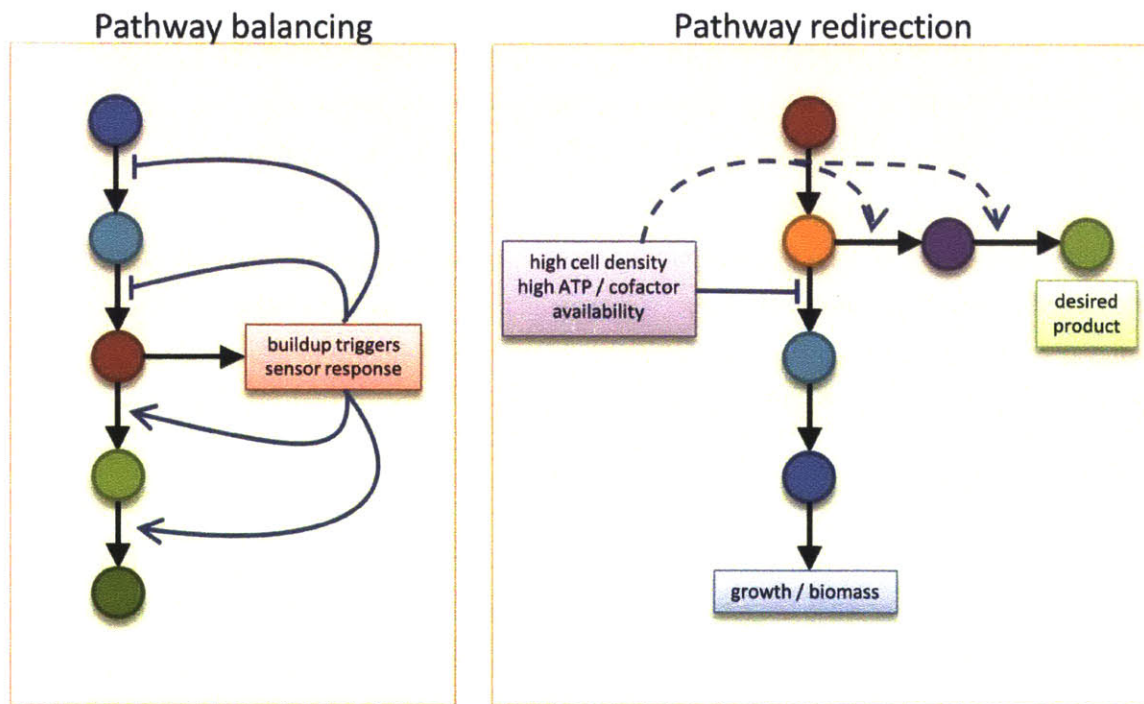
Fig. 1.2 | Typical implementations of dynamic control in metabolic engineering.
For "pathway balancing", buildup of an undesired intermediate is used to trigger repression of upstream enzymes and activation of downstream enzymes. The sensing of intermediate buildup may be direct (binding of the target small molecule) or indirect (sensing of cofactor imbalance, growth inhibition). "Pathway redirection" is typically associated with splitting intermediate flux between cellular growth and energy production and a pathway for a desired product. In this case, some information about cellular state, such as biomass concentration, is used to trigger knockdown of enzyme(s) in the cell's native metabolism and/or upregulation of the pathway toward the desired product.

There is also significant interest in controlling the interplay of multiple genes and managing multiple pathway fluxes. In a "genetic switchboard" developed in *E. coli*, Callura *et. al.* (Callura et al., 2012) demonstrated control of multiple native metabolic enzymes. Addition of different inducer combinations allowed switching of flux between glycolysis, the pentose phosphate pathway, and the Entner-Doudoroff pathway, resulting in changes in relative metabolite pools. While not directly connected to a heterologous pathway, the altered intracellular metabolite pools demonstrate the potential of more complex approaches for dynamically rerouting carbon fluxes.

The concept of multi-gene control can be expanded to heterologous pathway balancing. Two recent examples from the Keasling lab focused on dynamic control of multi-gene expression modules. In the first case, the transcriptional regulator FadR was used to control expression of genetic modules involved in the synthesis of fatty acid ethyl esters (FAEE) (Zhang et al., 2012). Because the native *E. coli* promoters interacting with FadR have limited dynamic range, more responsive synthetic promoters were designed by placing FadR and LacI binding sequences in the phage lambda and T7 promoters, resulting in up to a 60-fold change in fluorescence when tested for RFP expression in the presence and absence of oleic acid. These promoters were placed upstream of the modules involved in ethanol production, so that biosynthesis was only induced in the presence of fatty acids, avoiding wasting carbon for excess ethanol production and resulting in improved titers of FAEE. Importantly, a series of constitutive promoters was also tested for driving expression of the modules, to see whether a static balancing of expression could have achieved the same result; in this case, it was found the dynamic system was still superior with 2-fold higher FAEE titers than any of the thirty constitutive promoter combinations tested.

A modular approach was also employed to avoid buildup of the toxic intermediate FPP in the production of amorphadiene (Dahl et al., 2013). With no known FPP responsive transcription factors, whole-genome transcriptional analysis was used to identify candidate FPP responsive promoters. Promoters were identified that showed both up and downregulation in response to FPP, allowing a system to be developed with approximately a three-fold decrease in expression of the upstream FPP production module and four-fold increase in expression of the downstream consumption module upon FPP buildup. A similar strategy was recently used by Xu *et. al.* to balance malonyl-CoA pools for fatty acid production (Xu et al., 2014). Malonyl-CoA responsive promoters were designed based on FapR, a malonyl-CoA responsive transcription factor from *Bacillus subtilis*, allowing both upregulation and downregulation of gene expression in response to increasing malonyl-CoA levels (Xu et al., 2013). These promoters were used to decrease expression of the upstream malonyl-CoA production operon (*accADBC*) and increase expression of the downstream consumption operon (*fabADGI tesA'*) upon buildup of malonyl-CoA, resulting in oscillatory levels of intracellular malonyl-CoA and a 2.1-fold improvement in fatty acid titers over the unregulated pathway. With an appropriate choice of metabolic modules, for instance splitting modules at a metabolic branch point or at points where intermediate buildup has already been observed, a dynamic approach can prove very valuable. The optimal balance for a set of static

promoters will represent some balance over the average of all cellular conditions in a fermentation, which may not be the best balance at any given time point.

1.2.3 Strategies for development of new dynamic systems

A key factor in developing a system for dynamic pathway regulation is often finding an appropriate sensor system. Applications based on quorum sensing signals offer the ability to control response based on cell density, an important parameter for many metabolic engineering applications. Quorum sensing promoters have been used to drive protein expression and effect changes in cell physiology for a variety of applications, from delaying recombinant protein synthesis (Kobayashi et al., 2004; Tsao et al., 2010) to sensing pathogens (Saeidi et al., 2011). Through protein engineering, the affinity of the regulator protein for its cognate autoinducer can be attenuated, allowing the system to be tuned for control of induction time (Collins et al., 2005; Shong et al., 2013). Stationary phase promoters (Miksch et al., 2005) and autoinduction medium (Peti and Page, 2007) have also been successfully used as indirect methods of sensing cell density for applications like delayed recombinant protein expression. When sensing of a specific small molecule product or intermediate is desired, it may be possible to utilize one of many previously characterized transcription factors. Several recent reviews have addressed the current state-of-the-art in biosensors and their potential applications for both high-throughput screening and metabolic engineering (Michener et al., 2012; Schallmey et al., 2014; Zhang and Keasling, 2011). Protein engineering techniques can be used to alter the specificity of known transcription factors or increase their affinity for molecules of interest (Chen and Zeng, 2013).

In cases where no responsive promoter / regulator system has been identified for the metabolite or product of interest, decreases in the cost of RNAseq have expanded the opportunities for screening promoter response to larger libraries of small molecules. Additionally, a library is available with GFP expression driven by nearly 2,000 *E. coli* promoters, which can be used in fluorescence-based screening for small molecule responsive promoters (Zaslaver et al., 2006). In these screens, it may not be possible to identify the mechanism of promoter regulation, making it more difficult to apply in new systems, and generally limiting the applicability to a single organism. Additionally, even once identified, responsive promoters may not have the desired basal transcription level or dynamic range to be used in the desired metabolic engineering application. However, in this area, utilizing tools from synthetic biology will be very valuable. Rather than directly controlling the protein of interest from a responsive promoter, the promoter can be integrated into a larger genetic control system, allowing the output response to be

modulated. A number of strategies have already been demonstrated for amplifying (Karig and Weiss, 2005) and inverting (Yokobayashi et al., 2002) a signal from a biosensor or maintaining output even after the initial small molecular inducer disappears (Gardner et al., 2000). Multiple biosensors can also be integrated into cellular logic gates, allowing the response to be fined tuned against different combinations of signals (Anderson et al., 2007). The robustness of these logic gates is also being explored in the context of industrial strains and fermentation conditions, which are relevant for eventual application in pathways for large scale production of chemicals (Moser et al., 2012).

Dynamic control of metabolic enzyme levels and activities can be exerted not only at the transcriptional level, but also at the post-transcriptional and post-translational level. Fig. 1.3 illustrates how implementation of dynamic control might be envisioned at each level. Some of the initial applications of RNA-based control for metabolic engineering purposes have included the use of anti-sense and small RNA constructs (Kim and Cha, 2003; Yoo et al., 2013). Small RNAs can be designed for a wide variety of targets, providing a useful system for screening the effect of changing expression of multiple proteins, although these still require a responsive transcriptional element to drive expression of the regulatory RNA at the appropriate time. In addition to using anti-sense strategies, there are a variety of other routes for implementing RNA-based control, which could offer the opportunity to utilize RNA in a sensing capacity, through the use of aptamers that bind to small molecules. RNA-based control of gene expression via riboswitches has been demonstrated, both when the regulatory element is included on the mRNA of the gene of interest (Lynch and Gallivan, 2009) and in the case of *trans* acting RNAs (Bayer and Smolke, 2005). In both cases, binding of a small molecule effector to the RNA resulted in changes in the folded structure, which can be exploited to block or unblock the ribosome binding site, resulting in a change in translation of the protein of interest. Other mechanisms of riboswitch action exist, including ligand-dependent self cleavage and transcriptional attenuation due to ligand-dependent formation of a hairpin acting as a transcriptional terminator. Riboswitches have been discovered that bind naturally to purines and their derivatives, amino acids, protein coenzymes, and metal ions (Serganov and Patel, 2012), but by replacing the sensing domain with RNA aptamers, synthetic riboswitches and ribozymes have been developed which respond to theophylline (Sharma et al., 2008; Soukup and Breaker, 1999). A tetracycline aptamer has also been used to control gene expression in yeast by insertion in the 5' UTR without use of a natural riboswitch scaffold (Hanson et al., 2003). To expand the library of possible ligands, SELEX techniques can be used to screen for novel aptamers (Ellington and Szostak, 1990), although the integration of the binding domain with the existing mRNA structure requires careful

development. Overall, RNA-based strategies offer significant flexibility to easily target multiple genes for control of expression, as well as to develop RNA expression cascades, which could be used for more complex genetic controls (Lucks et al., 2011).
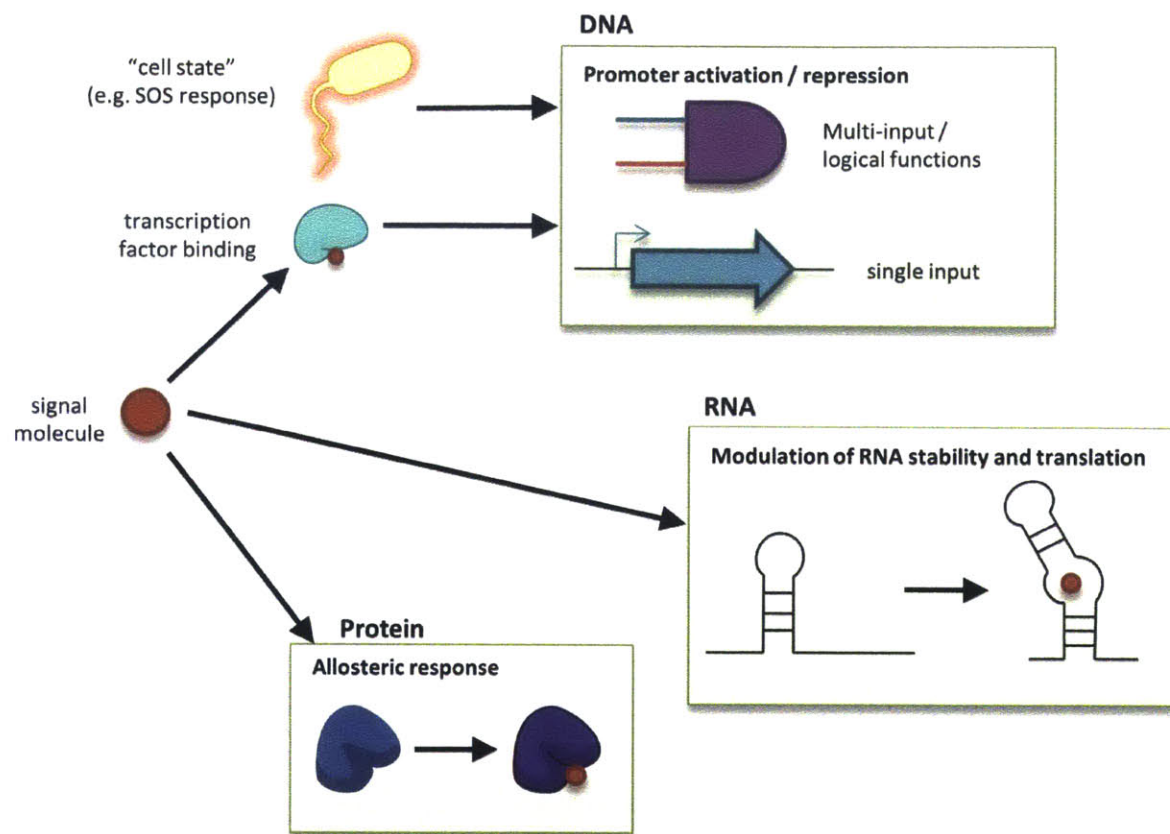
Fig. 1.3 | Strategies for dynamically modulating enzyme activity.
After sensing of a relevant condition or small molecule, control of enzyme activity can be exerted at the transcriptional, post-transcriptional, and post-translational level. At the transcriptional level, interactions between transcription factors and relevant small molecules can be exploited to activate or repress gene expression. At the post-transcriptional level, use of RNA aptamers can provide a method for controlling translation of the relevant mRNA. Control at the post-translational level is possible in some cases using strategies such as engineered allostery.

Post-translational control becomes more complicated, as this relies on changing the structure of the target enzyme. Many natural enzymes that exert significant flux control within a pathway are allosterically regulated by cofactors or pathway products, and a number of attempts have been made to engineer new allosteric sites into existing enzymes. One strategy that has been successfully implemented is that of domain insertion, where a protein domain that undergoes a conformational

change upon exposure to a stimulus, such as a small molecule, is inserted within the sequence of an existing protein (Ostermeier, 2005). Ideally, the catalytic activity of the original protein is then coupled to the presence of the stimulus. This approach has been successfully implemented in order to couple the activity of β-lactamase to the presence of heme and to couple the activity of *E. coli* dihydrofolate reductase to light exposure (Edwards et al., 2010; Lee et al., 2008). While this approach could potentially offer targeted control of enzyme activity, allowable insertion sites are hard to predict and extensive screening is required to identify protein variants that retain both high activity and significant allosteric response. An alternative strategy for post-translational control is inducible protein degradation, through selective exposure of degradation tags by cleavage (Jungbluth et al., 2010) or use of tags requiring an additional adaptor protein to facilitate proteolysis (McGinness et al., 2006). However, as in the case of antisense RNA, transcriptional control is still required to drive expression of the second component required for cleavage or proteolysis.

As an alternative to feedback loops based on intracellular sensors like RNA or proteins, responsive strains can also be combined with computational control systems, allowing feedback loops to be developed based on external process variables such as dissolved oxygen or off gas composition. Inexpensive inducers such as heat, or even pulses of light could then be used to affect the desired changes in cellular state. By fusing the Gal4 DNA-binding and activation domains to the light-responsive PhyB/PIF module, Milias-Argentis *et. al.* were able to demonstrate a feedback control system for YFP expression in yeast based on pulses of light (Milias-Argeitis et al., 2011). Light-based control of gene expression has also been demonstrated in mammalian cells, where a signaling cascade initiated by a conformational change in melanopsin due to photo-isomerization of 11-cis retinal was used to trigger transgene expression in human embryonic kidney cells. Control of transgene expression was successfully demonstrated both in bioreactors and in implants in mice (Ye et al., 2011). Future applications will need to address the limited penetration of light in tissues and in high-density bacterial cultures. In the case of mammalian tissues, use of near infrared wavelengths can improve penetration depths from millimeters to a few centimeters (Ryu and Gomelsky, 2014); however, application of light-controlled gene expression in fermentation vessels at the meter scale would still present a number of design challenges.

As with static systems, fine-tuning of expression in dynamic systems will still be required. This becomes especially important when considering control of enzymes in central metabolism, where baseline

expression levels determine cell physiology. Degenerate oligos generated using tools such as the RBS Library Calculator (Salis, 2011) provide a basis for rationally screening across a range of expression levels. Combining this with high throughput, scarless recombineering techniques such as MAGE (Wang et al., 2012) can provide a platform for screening libraries of strains.

1.2.4 Discussion and future directions in the field

Dynamic strategies for metabolic engineering have shown promise for conditional knockdown of essential genes and for balancing pathway fluxes in response to fermentation conditions. Natural cellular systems exhibit a wide variety of dynamic controls, such as allosteric inhibition or transcriptional repression via feedback from downstream metabolites. Many of these can be harnessed for metabolic engineering and integrated into novel applications.

While dynamic systems have shown potential for improvements in yield and titer, gains relative to static control are in many cases limited by the increased difficulty of fully exploring the production space in these systems. Rapid screening using previously developed constitutive promoter libraries facilitates optimization of steady state expression levels. Current dynamic systems often rely on discovery of specific small-molecule responsive promoters, which may not result in ideal expression ranges for system performance, especially when considering modulation of native enzyme expression.

However, methods for rapidly altering expression levels and balancing pathways, which have been already successfully applied for static control, will also facilitate development of dynamic control. Dynamic systems offer a much larger number of "control knobs", and recent modelling efforts have shown that careful choice of system architecture and expression levels is required for optimal outcomes to be achieved (Stevens and Carothers, 2015). Moving forward, both experimental and computational tools will be needed to fully exploit the potential of these systems. New technologies for screening biosensors and evolving their specificity will certainly push forward this area as well. Next generation gene synthesis technologies can reduce the cost of screening multiple system architectures. Combinatorial assembly techniques for combining short synthesized pieces of DNA into large expression cassettes have been used in applications like refactoring of complex pathways (Smanski et al., 2014), and provide a platform for screening any type of multipart cellular system.

As lab scale applications are improved, a future challenge will be implementation of dynamic control strategies in industrial strains and fermentation systems (Moser et al., 2012; Shiue and Prather, 2012). The concept could be quite valuable, as it would allow the cell to adapt in a pre-defined manner to changing conditions within the fermentation. In the laboratory, balancing of growth and production or balancing of pathway intermediate levels typically occurs under well-mixed conditions, where substrate concentrations vary slowly and continuously in one direction. However, at large scale, microorganisms are expected to move quickly through substrate and oxygen gradients. Scale-down studies have shown that for *E. coli*, short cycles of residence between an anoxic zone (1 minute) and a well-mixed zone (9 minutes), resulted in decreases in biomass yield and increases in formic acid production similar to those observed in large-scale fermenters (Xu et al., 1999). In design of industrially robust systems, fast response time, reversible response, and genetic stability of components will play a role in future success. Drawing from both natural and engineered systems, we can develop "smarter" cells, in which native metabolism is consistently balanced with heterologous pathways, even under changing conditions.

1.3 Thesis objectives

As discussed in the previous section, a number of recent works have focused on experimental and theoretical advantages associated with redirecting flux in central metabolism through dynamic control of enzyme levels. However, many of these systems have been optimized on plasmids or at relatively high expression levels, making them difficult to integrate in context with heterologous biosynthetic pathways that are already taxing to the host cells (Cardinale and Arkin, 2012). Dynamic control systems which could be integrated into production strains with minimal change in baseline performance and rapid response time would provide a valuable advantage in microbial production of chemicals.

In the Prather Lab, previous work has focused on control of enzymes in central carbon metabolism at the transcriptional and post-transcriptional levels (Solomon et al., 2012b). In one case, control of glucose uptake through the use of antisense mRNA to glucokinase was examined. A number of limitations were observed for this type of system. Notably, as growth slows due to reduced glucose uptake, dilution of protein due to cell growth decreases. This offsets the decrease in translation due to the presence of antisense mRNA, resulting in a reduced change in steady state protein levels. Similar

limitations have been noted for attempts to use genetic circuits outside the exponential growth phase, when dilution due to growth is too slow for quick response to be achieved.

This work focuses on utilization of controlled protein degradation strategies for demonstration of metabolic switching to increase glucose-6-phosphate pools and improve glucaric acid production. Protein degradation provides an attractive option for modulating enzyme levels, allowing for rapid changes in steady state levels of the target protein regardless of growth rate. SsrA tag variants have been reported which have varying degradation rates dependent on the presence and absence of SspB, an adaptor protein that tethers target proteins to ClpXP (Davis et al., 2011; McGinness et al., 2006). Adaptor protein expression can be controlled via a number of transcriptional strategies, allowing for optimal timing of induced protein degradation.

Beyond the demonstration of the initial switching strategy, which requires outside intervention for induction of protein degradation, this work considers development of fully autonomous systems, where the cells change their own environment in such a way that switching is automatically triggered at the optimal time. Some of these systems were discussed in Section 1.2.3, with quorum sensing and nutrient starvation being the most applicable to switching between biomass formation and small-molecule product formation.

In this context, the work presented in this dissertation aims to do the following:

1. Demonstrate a viable system for modulating levels of enzymes in central metabolism through controlled degradation of phosphofructokinase-I (Pfk-I) and its application for improving production of *myo*-inositol, an intermediate in glucaric acid production.

2. Expand this system to glucaric acid production, including investigation of optimal time for Pfk-I knockdown and development of fed-batch strategies to maximize yield and titer of glucaric acid.

3. Explore strategies for autonomous induction of Pfk knockout based on nutrient starvation and quorum sensing, and demonstrate how these systems can be tuned for optimal induction time and improvement of *myo*-inositol production.

1.4 Thesis organization

This thesis is organized into five chapters. Chapter 1 discusses the project motivation and provides background and scope for the project, including examples of how dynamic metabolic control can be implemented. Chapter 2 demonstrates a system for controlled degradation of the central metabolic enzyme phosphofructokinase-I (Pfk-I) and its application for improving production of *myo*-inositol, an intermediate in glucaric acid production. Chapter 3 discusses the expansion of this system to glucaric acid production, including investigation of optimal time for Pfk-I knockdown and development of fed-batch screening strategies to maximize yield and titer of glucaric acid. Chapter 4 details strategies which were explored for autonomous control of Pfk-I activity, including systems based on phosphate starvation and on quorum sensing. The remarks in Chapter 5 address the overall implications of the work and future directions for study, especially with respect to autonomous systems.

Chapter 2: Dynamic knockdown of *E. coli* central metabolism for redirecting fluxes of primary metabolites

Abstract

Control of native enzyme levels is important when optimizing strains for overproduction of heterologous compounds. However, for many central metabolic enzymes, static knockdown results in poor growth and protein expression. We have developed a strategy for dynamically modulating the abundance of native enzymes within the host cell and applied this to a model system for *myo*-inositol production from glucose. This system relies on controlled degradation of a key glycolytic enzyme, phosphofructokinase-I (Pfk-I). Through tuning Pfk-I levels, we have been able to develop an *E. coli* strain with a growth mode close to wild type and a production mode with an increased glucose-6-phosphate pool available for conversion into *myo*-inositol. The switch to production mode is trigged by inducer addition, allowing yield, titer, and productivity to be managed through induction time. By varying the time of Pfk-I degradation, we were able to achieve a two-fold improvement in yield and titers of *myo*-inositol.

2.1 Introduction

The introduction of heterologous enzymes into a microbial host to generate novel synthetic pathways poses a number of challenges, especially when the enzymes in those pathways compete with native enzymes for substrate. To counter this problem, common strategies utilized in rational strain design for overproduction of natural metabolites, such as gene knock-outs or promoter replacements, have typically been used (Lee et al., 2012; Tyo et al., 2010; Woolston et al., 2013). However, these approaches produce strains with only a few available control points, especially with respect to changing the cell's own metabolism during the course of a fermentation. The ideal flux balance for the production phase of a fermentation differs from the flux balance required at the beginning of a fermentation, when biomass production and expression of recombinant proteins are most important.

To overcome these limitations, a number of recent works have focused on experimental and theoretical advantages associated with redirecting flux in central metabolism through dynamic control of enzyme levels (Anesiadis et al., 2013; Callura et al., 2012; Farmer and Liao, 2000; Solomon et al., 2012b; Soma et al., 2014; Torella et al., 2013). While the use of inducible promoters to turn on heterologous gene expression in *E. coli* through small molecule inducers or temperature change has been well developed, methods for dynamically knocking down expression of native genes are more limited. The genetic devices developed in the context of synthetic biology offer a number of possible ways to achieve gene regulation in response to extracellular and intracellular conditions (Holtz and Keasling, 2010). However, many of these systems have been optimized on plasmids or at relatively high expression levels, making them difficult to integrate in context with heterologous biosynthetic pathways that are already taxing to the host cells (Cardinale and Arkin, 2012). Dynamic control systems which could be integrated into production strains with minimal change in baseline performance would provide a valuable advantage in microbial production of chemicals.

A potentially useful node from controlling fluxes in primary metabolism is the metabolic branch point at glucose-6-phosphate (G6P). G6P can be routed into native metabolism through both glycolysis and the oxidative pentose phosphate pathway, as well as into heterologous production of *myo*-inositol via INO1 from *Saccharomyces cerevisiae* (Hansen et al., 1999). *Myo*-inositol can be further converted into other useful products, such as glucaric acid, a biopolymer precursor (Werpy and Petersen, 2004) and *scyllo*-inositol, which has been studied as a therapeutic for Alzheimer's (Yamaoka et al., 2011). The pathway for glucaric acid has already been demonstrated in *E. coli* (Moon et al., 2009) and theoretical yields of

near 100% are possible; however, G6P must be directed into this pathway at the expense of central metabolism. Previous studies have focused on controlling the G6P utilization in glycolysis versus the pentose phosphate pathway (Callura et al., 2012), but dynamic redirection of G6P into a heterologous pathway has not been demonstrated. We therefore focused on control of phosphofructokinase (Pfk-I) level as a method to direct G6P into *myo*-inositol production and restrict biomass formation. Redirecting primary metabolism poses unique challenges, as heterologous pathway enzymes are often selected from secondary metabolism or may be acting on non-native substrates, while the central metabolic enzymes utilize primary metabolites very efficiently. Global studies have indicated central metabolic enzymes typically have a higher catalytic efficiency than enzymes in secondary metabolism and are likely to be operating on a substrate pool near the K_M value of the enzyme (Bar-Even et al., 2011; Bennett et al., 2009).

To minimize lag time associated with dilution of stable proteins and generate a quick response as well as large dynamic range, we have implemented post-translational control of Pfk through use of modified SsrA tags. A number of SsrA tag variants have been reported which alter the half-life of the tagged protein or have varying degradation rates dependent on the presence and absence of SspB, an adaptor protein that tethers target proteins to ClpXP (Andersen et al., 1998; Davis et al., 2011; McGinness et al., 2006). By appending such a tag to the coding sequencing of Pfk-I and knocking out the native copy of *sspB*, the half-life of Pfk-I can be controlled through expression of SspB from an inducible promoter. This strategy allows rapid changes in the steady-state level of Pfk-I to be achieved. Using this system in *E. coli*, we were able to achieve increases in both titer and yield of *myo*-inositol (MI), a precursor in glucaric acid production.

2.2 Materials and methods

2.2.1 Strains and plasmids

E. coli strains and plasmids used in this study are listed in Table 2.1. *E. coli* strain DH10B was used for molecular cloning and plasmid preparation. Production strains were constructed utilizing MG1655 Δ*endA* (IB531) as a parent strain. Knockouts of *zwf, pfkB,* and *sspB* were accomplished via sequential P1 transduction from Keio collection donor strains (Baba et al., 2006). The kanamycin resistance cassette was removed after each transduction via expression of FLP recombinase from pCP20 (Datsenko and Wanner, 2000). The native *pfkA* locus was replaced with a version containing a constitutive promoter

32

(apFAB114) and 5′ UTR from the BIOFAB library (Mutalik et al., 2013) and the degradation tag AADENYSENYADAS (McGinness et al., 2006). The replacement at the *pfkA* locus was carried out via a "landing pad" method (Kuhlman and Cox, 2010). The *pfkA* coding sequence was amplified from the *E. coli* genome with primers which appended the promoter and UTR at the 5′ end and the degradation tag at the 3′ end of the gene. This product was cloned into the vector pTKIP-neo by restriction digest with HindIII and KpnI, yielding pTKIP-114pfkA(DAS+4). Lambda-red mediated recombination was used to introduce the tetracycline resistance marker and "landing pad" sequences amplified from pTKS/CS into the genome at the *pfkA* locus. The resultant strain was then transformed with pTKRED and pTKIP-114pfkA(DAS+4), and integration of the construct from the pTKIP plasmid into the genome was achieved as described previously (Kuhlman and Cox, 2010). The kanamycin resistance cassette remaining after integration was cured by expression of FLP recombinase from pCP20 to yield strain IB1643.

Integration of the *tetR-P$_{LteOt}$-sspB* cassette into the genome was carried out via "clonetegration" (St-Pierre et al., 2013). The coding sequence of *sspB* was amplified from the *E. coli* genome and cloned into pKVS45 via restriction digest to yield pKVS-SspB. The vector pKVS45 includes a TetR expression cassette originally amplified from pWW308 (Solomon et al., 2012b). The entire *tetR-P$_{Lteto}$-sspB* cassette was amplified from pKVS-SspB. The pOSIP-CH backbone was also PCR amplified and cycled 10x with the *tetR-P$_{LteOt}$-sspB* fragment according to the protocol for circular polymerase extension cloning (CPEC) (Quan and Tian, 2009). The CPEC product was used to transform strain IB1643 for integration at the HK022 locus. The phage integration genes and antibiotic resistance cassette were cured with pE-FLP as described in the previously published protocol (St-Pierre et al., 2013) to yield strain IB1863.

For construction of IB1014, integration cassettes for deletion of *ptsHIcrr* and replacement of the native *galP* promoter with a strong constitutive promoter were PCR amplified from the genome of previously developed phosphotransferase system deficient (PTS-), glucose utilizing (glucose+) strains (Solomon et al., 2012a). These cassettes contained the desired genomic deletion or promoter replacement, a kanamycin resistance cassette, and the upstream and downstream genomic homology. The PCR cassettes were sequentially integrated into IB1863 via lambda-red mediated recombination using the helper plasmid pKD46, and each kanamycin resistance cassette was cured by expression of FLP recombinase from pCP20 (Datsenko and Wanner, 2000).

During all integration steps, colonies were screened via colony PCR with OneTaq master mix. PCR amplifications for cloning or genomic integration were carried out with Q5 polymerase. Enzymes utilized for PCR amplification, restriction digests, and ligation were obtained from New England Biolabs (Ipswich, MA). Oligonucleotides were obtained from Sigma-Genosys (St. Louis, MO).

2.2.2 Culture medium and conditions

For plasmid preparation and genetic manipulations, strains were cultured in Luria-Bertani (LB) medium at either 30° or 37° C. Temperature sensitive plasmids were cured at 42° C.

M9 minimal medium supplemented with either 0.4% glucose or 0.4% glycerol was utilized for initial screening of promoters for *pfkA*. All additional cultures for measurement of growth and production were carried out at 30°C in a modified MOPS medium containing 10 g/L D-glucose, 3 g/L NH_4Cl, 1 g/L K_2HPO_4, 2 mM $MgSO_4$, 0.1 mM $CaCl_2$, 40 mM MOPS, 4 mM tricine, 50 mM NaCl, 100 mM Bis-Tris, 134 µM EDTA, 31 µM $FeCl_3$, 6.2 µM $ZnCl_3$, 0.76 µM $CuCl_2$, 0.42 µM $CoCl_2$, 1.62 µM H_3BO_3, and 0.081 µM $MnCl_2$. When noted, the medium was supplemented with an additional 0.2% casamino acids. For strains containing pTrc-INO1, carbenicillin (100 µg/mL) was added for plasmid maintenance. Seed cultures were initiated using a 1:100 – 1:500 dilution from LB cultures and were grown at 30°C for 18 - 24 hours in modified MOPS, until mid-exponential phase was reached. Working cultures of 50 ml in 250 ml baffled shake flasks were inoculated to OD = 0.05 from seed cultures, and for *myo*-inositol production experiments, 50 µM β-D-1-thiogalactopyranoside (IPTG) was added at inoculation. For induction of SspB in strain IB1863, anhydrotetracycline (aTc) was added at the times and concentrations indicated in the Results section. Samples were taken periodically for measurement of enzyme activity, protein levels, and extracellular metabolites.

2.2.3 Phosphofructokinase activity assays and Western blotting

All enzymatic activity assays were carried out on crude lysates. For preparation of lysates, samples of 5- 10 ml of cell culture were collected, frozen at -80°C, and then resuspended in 50 mM Tris-HCl, pH 7.4 (0.25 – 1 ml, depending on cell density). Cells were lysed via bead beating for 5 minutes and lysates clarified by centrifugation at 15,000 x g for 15 minutes. Phosphofructokinase activity was assayed using a protocol adapted from Kotlarz and Buc (Kotlarz and Buc, 1982; Kotlarz et al., 1975). The assay mixture consisted of 0.1 M Tris – HCl (pH 8.2), 10 mM $MgCl_2$, 1 mM ATP, 0.2 mM β-NADH, 1 mM fructose-6- phosphate (F6P), 1 mM NH_4Cl, 0.01% Triton X-100, 0.83 U aldolase, 0.42 U triosephosphate isomerase, and 0.42 U glycerophosphate dehydrogenase. Reaction progress was followed by measurement of

absorbance at 340 nm. One unit of Pfk activity was defined as the amount required to convert 1.0 µmole of ATP and D-fructose 6-phosphate to ADP and fructose 1,6-bisphosphate per minute at pH 8.2 and room temperature.

For Western blots to confirm disappearance of Pfk-I, lysis was carried out as for enzymatic assays. A 4-20% SDS-PAGE gel was run with 10 µg total protein per lane. Proteins were transferred from the PAGE gel to a nitrocellulose membrane and excess binding sites were blocked using 5% dry milk in TBS. The membrane was incubated at 4°C overnight with anti-Pfk-I rabbit polyclonal antibody (6.7 µg/ml) custom prepared by Genscript (Piscataway Township, NJ), rinsed, and incubated with HRP-conjugated goat anti-rabbit IgG polyclonal antibody (Santa Cruz Biotechnology, Dallas, TX) and StrepTactin-HRP (Bio-rad, Hercules, CA) at room temperature for one hour. Bands were visualized by treatment with Western blotting Luminol Reagent (Santa Cruz Biotechnology).

Total protein levels for normalization of enzymatic activities and Western blot loadings were measured using a modified Bradford assay (Zor and Selinger, 1996).

2.2.4 Measurement of intracellular glucose-6-phosphate and fructose-6-phosphate

Cultures of IB531, IB1863, and IB1014 were grown in triplicate in modified MOPS medium using the seed culture protocol outlined in Section 2.2.2. Working cultures were inoculated to OD = 0.02 and incubated at 30° C. For measurement of G6P buildup after Pfk-I degradation, aTc was added to the culture one hour before collection of the cell mass.

For intracellular metabolite measurements, 20-30 ml of cells in exponential phase (OD = 0.3 – 0.9) were collected via vacuum filtration through 0.45 µM Metricel GN-6 filters (Pall, Port Washington, NY). After filtration of the culture, the filters with cell mass were immediately immersed in 10 ml of 75% ethanol solution at 80° C. The solution was vortexed for 30 seconds, incubated at 80° C for 3 minutes, and vortexed again. The filter paper was then removed and the solution centrifuged for 10 minutes at 5000 x g to remove cell debris. Incubation in boiling 75% ethanol for 3 minutes has been previously shown to result in good extraction of sugar phosphates (Gonzalez et al., 1997). The solutions were stored at -80° C until evaporation for analysis.

The 75% ethanol solution was completely evaporated and the remaining solids resuspended in 200 μL water. Any solids which could not be dissolved in water were pelleted by centrifugation at 15,000 x g for 5 minutes. Enzymatic assays for G6P and F6P were carried out in 96-well plates in a Tecan infinite F200Pro plate reader (Männedorf, Switzerland). The assay solution consisted of 0.2 M triethanolamine, 0.2 mM NADP, and 5 mM $MgCl_2$ (Bergmeyer et al., 1983). After stabilization of the baseline, glucose-6-phosphate dehydrogenase was added to the assay solution and G6P levels were analyzed by following NADPH generation via fluorescence (excitation 340 nm, emission 450 nm). After complete turnover of G6P, F6P levels were analyzed by the addition phosphoglucose isomerase, which converted the remaining F6P to G6P. Intracellular metabolite levels were estimated assuming 0.4 gDCW/OD unit (Tseng et al., 2009) and an intracellular volume of 2 ml/gDCW, which would be expected for *E. coli* at a similar growth rate on glucose (Hiller et al., 2007).

2.2.5 Measurement of extracellular metabolites

Glucose, acetate, and *myo*-inositol levels were quantified by high performance liquid chromatography (HPLC) on an Agilent 1100 or 1200 series instrument (Santa Clara, CA) with an Aminex HPX-87H anion exchange column (300 mm by 7.8 mm; Bio-Rad Laboratories, Hercules, CA). Sulfuric acid (5 mM) at a flow rate of 0.6 mL/min was used as the mobile phase. Compounds were quantified from 10 μL sample injections using refractive index and diode array detectors. Column and refractive index detector temperatures were held at 35° C. Glucose uptake and acetate production rates were calculated using an estimated cell mass of 0.4 gDCW/OD unit (Tseng et al., 2009).

2.2.6 Characterization of BioFab promoters for Pfk-I expression

The *pfkA* locus was replaced as described in section 2.1 with a series of constructs containing various promoters from the BIOFAB library (Mutalik et al., 2013). Strains were cured of the kanamycin resistance cassette included with the insertion. Cultures were grown in triplicate in M9 minimal medium at 37° C with either 0.4% glucose or 0.4% glycerol as the carbon source for growth rate measurements. Samples were taken in mid-exponential phase for measurement of phosphofructokinase activities in crude lysates.

Table 2.1 | Strains and plasmids used in this study.

Strain / plasmid	Genotype	Reference / source
Strains		
DH10B	F⁻ *mcrA Δ(mrr-hsdRMS-mcrBC) φ80lacZΔM15 ΔlacX74 recA1 endA1 araD139 Δ(ara, leu)7697 galU galK λ-rpsL nupG*	Life Technologies (Carlsbad, CA)
MG1655	F⁻ λ⁻ *ilvG⁻ frb- 50 rph-1*	ATCC #700926
IB531	MG1655 *ΔendA*	Prather Lab
IB1375	MG1655 *ΔendA Δzwf*	This study
IB1379	MG1655 *ΔendA Δzwf ΔpfkB*	This study
IB1489	MG1655 *ΔendA Δzwf ΔpfkB ΔsspB*	This study
IB1643	MG1655 *ΔendA Δzwf ΔpfkB ΔsspB pfkA::114-pfkA(DAS+4)*	This study
IB1863	MG1655 *ΔendA Δzwf ΔpfkB ΔsspB pfkA::114-pfkA(DAS+4) HK022::tetR-Ptet-sspB*	This study
IB1014	MG1655 *ΔendA Δzwf ΔpfkB ΔsspB ΔptsHIcrr pfkA::114-pfkA(DAS+4) HK022::tetR-Ptet-sspB galP^q*	This study
IB531-I	IB531 / pTrc-INO1	This study
IB1863-I	IB1863 / pTrc-INO1	This study
IB1014-I	IB1014 / pTrc-INO1	This study
JW3197-1	F-, *Δ(araD-araB)567, ΔlacZ4787(::rrnB-3), λ⁻, ΔsspB756::kan, rph-1, Δ(rhaD-rhaB)568, hsdR514*	(Baba et al., 2006)
JW5280-1	F-, *Δ(araD-araB)567, ΔlacZ4787(::rrnB-3), λ⁻, ΔpfkB722::kan, rph-1, Δ(rhaD-rhaB)568, hsdR514*	(Baba et al., 2006)
JW1841-1	F-, *Δ(araD-araB)567, ΔlacZ4787(::rrnB-3), λ⁻, Δzwf-777::kan, rph-1, Δ(rhaD-rhaB)568, hsdR514*	(Baba et al., 2006)
Plasmids		
pCP20	Rep^a, Amp^R, Cm^R, FLP recombinase expressed by λ p_r under control of λ cI857	CGSC #7629
pKD46	*ori*R101, *repA*101ts, Amp^R, *araC*, araBp-λγ-λβ-λexo	CGSC #7739
pE-FLP	*ori*R101, *repA*101ts, Amp^R, FLP recombinase expressed by pE	(St-Pierre et al., 2013)
pKVS45	*p*15A, Amp^R, *tetR*, P_{Tet}	(Solomon et al., 2012b)
pKVS-SspB	pKVS45 with RBS B0034 + *E. coli* SspB inserted at the EcoRI and BamHI sites	This study
pOSIP-CH	pUC *ori*, RK6γ *ori*, Cm^R, *attP* HK022, ccdB, HK022 integrase expressed by λ p_r under control of λ cI857	(St-Pierre et al., 2013)
pTKIP-neo	ColE1(pBR322) *ori*, Amp^R, Kan^R	(Kuhlman and Cox, 2010)
pTKRED	*ori*R101, *repA*101ts, Spec^R, *araC*, P_{lac} λγ λβ λexo *lacI*, P_{araB} I-SceI	(Kuhlman and Cox, 2010)
pTKS/CS	*p*15A, Cm^R, P_{lacIq} *tetA*	(Kuhlman and Cox, 2010)
pTrc-INO1	pTrc99A with *S. cerevisiae* INO1 inserted at the EcoRI and HindIII sites	(Moon et al., 2009)

2.3 Results

2.3.1 Selection of phosphofructokinase-I as a control point for glucose-6-phosphate flux

The primary native enzymes acting on the branch point metabolite G6P are phosphoglucose isomerase (Pgi) and glucose-6-phosphate dehydrogenase (Zwf). Although knockout of these enzymes will result in a strain that cannot consume G6P (Shiue et al., 2015), they are not necessarily appropriate targets for dynamic control. The interconversion between G6P and fructose-6-phosphate (F6P) catalyzed by Pgi is near equilibrium within the cell, indicating that the enzyme may not exert significant control over flux (Stephanopoulos et al., 1998). Previous reports from *in vitro* simulation of glycolysis indicate that Pfk exerts significant control over the utilization of G6P (Delgado et al., 1993).

To better understand where control of G6P flux toward *myo*-inositol lies in this system in *E. coli,* a basic model of G6P consumption was constructed, using available *in vitro* kinetic data and published information on steady-state flux distribution, intracellular metabolite levels, and cofactor levels during growth on glucose (additional information can be found in Appendix A). The reaction catalyzed by INO1, *myo*-inositol-1-phosphate synthase from *Saccharomyces cerevisiae,* was included as a competing reaction to generate the target heterologous compound *myo*-inositol. This initial model was used to explore inherent kinetic limitations, but did not account for changes in downstream regulation, glucose uptake rate, and cofactor pools, which occur as the levels of glycolytic enzymes are varied.

The model was used to predict steady-state rate of G6P consumption by INO1 as a function of enzyme level knockdown (Fig. 2.1). 25% knockdown of Pfk is predicted to increase flux through INO1 nearly two-fold, while almost complete knockdown of Pgi would be required to achieve this increase in flux. The predicted increase in flux is also consistent with the reported K_M value of INO1, which has been estimated for G6P *in vitro* at 1.18 mM (Majumder et al., 1997). Given that intracellular G6P is predicted to be near this level, it could be expected that INO1 is not already saturated with substrate and might have capacity for increasing turnover. Based on the predicted increases in flux towards *myo*-inositol with control of Pfk levels, this enzyme was selected for further development as a control point.
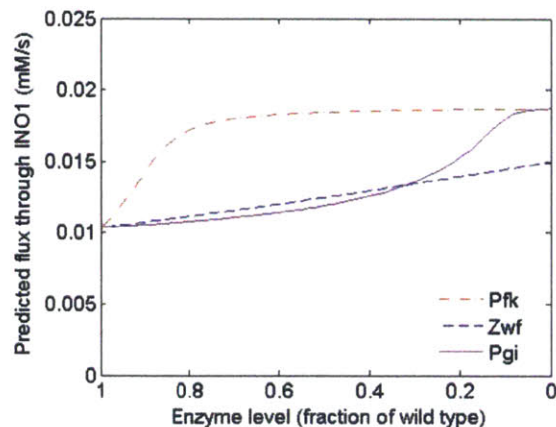
Fig. 2.1 | Kinetic analysis of flux through INO1 with predicted changes in flux through INO1 as the levels of the native metabolic enzymes Pgi, Pfk, and Zwf are varied.

2.3.2 Control of glucose flux and growth via controlled degradation of Pfk-I

With Pfk as the target for control, a strain background was developed that would allow the effect of Pfk knockdown to be cleanly observed (Fig. 2.2A). Pfk exists as two isozymes in *E. coli*, and the major form, Pfk-I, accounts for more than 90% of the observed activity (Keseler et al., 2011). Pfk-I was selected as the target enzyme for control, while the isozyme Pfk-II was eliminated by knockout of *pfkB*. Additionally, *zwf* was knocked out to eliminate G6P flux into the pentose phosphate pathway, generating strain IB1379. These knockouts resulted in a 13% reduction in growth rate on modified MOPS minimal medium relative to the parent strain IB531 (Table 2.2).

Table 2.2 | Growth rates of intermediate strains in construction of IB1863.
Cultures were grown in triplicate at 30° C in modified MOPS minimal medium as described in Section 2.2.2. Growth rates given as triplicate mean ± SD.

Strain	Growth rate (1/hr)	% growth decrease relative to IB531
IB531	0.35 ± 0.002	--
IB1375	0.31 ± 0.007	13%
IB1379	0.30 ± 0.01	14%
IB1489	0.31 ± 0.005	13%
IB1643	0.28 ± 0.02	21%
IB1863	0.30 ± 0.01	14%
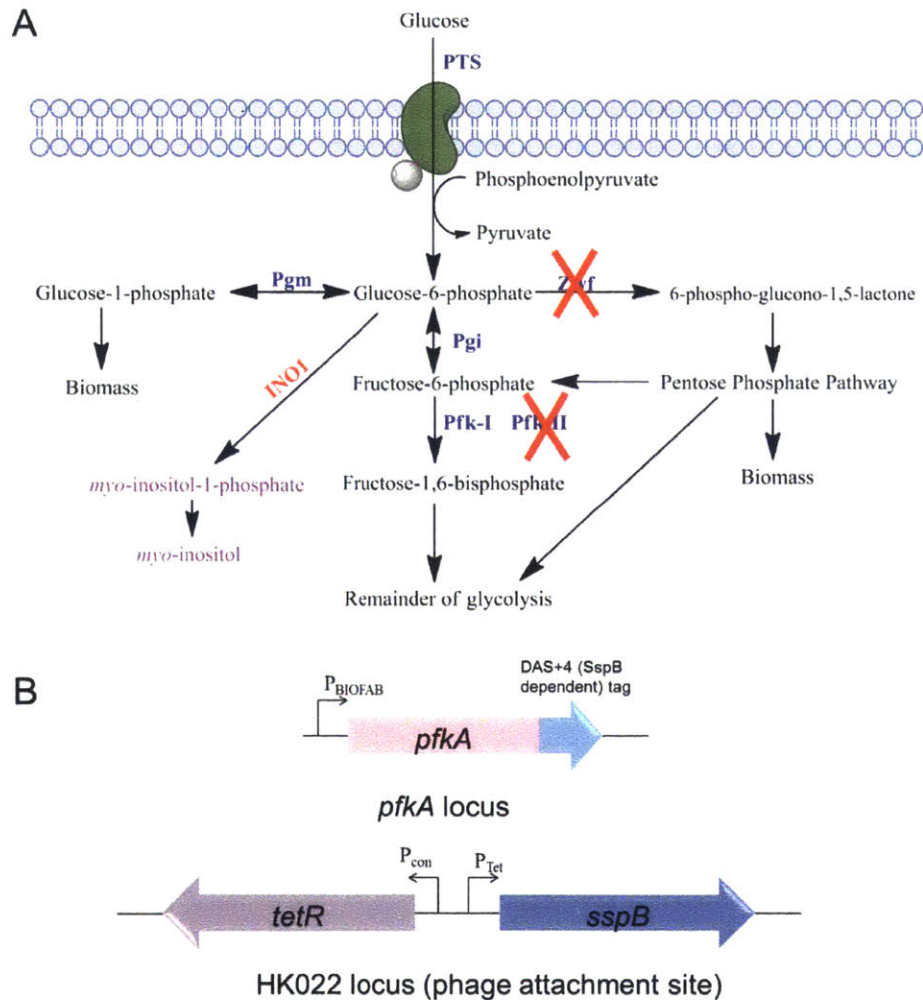
Fig. 2.2 | Construction of a switchable strain for *myo*-inositol production.
(A) Utilization of G6P in the cell, with gene knockouts to make Pfk-I the sole control point for G6P utilization. (B) Modifications to the *pfkA* and *HK022* loci to generate aTc inducible control of Pfk-I degradation.

To achieve dynamic knockdown of Pfk-I, a system based on controlled protein degradation was utilized. The coding sequence of *pfkA* was altered by appending a modified SsrA tag previously developed by McGinness *et. al.*, which results in rapid degradation of the target protein in the presence of the native *E. coli* adaptor protein SspB, but slow degradation in the absence of that protein (McGinness et al., 2006). Degradation of Pfk-I by ClpXP upon addition of an ssrA tag sequence was confirmed (Appendix B), indicating this system would be appropriate for further development. Native regulation of Pfk-I expression was disrupted by replacement of the native promoter sequence, which contains a binding

40

site for the transcription factor Cra, with a constitutive promoter selected from the BIOFAB modular library (Mutalik et al., 2013).   Six promoters from the low range of this library were tested. All promoters showed Pfk activities higher than that observed with the wild-type for untagged Pfk, and some of the replacements resulted in growth defects, which did not correspond with Pfk activity level. The promoter selected for further testing (apFAB114) showed no growth defect after integration and had the second lowest Pfk activity among the promoters tested, although the activity was still six-fold higher than wild type (Table 2.3). To make the default state "ON" (slow degradation of Pfk-I), SspB was knocked out at its native locus. Control was initially tested through aTc-inducible expression of SspB from the plasmid pKVS-SspB. This did not result in complete growth arrest in the "OFF" state, possibly due to plasmid loss or instability (data not shown). To improve system performance, the tet-expression cassette for SspB was integrated into the genome at the phage attachment site, HK022 (Fig. 2.2B), resulting in much better dynamic range of the system.

Table 2.3 | Characterization of BIOFAB promoters for Pfk-I expression.
Growth rates and Pfk activity are given as the triplicate mean ± SD. Red text = poorest growth in that medium, green text = best growth in that medium.

Promoter #	Stated promoter strength	0.4% Glucose		0.4% Glycerol	
		Growth rate (1/hr)	Activity (U/mg total protein)	Growth rate (1/hr)	Activity (U/mg total protein)
114	3.35	0.52 ± 0.001	4.49 ± 0.24	0.33 ± 0.006	5.41 ± 0.53
84	4.73	0.30 ± 0.002	5.20 ± 0.80	0.22 ± 0.005	7.99 ± 1.74
113	5.32	0.46 ± 0.003	4.75 ± 0.22	0.25 ± 0.002	5.61 ± 0.32
112	17.31	0.33 ± 0.001	3.38 ± 0.15	0.33 ± 0.003	3.61 ± 0.15
104	126.83	0.42 ± 0.02	8.01 ± 0.49	0.34 ± 0.002	10.08 ± 1.04
111	327.28	0.35 ± 0.002	9.45 ± 0.74	0.31 ± 0.004	10.22 ± 1.58
wild type		*0.51 ± 0.007*	*0.71 ± 0.04*	*0.38 ± 0.003*	*0.88 ± 0.08*

The resultant strain, IB1863, showed a 15% reduction in growth rate relative to IB531 on minimal medium (Fig. 2.3A). IB1863 and IB531 maintained similar growth profiles and no effect was seen on final OD. The baseline Pfk activity in IB1863 in the absence of induced SspB was 1.8X higher than IB531, lower than in the case of untagged Pfk-I due to low-level background degradation of Pfk-I, possibly due to leaky expression of SspB. However, upon addition of anhydrotetracycline (aTc) to induce expression of SspB from the $P_{L-tetO-1}$ promoter, Pfk-I activity in IB1863 declined very rapidly, decreasing to only 35% of wild type within one hour of SspB induction and 18% of wild type after 4 hours (Fig. 2.3B). The

activity decline corresponded with observed growth arrest in the aTc treated flasks, which showed over 90% reduction in growth rate. The growth arrest and activity reduction were stable over the 16 hour time period tested. Some decline in Pfk activity at stationary phase can be observed in the absence of SspB induction. A portion of this may be due to leaky SspB expression. Tests with the promoter replacement alone, in the absence of inducible SspB, indicate that this can also be attributed to decreased Pfk expression from the constitutive promoter in the stationary phase (Table 2.4). Western blotting with anti-Pfk-I showed consistent levels of the protein over 16 hours in untreated IB1863, while Pfk-I levels were below the limit of detection for cultures treated with aTc (Fig. 2.3C). Overexpression of SspB from pKVS-SspB was also tested in a *sspB-* background in the absence of tagged Pfk-I and no change in activity was seen, confirming inducible SspB overexpression alone had no effect (Fig. 2.4). These results indicate that Pfk-I degradation can be controlled through SspB induction and can be used to alter cellular phenotype.
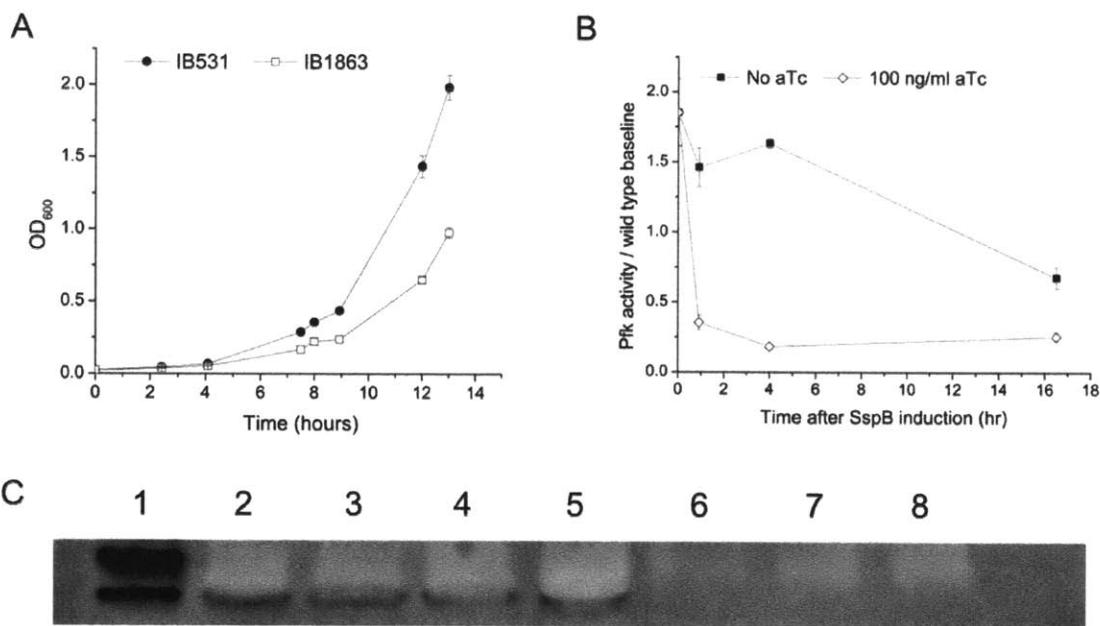
Fig. 2.3 | Performance of IB1863 in growth (Pfk-I ON) and production modes (Pfk-I OFF) in modified MOPS minimal medium at 30° C.
(A) Baseline growth of IB1863 in comparison to parent strain IB531. (B) Decline in Pfk activity in crude lysates in response to induction of SspB with aTc. (C) Western blot confirming disappearance of Pfk-I protein from crude lysates. Lane 1: Western C ladder, lane 2: Initial culture of IB1863 before split for aTc treatment (t = 0), lanes 3 – 5: Untreated IB1863 (t = 1, 4, 16 hours), lane 6 – 8: IB1863 treated with aTc (t = 1, 4, 16, hours after treatment).

Table 2.4 | Pfk activity for IB531 (wild type *pfkA* promoter), IB1643 (constitutive BIOFAB *pfkA* promoter, Δ*sspB* background), and IB1863 (constitutive BIOFAB *pfkA* promoter, P$_{LtetO}$ *sspB*) in exponential and stationary phase in cultures.
Cultures were grown at 30° C in modified MOPS minimal medium with 10 g/L glucose. Pfk activity is given as triplicate mean ± SD.

	Pfk activity (U/mg total protein)		
	IB531	IB1643	IB1863
Exponential phase	0.76 ± 0.04	1.69 ± 0.04	1.25 ± 0.17
Early stationary phase	0.78 ± 0.03	1.32 ± 0.14	0.53 ± 0.06
% change exponential to stationary	2.6%	-21.9%	-57.6%
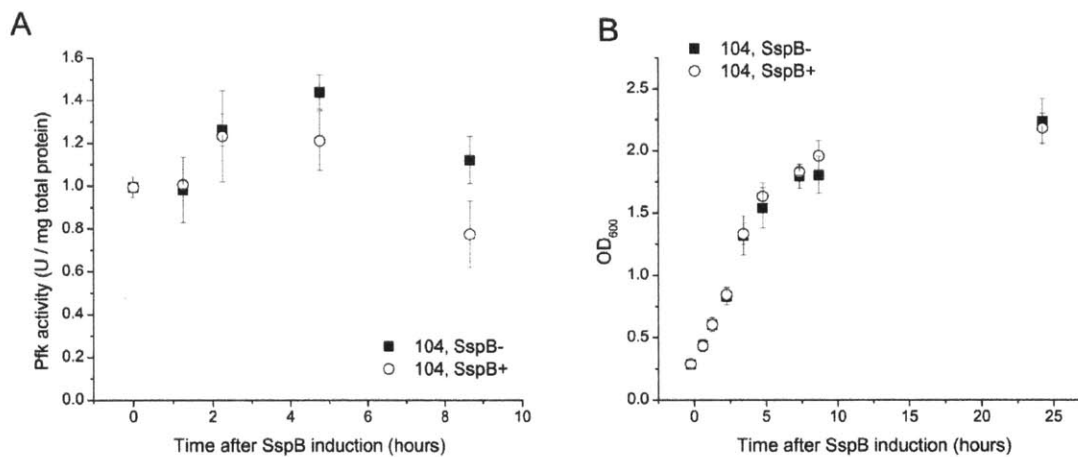
Fig. 2.4 | Pfk activity (A) and growth (B) in promoter library strain 104 with untagged Pfk-I.
Black squares indicate cultures with no induction of SspB, while open circles indicate cultures with SspB expression induced from pKVS-SspB by addition of 100 ng/ml aTc.

The degree of growth arrest can be modulated through titration of inducer, allowing the entire dynamic range to be utilized, with growth rates between 0.05 hr^{-1} and 0.30 hr^{-1} at 30° C (Fig. 2.5). The system shows full induction at an aTc concentration of 1 ng/ml. Previous characterization of the P$_{Ltet-O}$ promoter in a plasmid context indicated that 10 ng/ml of aTc was required for full induction (Lutz and Bujard, 1997). The relative change is likely due to differences in the amount of TetR produced through genomic versus plasmid-based expression. At a concentration of 1 ng/ml, there are 1.4×10^{15} molecules/L of aTc available in the medium. Given a biomass concentration of 10^{12} cells/L (approximately OD 1), this only provides enough aTc molecules to bind to 700 TetR molecules per cell, likely below the level produced from plasmid-based expression. The affinity of TetR for aTc is also well below the concentrations added to the medium, with the K$_D$ for [aTc-Mg]$_2^+$ binding reported as 8×10^{-13} M (Kamionka et al., 2004).
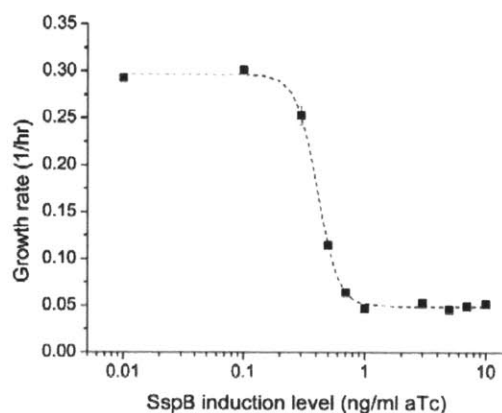
Fig. 2.5 | Growth rate of IB1863 as a function of aTc concentration added to the medium at inoculation.
Dotted line represents fit to Hill function with n=5. All points represent triplicate mean ± SD.
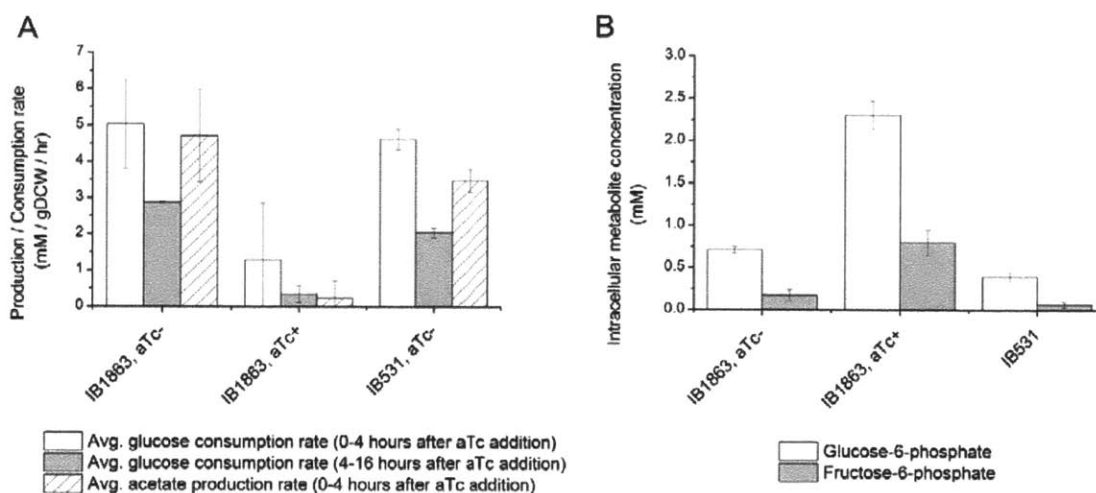
Fig. 2.6 | Effect of Pfk-I knockdown on carbon utilization in modified MOPS minimal medium at 30° C.
(A) Glucose consumption and acetate production rates in IB1863 and IB531. Glucose consumption was measured at 4 hours and 16 hours after addition of aTc to the indicated cultures and uptake rate was averaged across the given time period. (B) Intracellular G6P and F6P pools in IB1863 and IB531. Cells were collected in exponential phase and intracellular metabolites were extracted into boiling 75% ethanol. For cultures treated with aTc, cells were collected one hour after aTc addition to the culture. Plots depict the triplicate mean ± SD.

Glucose uptake and acetate production rates were also measured in IB1863. In the ON state, IB1863 shows a profile almost identical to IB531, but as expected in the OFF state, glucose uptake is greatly reduced (Fig. 2.6A). Acetate production is also lower, indicative of reduced flux into lower glycolysis.

44

Additionally, intracellular levels of glucose-6-phosphate and fructose-6-phosphate were elevated in the OFF state due to limited flux into lower glycolysis (Fig. 2.6B). Based on the thermodynamics of the G6P to F6P interconversion, it is expected that the sugar phosphate pool will be approximately 67% G6P and 33% F6P at equilibrium (Stephanopoulos et al., 1998). The intracellular metabolite measurements in IB1863 show a pool of 75% G6P and 25% F6P for Pfk-I knockdown and 80% G6P and 20% F6P for the control condition, consistent with the expectation that the reaction catalyzed by Pgi is near equilibrium, as discussed in the kinetic model in Section 2.3.1.

2.3.3 Application of the Pfk-I valve to *myo*-inositol production

Strains IB1863 and IB531 were transformed with pTrc-INO1, enabling IPTG-inducible expression of INO1, which catalyzes the conversion of G6P to *myo*-inositol-1-phosphate (MI1P). MI1P is then converted to MI by an endogenous phosphatase in *E. coli* (Hansen et al., 1999; Moon et al., 2009). In all cultures, INO1 expression was induced at inoculation through addition of 50 μM IPTG. Fermentations were carried out for 78 hours in shake flasks containing modified MOPS minimal medium and 10 g/L glucose. MI titers were assayed at the conclusion of the experiment. Switching of IB1863 between growth (Pfk-I ON) and production (Pfk-I OFF) modes was controlled through addition of 100 ng/ml aTc to induce SspB at t = 0, 11.5, 18, 32, and 47 hours.

Strong growth arrest was seen after induction of SspB in IB1863-I, except in the case of aTc addition at 47 hours, where the strain was in stationary phase (Fig. 2.7A). Activity measurements at 48 hours indicated an average 56% reduction in Pfk activity across all samples with SspB induced relative to those without SspB induction for IB1863-I and a 52% reduction in Pfk activity relative to the control strain IB531-I (Fig. 2.7B). The Pfk-I knockdown was quite consistent across SspB induction times, although for cultures with SspB induced at 47 hours, Pfk-I knockdown did differ between replicates, probably due to the short time available for Pfk-I degradation and the difference in relative growth phase of the replicates at that point.
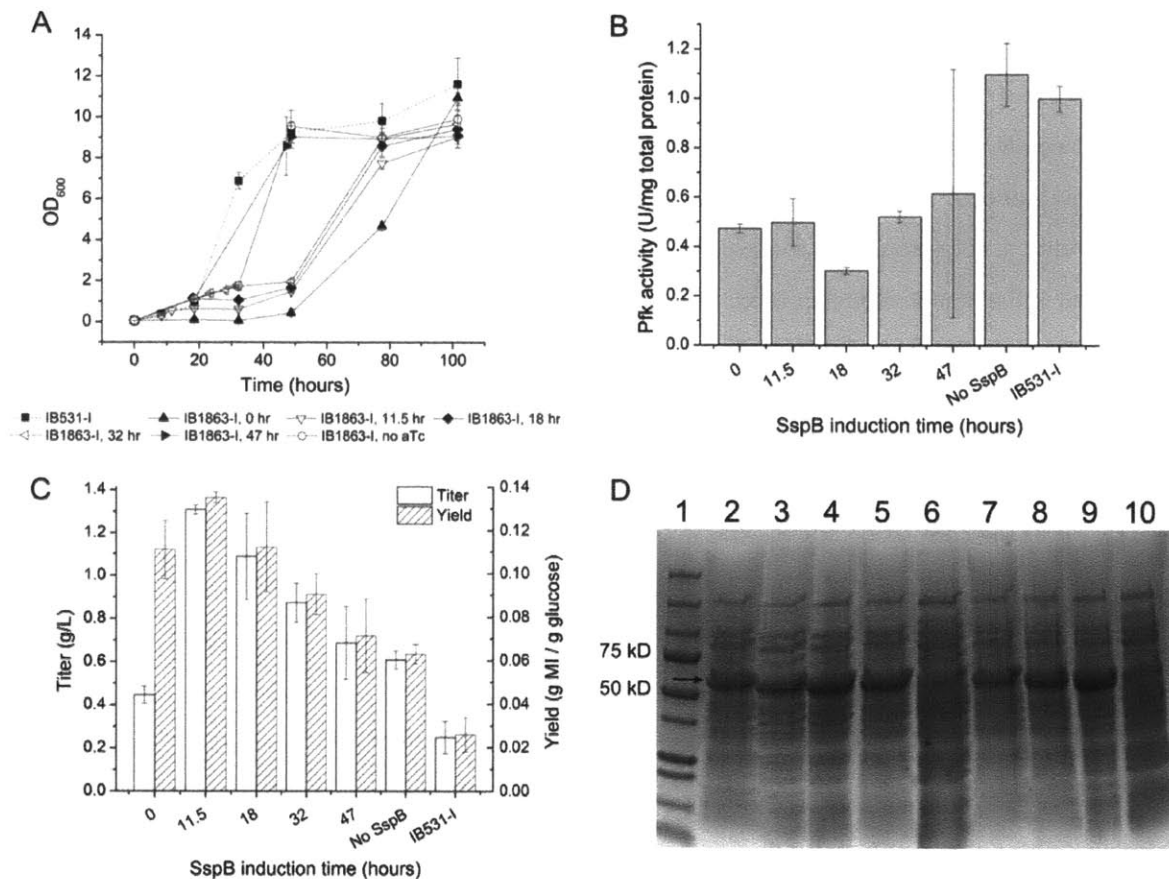
Fig. 2.7 | Effect of Pfk-I knockdown on MI production from glucose.
(A) Growth of IB531-I and IB1863-I with aTc added at times varying from 0 to 47 hours. Points represent duplicate mean ± SD. (B) Pfk activity in all cultures at 48 hours as a function of SspB induction time. "No SspB" refers to IB1863-I without induction of SspB by aTc addition and IB531-I shows the MG1655 ΔendA control. (C) Yield and titer of MI at 78 hours as a function of SspB induction time in IB1863-I. (D) SDS-PAGE gel showing representative INO1 expression (indicated at arrow) in IB531-I and IB1863-I. Lane 1: ladder, lanes 2 - 5: expression at 18 hours (IB531-I, IB1863-I with aTc at t = 11.5 hours, IB1863-I with aTc at t = 18 hours, IB1863-I without aTc), lanes 6 – 10: expression at 48 hours (IB531-I, IB1863-I with aTc at t = 11.5 hours, IB1863-I with aTc at t = 18 hours, IB1863-I with aTc at t = 32 hours, IB1863-I without aTc). Plots (A) - (C) depict duplicate mean ± SD for cultures with timed SspB induction and triplicate mean ± SD for uninduced IB1863-I and IB531-I controls.

Both theoretical (Anesiadis et al., 2008; Gadkar et al., 2005) and experimental studies (Solomon et al., 2012b; Soma et al., 2014) have indicated that there should be an optimal time for knockdown of a growth-coupled or essential gene within a fixed batch time to maximize product titer and yield. The theoretical work uses dynamic flux balance (dFBA) simulations to show that very early knockdown will result in the highest yields, but potentially incomplete carbon utilization within the batch, while later knockdown will result in lower yields, as more carbon is used for biomass, but faster consumption of the

available substrate given the higher concentration of biocatalyst. The earliest knockdown time that allows complete consumption of glucose should then give the highest titer in the batch. The experimental work to date shows the tradeoff can be more nuanced, as very early induction of gene knockdown, while in theory delivering highest yields, can result in unexpectedly poor growth (Soma et al., 2014). As expected, MI yield and titer varied as a function of induction time, with the highest yield and titers when SspB was induced at 11.5 hours (OD = 0.5). This resulted in a more than two-fold improvement in titers due to controlled Pfk-I degradation, with 1.31 g/L MI produced with SspB induction at OD = 0.5 compared to 0.61 g/L MI without SspB induction, and a five-fold improvement over the 0.25 g/L MI observed for the parent strain IB531-I (Fig. 2.7C). Delaying induction of SspB beyond 11.5 hours in this 78 hour batch resulted in the expected lower yields and lower titers, as more carbon was directed into biomass formation, with yields converging to those shown in the control without SspB induction. At the other extreme, induction of SspB at inoculation resulted in lower titers due to incomplete consumption of glucose after 78 hours. However, the yield was also lower, falling outside the trend of expected higher yields at earlier SspB induction times. It was thought that this might be due to poor recombinant protein expression, but SDS-PAGE analysis indicated INO1 was expressed at levels comparable to the other conditions (Fig. 2.7D), so the reduced yield may be due to broader limitations in metabolic capacity when early glucose uptake is restricted. Overall, these results indicate that it is possible to improve *myo*-inositol yields and titers by delaying knockdown of Pfk-I rather than using a static knockdown strategy, and that the optimal induction time will depend on the desired batch length. Further optimization of the timing of both INO1 expression and Pfk-I knockdown could be used to minimize the time required for biomass formation and allow for the highest flux toward *myo*-inositol within the biomass formed, maximizing productivity rates.

It was noted that by 78 hours, formation of biomass had resumed even in cultures in which growth had been arrested. This corresponded with some recovery in Pfk activity, likely indicating selection for cells that have accumulated mutations preventing the degradation of Pfk-I (Fig. 2.8). Section 2.3.4 provides a more detailed discussion of one observed mechanism of inactivation. While it would be most desirable to maintain full knockdown throughout the course of the fermentation, there is still a significant period of reduced Pfk activity, which provides sufficient time for flux redirection. It would be expected that having a larger proportion of cells in the culture with increased Pfk activity would hurt *myo*-inositol yield due to increased glucose utilization for biomass, but the trend shows that earlier induction of Pfk degradation, leaving the most glucose available for any "escaped" cells to consume, still resulted in

higher yields and titers. As a result, we do not think that escape is driving the differences in yield and titer observed.
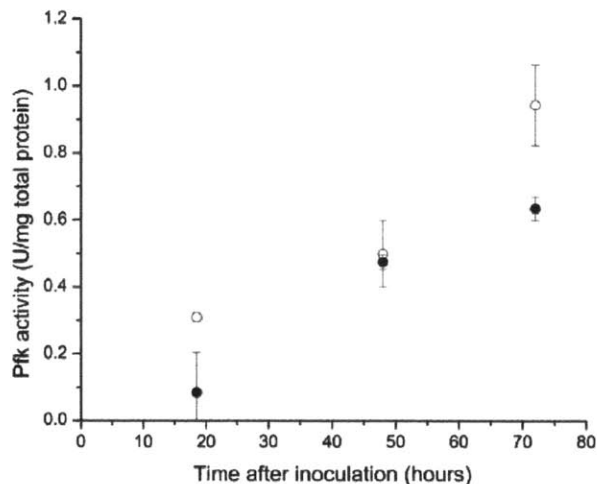
Fig. 2.8 | Pfk activity as a function of time in selected cultures of IB1863-I.
Filled circles represent cultures with SspB induced at inoculation (OD = 0.05) and open circles represent cultures with SspB induced at 11.5 hours (OD = 0.55). Points indicate duplicate mean ± SD.

Analysis of lysates by SDS-PAGE showed similar expression of INO1 during exponential growth at 18 hours for IB531-I and for IB1863-I with and without SspB induction (Fig. 2.7D), indicating that differences in initial expression of INO1 were not a primary factor in influencing yield. At 48 hours, cultures containing IB531-I and untreated IB1863-I had reached stationary phase, and showed reduced INO1 expression, while those cultures in growth arrest after SspB induction still showed high levels of INO1 expression. Growth arrest due to dynamic Pfk-I knockdown appears to yield a metabolic state in which recombinant protein levels can still be maintained.

2.3.4 Genetic stability of Pfk-I valve system

Any system relying on arrest of cellular growth is naturally applying a strong selection for compensatory mutations. In this particular system, any mutation that prevents the degradation of Pfk-I after aTc additional will provide a relative fitness advantage, and those cells will eventually become the predominant population. Possible points for mutation include the degradation tag on *pfkA*, the coding sequence or promoter for *sspB*, and the coding sequence or promoter for *clpX* and *clpP*. To determine if these mutations did occur in escaped cells, strain IB1863 was grown in triplicate in modified MOPS

minimal medium with glucose and aTc was added at OD 0.25. The cells showed very slow growth for 48 hours, but between 48 and 72 hours, grew rapidly and consumed all available glucose. At that time, samples from all three flasks were streaked onto LB agar. New cultures were also started from these flasks, and they no longer showed growth arrest in response to aTc addition, indicating the observed growth was not due to breakdown of inducer.

Colony PCR was then carried out on two colonies isolated from each flask using primers that amplified the regions containing *pfkA(DAS+4)*, *clpX*, and the *sspB* expression cassette. In these 6 colonies, *clpX* and *pfkA(DAS+4)* amplification resulted in the expected band sizes and sequencing of the PCR products also returned the correct sequences. Amplification of the *sspB* cassette resulted in 4 cases of PCR products with a larger than expected band size and 2 cases of no amplification. Three of the recovered PCR products were sent for sequencing and revealed an insertion that disrupted up to 36 base pairs of *sspB* and separated it from the tet promoter (Fig. 2.9). A BLAST search revealed that the insertion sequence matched that found in the IS2 insertion element. To improve the stability of such constructs, it might be beneficial to utilize a modified strain background with mobile genetic elements deleted. Fluctuation assays comparing one such reduced genome strain to MG1655 showed that 24% of loss of function mutations in MG1655 were caused by IS transpositions, and those could be eliminated in the IS-free strain MD41 (Pósfai et al., 2006). An alternative using the existing strain background could be to add an essential gene or toxin/antitoxin system to the *sspB* expression cassette to limit the possible locations where transposable elements could successfully be inserted and not cause cell death.

P_{tet}

-35   -10   +1

...tccctatcagtgatagagattgacatccctatcagtgatagagatactgagcacctaggtttctccatacccgtttttttgggctagcgaattc

RBS   sspB

aaagaggagaaatactagatggatttgtcacagctaacaccacgtcgtccctatctgctgcgtgcatt...

insertion site 1   insertion site 2, 3
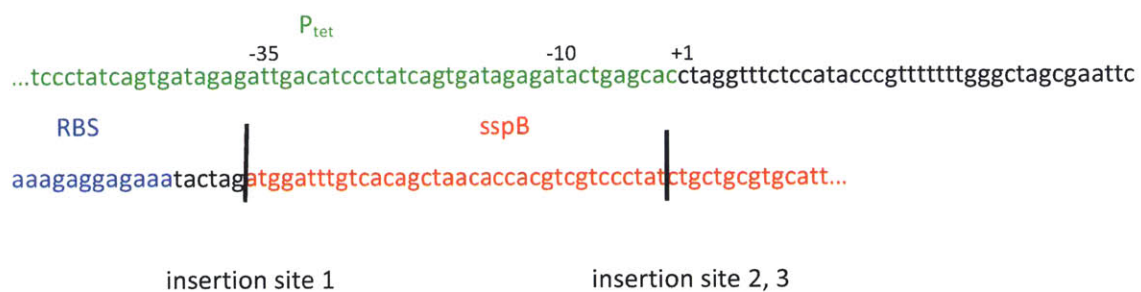
Fig 2.9 | Locations of IS2 insertions in *sspB* expression cassette.
Three instances of the IS2 insertion were found during sequencing. One insertion was immediately in front of the *sspB* coding sequence (insertion site 1), while the remaining two were at the same site, 36 bp into the *sspB* coding sequence (insertion site 2, 3).

In addition to improving genetic stability of the Pfk-I valve system itself, high stability of INO1 expression is required to reach high yields of MI. To understand the baseline stability of INO1 expression from pTrc-INO1, plasmid loss and INO1 expression was monitored in IB531-I under the minimal medium production conditions used in 2.3.3. Culture samples were diluted as appropriate and plated on LB agar plates with and without antibiotic selection. Lysates were analyzed by SDS-PAGE with loadings normalized to total protein. Significant plasmid loss occurred between 24 and 36 hours (Fig 2.10A), corresponding with more rapid growth and a decrease in INO1 as a fraction of total protein (Fig. 2.10B). While approximately 77% of cells were ampicillin resistant at 24 hours (contained pTrc plasmid), only 2.9% were resistant by 35 hours. Genomic integration of INO1 could improve stability; however high expression will still be important. Tests utilizing the low-copy plasmid pMMB-INO1 showed no plasmid loss, but reconfirmed the previous observation that INO1 activity was insufficient for MI production (Moon et al., 2009).
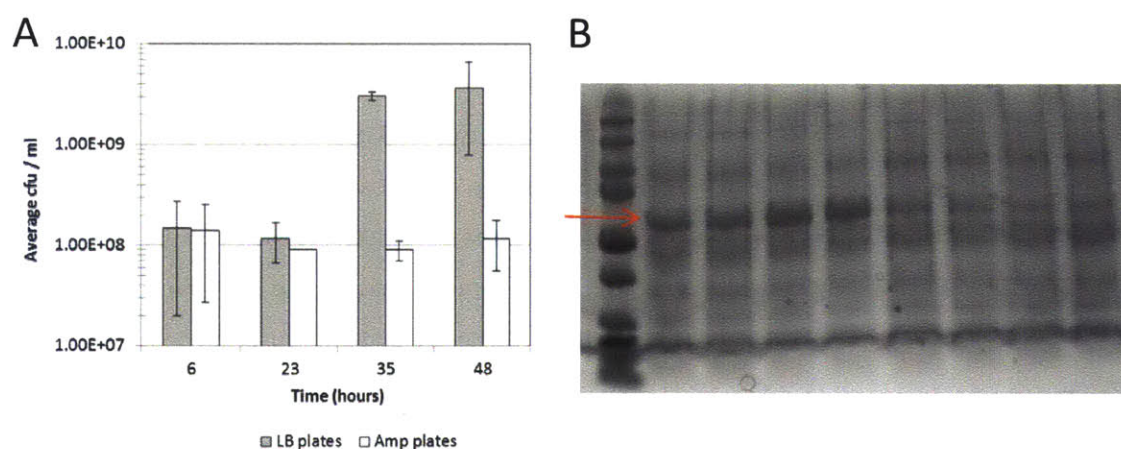
Fig. 2.10 | Plasmid loss and INO1 expression in IB531-I.
(A) Colony counts on plates without (gray) and with (white) antibiotic selection for pTrc-INO1. Bars represent triplicate mean ± SD. (B) SDS-PAGE analysis of INO1 expression over time. Loadings were normalized to total protein concentration measured by Bradford assay. Red arrow indicates location of INO1 band. Lane 1: ladder, lanes 2/3: 6 hours, lanes 4/5: 23 hours, lanes 6/7: 35 hours, lanes 8/9: 48 hours.

2.3.5 Application of the Pfk-I valve in a PTS- strain background

Another factor important for maximizing MI productivity is maintenance of a high glucose uptake rate. However, uptake of glucose via the phosphotransferase system (PTS) is expected to be limited by downstream availability of phosphoenolpyruvate (PEP) when flux through Pfk-I is restricted. To test the effect of Pfk-I knockdown when glucose uptake is independent of the PTS, a PTS- glucose+ strain was

generated via deletion of *ptsHIcrr* and constitutive expression of *galP*, manipulations which were previously shown to impart a PTS- glucose+ phenotype (De Anda et al., 2006; Solomon et al., 2012a). This strain, IB1014, showed a significant reduction in growth on glucose compared to IB1863, with a baseline growth rate of 0.13 hr^{-1} in glucose minimal medium at 30°C, less than half of that observed for IB1863. However, the behavior of the strain upon induction of SspB was still consistent and addition of aTc resulted in strong growth arrest, with over 90% reduction in growth rate (Fig. 2.11A). G6P levels were also measured in the strain with and without induction of SspB. Similar to IB1863, induction of SspB resulted in an increase in the G6P pool in IB1014 (Fig. 2.11B). These results indicate that the Pfk-I knockdown strategy should be applicable for G6P accumulation in a PTS- background and that the growth arrest observed in IB1863 was not dependent upon PEP limitation driving reduced glucose uptake.
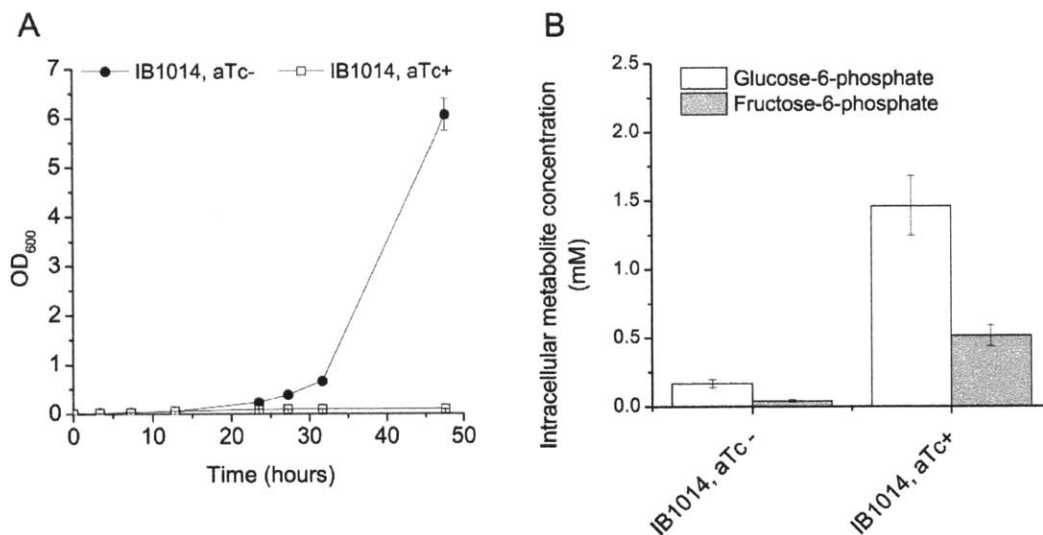
Fig. 2.11 | Characterization of IB1014 in modified MOPS minimal medium + 10 g/L glucose at 30° C. (A) Growth of IB1014 without aTc addition and with aTc addition at OD = 0.06. (B) Intracellular G6P and F6P pools in IB1014 with and without induction of SspB by aTc addition. Cells were collected in exponential phase and intracellular metabolites were extracted into boiling 75% ethanol. For cultures treated with aTc, cells were collected one hour after aTc addition to the culture. Plots depict the triplicate mean ± SD.

IB1014 was also transformed with pTrc-INO1 to test *myo*-inositol production. In the modified MOPS minimal medium with 10 g/L glucose used for testing of IB1863-I, IB1014-I showed no growth after 36 hours when INO1 was expressed at inoculation. IB1014-I was then tested in the same base medium and with the same INO1 induction conditions, but with additional supplementation of 0.2% casamino acids.

51

Casamino acid supplementation restored growth, although IB1014-I was still significantly impaired in growth relative to the wild type (PTS+) control IB531-I. At various time points during the fermentation in casamino acid supplemented medium, 100 ng/ml aTc was added to cultures of IB1014-I knock down Pfk-I activity. The growth patterns observed were qualitatively similar to those seen for IB1863-I, with growth arrest occurring at initial aTc addition and eventual accumulation of biomass at long times (Fig. 2.12). Culture supernatant was analyzed by HPLC, but MI titers were below 0.1 g/L in IB1014-I and could not be accurately quantified. Given the poor titers, additional production experiments were not pursued in this strain. The strain could possibly be improved through adaptation on glucose or upregulation of Glk, although strong overexpression of Glk has been shown to be detrimental (Solomon et al., 2012a).
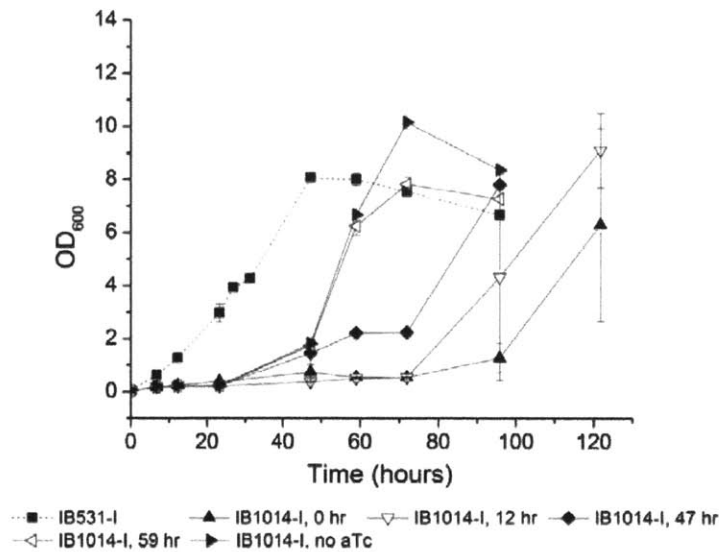
Fig. 2.12 | Growth of IB531-I and IB1014-I in modified MOPS minimal medium supplemented with 10 g/L glucose and 0.2% casamino acids.
50 µM IPTG was added at inoculation for induction of INO1 expression. IB1014-I cultures were either untreated (no aTc) or SspB was induced via addition of 100 ng/ml aTc at the following times: t = 0 (inoculation), 12 hours, 47 hours, and 59 hours. Points represent duplicate mean ± SD.

2.4 Discussion

In the production of MI, there is a direct competition between cellular growth and carbon flux toward product. Given this tradeoff, it is very difficult to engineer a static knockdown strategy which will not result in detrimental effects on host strain physiology, including poor growth and poor expression of recombinant proteins. To overcome this, we focused on development of a host strain that retains the

positive characteristics of the parent strain with regard to growth and glucose uptake, but can be switched to a production mode with reduced carbon utilization for biomass.

Strain IB1863 was engineered to make Pfk-I the sole control point for utilization of G6P and F6P, linking cellular growth to steady-state levels of this enzyme. Through addition of an SspB-dependent degradation tag to the coding sequence of Pfk-I, the steady-state level could be controlled by expression of SspB from an inducible promoter. After these changes, IB1863 showed a modest reduction in growth rate compared to the parent strain in untreated cultures, but addition of aTc could be used to control glucose uptake, reducing growth by more than 80%. Coupling this with expression of INO1 allowed a two-fold increase in MI yield and titer to be achieved when utilizing glucose as a sole carbon source.

Notably, the greatest improvement in yield and titer came with delayed induction of SspB, indicating that the dynamic control of Pfk-I, rather than static downregulation, was necessary in order to achieve the best performance. The full extent of the system can still be explored, including combinations of different induction times and induction levels for both INO1 and SspB, allowing a variety of biomass and production tradeoffs to be tested. A particularly interesting possibility for use of this system might be in a fed-batch fermentation, where Pfk knockdown is induced after a suitable period of biomass formation and glucose is then fed at a rate matching the uptake needed for *myo*-inositol production and for minor glycolytic flux supporting cell maintenance.

Explorations of similar systems with dFBA indicate that there should be an optimal point for maximum productivity (Anesiadis et al., 2013). Given that the deletion of *pfkA* in the *Δzwf ΔpfkB* background used is lethal, the productivity of a static knockout strain is zero, and dynamic control is especially appealing for this type of system. While we did not observe the direct trade-off between yield and titer predicted in the dFBA work at the batch length tested in this study, as both titer and yield increased with dynamic control in this case, productivity trends would still be important to consider, especially for a fed-batch case relying on formation of a fixed initial amount of biomass.

In addition to testing of the system in a strain relying on glucose uptake via the PTS, we also tested the applicability of Pfk-I control in a strain where glucose uptake is independent of PEP utilization. Our results showed that increases in the G6P pool could still be achieved in a PTS- background. While the particular PTS- strain examined in this study would require significant optimization to support MI

production, ultimately, a strain where glucose uptake is decoupled from PEP utilization could offer the highest theoretical yields for products derived from G6P. Reducing equivalents or ATP produced within a heterologous pathway could be used to drive glucose uptake, maintaining glucose utilization even as metabolites in lower glycolysis are depleted.

2.5 Conclusions

In this study, we demonstrated controlled degradation of Pfk-I as a novel method for redirecting flux of G6P into a heterologous pathway. Upon addition of aTc to induce expression of SspB, Pfk-I was degraded and carbon flux into biomass was halted. This system was used to achieve improvements in both yield and titer of MI on glucose as a sole carbon source. The rapid, dynamic nature of the switching allows desirable cellular phenotypes (rapid growth, high expression of recombinant proteins) to be preserved during the growth phase of a fermentation, while still achieving reduced flux into central metabolism during the production phase. While this specific system was designed to be coupled with the first step in a pathway for glucaric acid production, it could be more broadly applied to any pathway with G6P or F6P as a branch point. This could include production of other *myo*-inositol derivatives, including *scyllo*-inositol, which has been studied for therapeutic uses (Yamaoka et al., 2011) or redirection of flux into the pentose phosphate pathway in response to cellular demand for NADPH, which is important when expressing pathways with high cofactor requirements, such as fatty acid biosynthesis.

Chapter 3: Improvement of glucaric acid production via a "metabolite valve"

Abstract

D-glucaric acid can be used as a building block for biopolymers, as well in the formulation of detergents and corrosion inhibitors. A biosynthetic route for production in *E. coli* has been developed (Moon et al., 2009). Previous work with the glucaric acid pathway has indicated that competition with endogenous metabolism may limit carbon flux into the pathway. Our group has recently developed an *E. coli* strain where phosphofructokinase (Pfk) activity can be dynamically controlled and demonstrated its use for improving yields and titers of the glucaric acid precursor *myo*-inositol on glucose minimal medium (Brockman and Prather, 2015). In this work, we have explored the further applicability of this strain for glucaric acid production in a supplemented medium more relevant for scale-up studies, under batch conditions and with glucose feeding via starch hydrolysis. It was found that glucaric acid titers could be improved by up to 42% with appropriately timed knockdown of Pfk activity during glucose feeding.

3.1 Introduction

D-glucaric acid was identified by the United State Department of Energy as a top value-added chemical for production from biomass (Werpy and Petersen, 2004). It has a number of potential applications, including use in biopolymers (Kiely and Chen, 1994) and as a detergent builder or corrosion inhibitor (Smith et al., 2012). Glucaric acid can be produced through nitric acid oxidation of glucose (Mehltretter and Rist, 1953), but a biological route to glucaric acid production could potentially provide several advantages, including mild processing conditions and high selectivity for the product of interest.

Production of D-glucaric acid in *Escherichia coli* was previously demonstrated by our group via expression of heterologous enzymes from three different organisms (Moon et al., 2009). Titers of 1.13 g/L glucaric acid were achieved in strain BL21 in LB medium supplemented with 10 g/L glucose. Following demonstration of the initial pathway, some increases in glucaric acid titers were achieved through improved strategies for expression of the *myo*-inositol oxygenase (MIOX) enzyme, which was one of the limiting factors in glucaric acid production in LB supplemented with glucose or *myo*-inositol (Moon et al., 2010; Shiue and Prather, 2014). However, competition for glucose-6-phosphate (G6P) between native *E. coli* enzymes and the first enzyme in the glucaric acid pathway, *myo*-inositol-1-phosphate synthase (INO1), is also a concern. High level expression of INO1 is required for detectable *myo*-inositol and glucaric acid production, indicating it competes poorly against endogenous metabolism for substrate (Moon et al., 2009). Additionally, the second pathway enzyme, MIOX appears to be stabilized by its substrate, *myo*-inositol, so more rapid accumulation of *myo*-inositol may help reduce limitations in MIOX activity as well.

With this in mind, our group has explored strategies for development of strains capable of accumulating G6P and directing greater fluxes of this metabolite into production of glucaric acid and *myo*-inositol. By eliminating the pathways for glucose catabolism in the production strain, and feeding alternative carbon sources, high yields of glucaric acid from glucose could be achieved (Shiue et al., 2015). However, the rate of glucose uptake in this strain was quite slow, especially in minimal medium, and its use was limited to mixed sugar substrates. It was recently shown that by dynamically controlling the phosphofructokinase (Pfk) activity in the cell, the pools of G6P could be increased during growth on glucose minimal medium, along with the yields and titers of the glucaric acid precursor *myo*-inositol (Brockman and Prather, 2015). In this work, we explored the expanded utility of this system for production of glucaric acid from glucose in a semi-defined medium under batch conditions and a fed-

batch condition simulated by glucose release from starch hydrolysis. Improvements in glucaric acid titer of up to 42% were achieved through appropriately timed induction of Pfk activity knockdown during the fermentation.

3.2 Materials and methods

3.2.1 Strains and plasmids

E. coli strains and plasmids used in this study are listed in Table 3.1. Strains IB1863 and IB1379 were constructed by our group previously (Brockman and Prather, 2015). To eliminate glucaric acid catabolism in strain IB1863, knockouts of *gudD* and *uxaC* were carried out via sequential P1 transduction from Keio collection donor strains (Baba et al., 2006). The kanamycin resistance cassette was removed after each transduction via expression of FLP recombinase from pCP20 (Datsenko and Wanner, 2000). The λDE3 lysogen was integrated into this strain using a λDE3 Lysogenization Kit (Novagen, Darmstadt, Germany), generating strain IB1486. To generate the Δ*pfkA* control strain IB2255, serial P1 transductions were also carried out in IB1379 to knockout *pfkA, gudD,* and *uxaC,* and the λDE3 lysogen was integrated as described above. Construction of plasmids for production of glucaric acid, pRSFD-IN-MI and pTrc-udh, was described previously (Moon et al., 2009; Yoon et al., 2009).

3.2.2 Culture medium and conditions

For plasmid preparation and genetic manipulations, strains were cultured in Luria-Bertani (LB) medium at either 30° or 37° C. Temperature sensitive plasmids were cured at 42° C.

Glucaric acid production experiments were carried out in T12 medium containing 7.5 g/L yeast extract, 7.5 g/L soytone, 7 g/L Na_2HPO_4, 3 g/L KH_2PO_4, 0.5 g/L NaCl, 3 g/L $(NH_4)_2SO_4$, 4 mM $MgSO_4$, and the indicated amount of glucose and/or starch plus amyloglucosidase (Sigma A7095).

For experiments in the BioLector (m2p labs, Baesweiler, Germany), starter cultures were incubated in culture tubes at 30° C overnight in T12 supplemented with 10 g/L glucose and diluted 1:100 into working cultures. Working cultures were incubated at 30° C, 1200 rpm, and 80% relative humidity in the BioLector. A working volume of 1 ml was used in the BioLector 48-well flower plate, and plates were sealed with gas-permeable sealing foil with evaporation reduction (m2p labs). To induce expression of enzymes required for glucaric acid production, 100 μM β-D-1-thiogalactopyranoside (IPTG) was added to

working cultures at inoculation. For induction of SspB in strain IB1486 to knock down Pfk activity, 100 ng/ml anhydrotetracycline (aTc) was added at the times indicated in the Results section. At the indicated time points, the contents of the sample well were removed for measurement of glucaric acid production and residual glucose levels.

For experiments in shake flasks, starter cultures were grown to mid-exponential phase (OD ~ 5) in flasks containing 30 ml T12 + 10 g/L glucose and used to inoculate 30 ml working cultures to a starting OD = 0.05. Working cultures were incubated in 250 ml baffled shake flasks at 30° C, 80% humidity, and 250 rpm. IPTG (100 μM) was added at inoculation and aTc (100 ng/ml) was added at the indicated time points. Flasks were sampled periodically for measurement of optical density, as well as for HPLC and biomass samples. Samples from all experiments were stored at -20° C until analysis.

3.2.3 Measurement of extracellular metabolites and starch

Glucose, glucaric acid, acetate, and *myo*-inositol levels were quantified by high performance liquid chromatography (HPLC) on an Agilent 1100 or 1200 series instrument (Santa Clara, CA) with an Aminex HPX-87H anion exchange column (300 mm by 7.8 mm; Bio-Rad Laboratories, Hercules, CA). Sulfuric acid (5 mM) at a flow rate of 0.6 mL/min was used as the mobile phase. Compounds were quantified from 10 μL sample injections using refractive index (glucose, *myo*-inositol, acetate, glucaric acid) and diode array detectors (glucaric acid, 210 nm). Column and refractive index detector temperatures were held at 65° C and 35° C respectively.

To quantify the amount of starch hydrolysis in fed-batch samples, samples were split at collection. Half of the sample was centrifuged at 15000 xg for 15 minutes and used for HPLC analysis as described above. The remaining portion of the sample was treated with 15 U/ml amyloglucosidase for 15 minutes at room temperature for full hydrolysis of remaining starch. After treatment, the sample was centrifuged for 5 minutes at 15000 xg and the glucose concentration was measured in the supernatant using a YSI 2900 Biochemistry Analyzer (YSI Life Sciences, Yellow Springs, OH). The difference between the glucose content measured in the fully hydrolyzed sample and the glucose content measured via HPLC in the sample without an additional hydrolysis step was used to calculate the content of unhydrolyzed starch.

The maximum amount of glucose that could be liberated from starch in the medium was determined by full hydrolysis of the starting medium with amyloglucosidase. To calculate glucose utilized by the cell, the amount of free glucose and the amount glucose generated from full hydrolysis of residual starch in a sample were subtracted from the maximum amount available in the medium. This value for consumed glucose was then used in the calculation of glucaric acid yield from glucose.

Table 3.1 | Strains and plasmids used in this study.

Strain / plasmid	Genotype	Reference / source
Strains		
LG1458	MG1655(DE3) *ΔgudD ΔuxaC*	Prather Lab
IB1863	MG1655 *ΔendA Δzwf ΔpfkB ΔsspB pfkA::114-pfkA(DAS+4) HK022::tetR-Ptet-sspB*	(Brockman and Prather, 2015)
IB1379	MG1655 *ΔendA Δzwf ΔpfkB*	(Brockman and Prather, 2015)
IB1486	MG1655(DE3) *ΔendA Δzwf ΔpfkB ΔsspB pfkA::114-pfkA(DAS+4) HK022::tetR-Ptet-sspB ΔgudD ΔuxaC*	This study
IB2255	MG1655(DE3) *ΔendA Δzwf ΔpfkB ΔpfkA ΔgudD ΔuxaC*	This study
JW2758-5	F-, *Δ(araD-araB)567, ΔlacZ4787*(::rrnB-3), *λ⁻, ΔgudD785::kan, rph-1, Δ(rhaD-rhaB)568, hsdR514*	(Baba et al., 2006)
JW3887-1	F-, *Δ(araD-araB)567, ΔlacZ4787*(::rrnB-3), *λ⁻, ΔpfkA775::kan, rph-1, Δ(rhaD-rhaB)568, hsdR514*	(Baba et al., 2006)
JW3603-2	F-, *Δ(araD-araB)567, ΔlacZ4787*(::rrnB-3), *λ⁻, ΔuxaC782::kan, rph-1, Δ(rhaD-rhaB)568, hsdR514*	(Baba et al., 2006)
IB1486-GA	IB1486 / pRSFD-IN-MI / pTrc-udh	This study
LG1458-GA	LG1458 / pRSFD-IN-MI / pTrc-udh	This study
IB2255-GA	IB2255 / pRSFD-IN-MI / pTrc-udh	This study
Plasmids		
pCP20	Rep^a, Amp^R, Cm^R, FLP recombinase expressed by $\lambda\ p_r$ under control of λ cI857	CGSC #7629
pRSFD-IN-MI	pRSR1030 *ori*, lacI, Kan^R, INO1 (*S. cerevisiae*) and MIOX (*M. musculus*) expressed under control of T7 promoter	(Moon et al., 2009)
pTrc-udh	pBR322 *ori*, lacI, Amp^R, Udh (*P. syringae*) expressed under control of Trc promoter	(Yoon et al., 2009)

3.2.4 Phosphofructokinase activity measurements

Phosphofructokinase activity assays were carried out as described in Chapter 2 (Brockman and Prather, 2015).

3.3 Results

Glucaric acid production was screened in strain IB1486-GA. This strain was derived from a previously developed strain, IB1863, where Pfk activity can be dynamically controlled through addition of aTc, which induces expression of an adaptor protein, SspB, that increases the rate of phosphofructokinase-I (Pfk-I) degradation to reduce activity (Brockman and Prather, 2015). IB1486 contains additional knockouts of *gudD* and *uxaC* to prevent glucaric acid catabolism, and also contains the DE3 lysogen for expression of T7 RNA polymerase. In previous work with IB1863, it was shown that dynamic knockdown of Pfk activity could result in increased production of the glucaric acid precursor *myo*-inositol in glucose minimal medium, but that correct timing of aTc addition was required to achieve maximum yields and titers. Very early switching to "production mode" by aTc addition may result in insufficient time for protein expression and formation of biomass to serve as biocatalyst. However, very late switching results in more utilization of glucose for growth, and less remaining glucose to be redirected into product formation.

In moving to glucaric acid production, screening for optimal aTc addition time was again required, due to changes in cellular growth rate from the burden of expression of the complete glucaric pathway and to the change in medium composition relative to the glucose minimal medium previously tested. The modified MOPS glucose minimal medium used for *myo*-inositol production in Chapter 2 was initially explored for glucaric acid production, but lag times of approximately 48 hours were observed, likely due to the burden associated with expression of all three pathway proteins. In addition to glucose, the new T12 medium used for testing of glucaric acid production contains yeast extract and soytone, which do provide supplemental carbon sources. While glucose would primarily be used as a feedstock for glucaric acid production, some additional carbon supplementation was desired in the medium to speed batch time and better represent a potential semi-defined scale up medium.

To facilitate rapid screening of a variety of aTc addition times in triplicate, cultures were grown in 48-well flower plates in a BioLector microbioreactor system. Glucaric acid production was screened in T12 medium in both batch conditions (15 g/L glucose at inoculation) and simulated fed batch conditions, where 3-5 g/L glucose was added at inoculation, and additional glucose was released slowly from 10 – 12 g/L starch solution by addition of amyloglucosidase.

3.3.1 Screening batch conditions for timing of Pfk knockdown

For screening of IB1486-GA under batch conditions, working cultures consisted of T12 medium with 15 g/L glucose and with 100 µM IPTG added at inoculation for induction of the glucaric acid pathway enzymes. Additions of aTc were made at times varying from 0 – 30 hours after inoculation. Fig. 3.1 illustrates the yields and titers of glucaric acid observed after 48 hours.
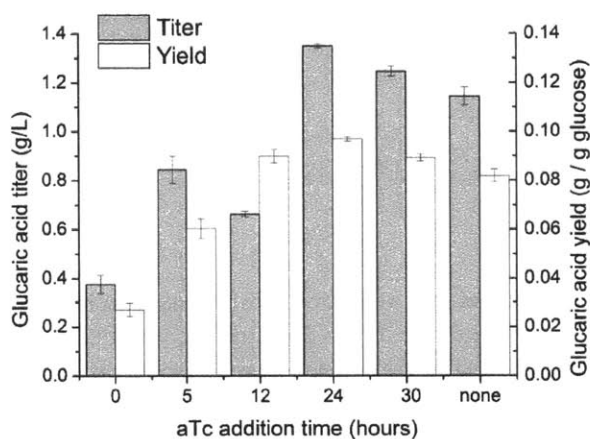
Fig. 3.1 | Yields (white bars) and titers (gray bars) of glucaric acid as a function of aTc addition time. Glucaric acid production was measured at 48 hours in T12 medium supplemented with 15 g/L glucose. Error bars represent triplicate mean ± SD.

Glucose was fully consumed in all cultures at 48 hours, except the culture with aTc addition at 12 hours. The highest titers of glucaric acid, 1.35 g/L, were achieved with aTc addition at 24 hours, representing an 18% improvement over the case of no Pfk switching. As expected, later switching after 24 hours resulted in somewhat lower titers, as more glucose had already been consumed for biomass and could not be redirected into glucaric acid production. Earlier switching resulted in lower titers either due to incomplete consumption of glucose, as in the case of 12 hour aTc addition, or due to an "escape" phenotype. The escape phenotype correlates with rapid growth to higher cell densities (Fig. 3.2A) and an increase in Pfk activity (Fig. 3.2B). Studies of the system based on IB1863 have indicated that this is due to a combination of inactivation of expression of the SspB protein required for degradation of Pfk-I through mutation or mobile element insertion and loss of plasmids containing pathway genes (Chapter 2). Very early addition of aTc results in high stress on the cell from a combination of limited glucose uptake and high protein expression for the glucaric acid pathway enzymes, which may result in more rapid selection for the escape phenotype.
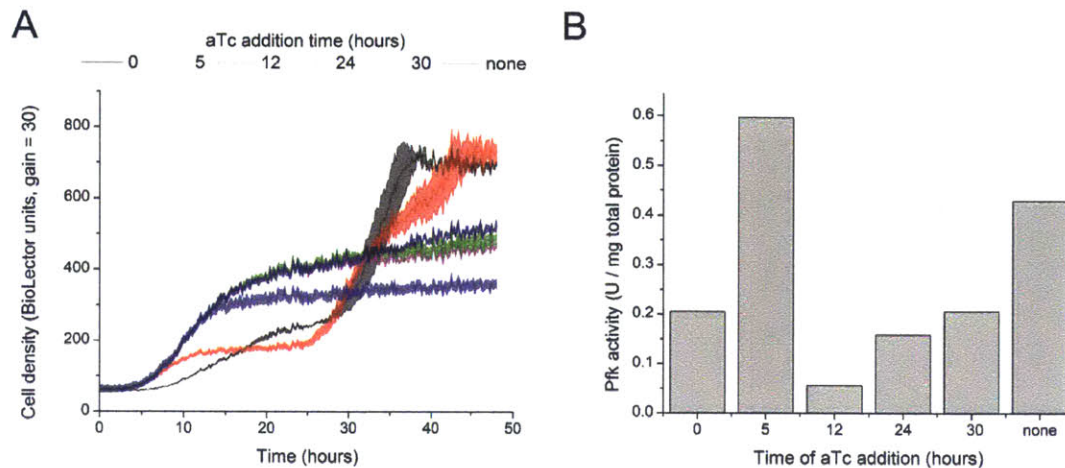
Fig. 3.2 | Growth profiles and Pfk activity at 48 hours for IB1486-GA in T12 + 15 g/L glucose.
(A) Growth of IB1486-GA with aTc addition at the times notes. Error bars represent triplicate mean ±
SD. (B) Pfk activity measured in selected wells from screening plate at 48 hours.

3.3.2 Screening fed-batch conditions for timing of Pfk knockdown

Fed batch conditions were initially screened in T12 medium with 3 g/L free glucose and 12 g/L starch,
with 100 μM IPTG added at inoculation for induction of the glucaric acid pathway enzymes. Feeding was
started at 12 hours by addition of 0.006 U/ml amyloglucosidase. As the starch hydrolysis rate declines
with time, secondary additions of 0.006 U/ml and 0.012 U/ml amyloglucosidase were carried out at 36
and 48 hours, giving the glucose release profile shown in Fig. 3.3. At the conclusion of the experiment,
in addition to the initial 3 g/L glucose, another 9.7 ± 0.7 g/L free glucose had been released in the
cultures on average. (For calculation of yield, unhydrolyzed starch was measured in individual wells via
the method outlined in Section 3.2.3).

In this system, maximum titers of 1.56 g/L could be achieved with aTc addition at either 24 or 32 hours
(Fig. 3.4A), a 42% improvement over no aTc addition. This improvement was larger than the batch
condition, likely due to differences in the amount of glucose still available for consumption after
addition of aTc. Early aTc addition at 12 hours did not result in improved titers, with the shape of the
growth curve indicative of escape (Fig. 3.4B). Measurement of Pfk activity also showed activity recovery
to levels at or above the case of no aTc addition.
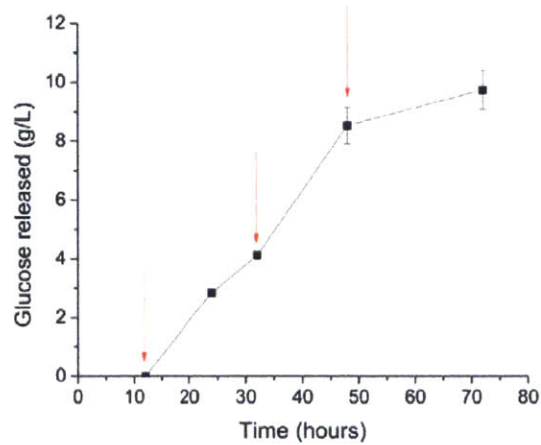
Fig. 3.3 | Glucose release via starch hydrolysis in T12 medium.
Amyloglucosidase additions are indicated by red arrows. Amyloglucosidase additions are indicated by red arrows: 0.006 U/ml at 12 and 36 hours, 0.012 U/ml at 48 hours.
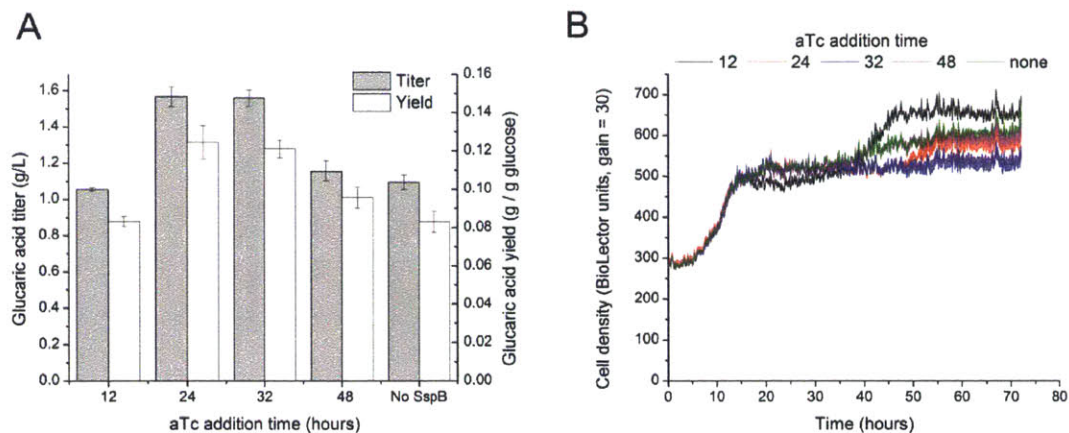
Fig. 3.4 | Growth and GA production in IB1486-GA in T12 + 3 g/L glucose + 12 g/L starch.
(A) Titers and yields of GA at 72 hours for aTc addition times from 12 – 48 hours. (B) Growth of IB1486-GA in T12 + 3 g/L glucose + 12 g/L starch. Starch addition resulted in higher opacity of medium at start of fermentation. Error bars represent triplicate mean ± SD.

3.3.3 Validation of fed-batch results under altered feeding conditions

Consistent improvements in glucaric acid titers could be observed by timed knockdown of Pfk activity under the conditions tested. To determine whether these improvements would be robust to moderate changes in culture conditions, a set of experiments was carried out under altered feeding conditions in the BioLector and also in shake flasks.

63

As the highest titers were achieved previously with Pfk knockdown at 24-32 hours, it would be expected that growth up to that point could be carried out under either batch or fed-batch conditions without significant changes to the outcomes. An alternative feeding strategy was tested with the initial free glucose increased to 5 g/L and feeding started at 24 hours, from a reservoir of 10 g/L starch. This was initially tested in 48 well plates in the BioLector microbioreactor, with amylase additions of 0.006 U/ml at 24 hours and 48 hours. The highest titers of 1.17 g/L were achieved with aTc addition at 36 hours, a 27% improvement over no aTc addition (Fig 3.5). Although titers were lower than in the original fed-batch screening, maximum yields were similar, as unhydrolyzed starch contents were higher under this feeding strategy, leaving only 9.7 g/L free glucose (initial dose and feeding) available for conversion to glucaric acid, versus 12.7 g/L in the previous test.
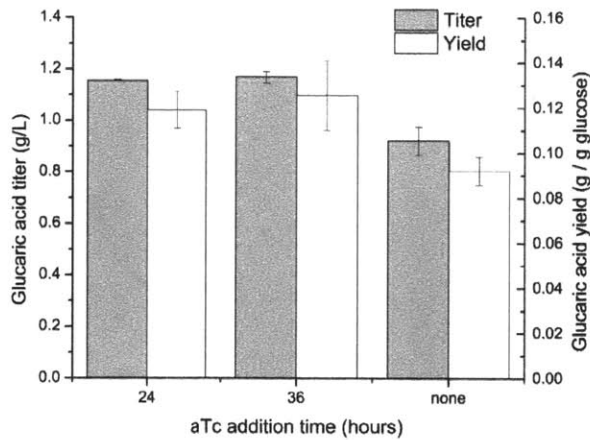
Fig. 3.5 | Titers and yields of glucaric acid at 72 hours for IB1486-GA in T12 + 5 g/L glucose + 10 g/L starch.
Amylase additions were carried out at 24 and 48 hours. Error bars represent triplicate mean ± SD.

The starch fed-batch strategy was also tested in shake flasks, both for IB1486-GA and for LG1458-GA, a wild-type MG1655 background with only *gudD* and *uxaC* knockouts. The cultures contained 5 g/L free glucose and 10 g/L starch. Free glucose was measured at 18 hours, and since glucose was already found to be exhausted, amylase addition was started at that time. Secondary additions were carried out at 40 and 48 hours. Despite the extra amylase addition, starch hydrolysis was again poorer in this condition, and resulted in 10.1 ± 0.5 g/L total free glucose available in the cultures on average. Baseline yields for IB1486-GA were still comparable with the previous tests and were similar to LG1458-GA. Addition of

aTc for Pfk knockdown at 24 hours resulted in a 28% improvement in titers over no aTc addition, although variability was higher in shake flasks than in previous testing in the BioLector (Fig. 3.6).
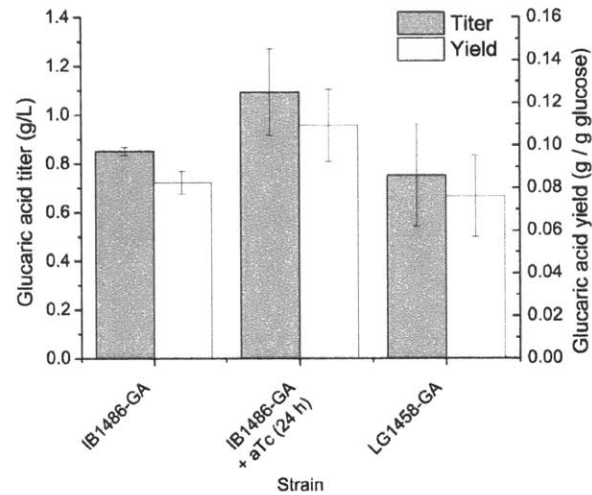
Fig. 3.6 | Yields and titers of glucaric acid in IB1486-GA and LB1458-GA in shake flasks with T12 + 5 g/L glucose + 10 g/L starch.
Amylase additions were carried out at 18, 40, and 48 hours. Error bars represent triplicate mean ± SD.

Growth (Fig. 3.7A) and activity measurements (Fig. 3.7B) showed trends similar to previous tests. However, activity comparison with the wild type LG1458-GA at 48 hours shows that IB1486-GA has significantly lower baseline activity than LG1458-GA before aTc addition, with aTc addition resulting in an additional decrease in activity of about 50%. The low baseline activity of IB1486-GA in T12 medium was unexpected, given that the parent strain, IB1863, always showed Pfk activity higher than the wild type in MOPS minimal medium with glucose (Chapter 2). While the mismatch in baseline activity did not cause a significant difference in titers between IB1486-GA and LG1458-GA under fed-batch conditions, this did affect batch performance strongly, as discussed in Section 3.3.4.
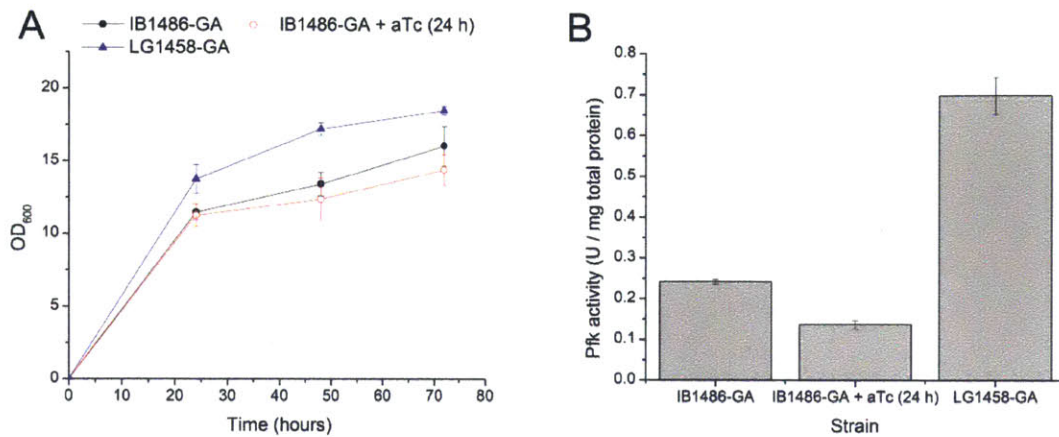
Fig. 3.7 | Growth and Pfk activity in IB1486-GA and LG1458-GA in T12 + 5 g/L glucose + 10 g/L starch with amylase addition at 18, 40, and 48 hours.
(A) Growth of LG1458-GA and IB1486-GA with and without aTc addition at 24 hours after inoculation.
(B) Pfk activity in these strains at 48 hours after inoculation. Error bars represent triplicate mean ± SD.

3.3.4 Shake flasks studies under batch conditions

Glucaric acid production was also tested in shake flasks under batch conditions. In shake flasks, batch testing resulted in high baseline variability in titers that made it difficult to validate improvements in the 20-40% range. However, the shake flask testing did provide some interesting insights into the metabolism of IB1486-GA versus the wild-type strain LG1458-GA. Significantly, under batch production conditions, acetate production varied greatly between the two strains, with LG1458-GA producing much higher levels of acetate. The fill volume of flasks in batch testing appeared to have an effect on acetate production IB1486-GA, potentially due to changes in aeration. In IB1486-GA, several cultures showed significant residual acetate at 48 hours in shake flasks with a 45 ml fill volume, while in previous testing in the BioLector, no acetate was observed at 48 hours. Testing at a lower fill volume (30 ml) resulted in reduced acetate accumulation at both 24 and 48 hours. A summary of observed acetate production in IB1486-GA and LG1458-GA in shake flasks is presented in Fig. 3.8A. Pfk activity measurements at 24 hours in IB1486-GA and IB1458-GA (Fig. 3.8B) showed that, as in the fed-batch case, Pfk activity in LG1458-GA was significantly higher, likely leading to metabolic overflow and acetate production.
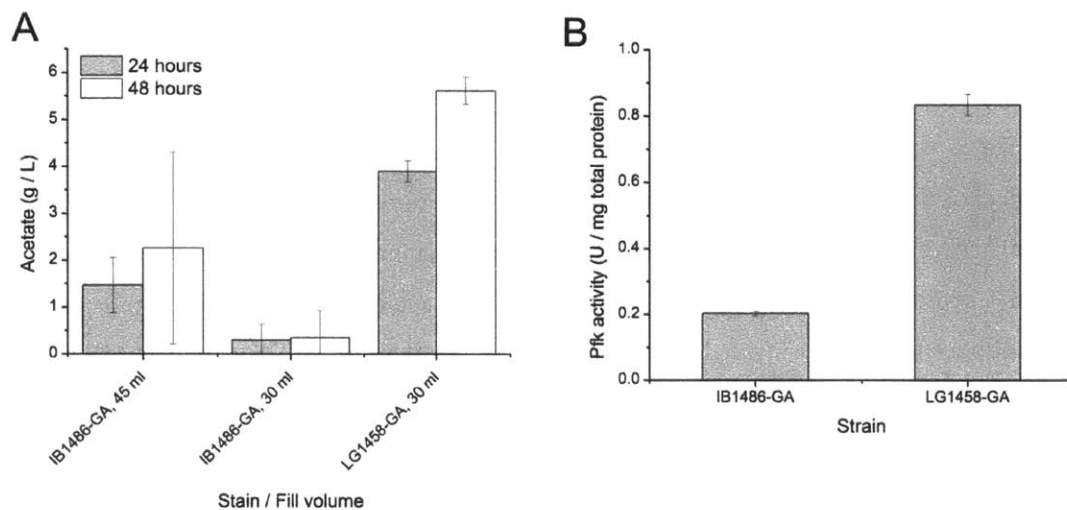
Fig. 3.8 | Acetate production and Pfk activity in IB1486-GA and LG1458-GA in T12 + 15 g/L glucose.
(A) Acetate production at 24 and 48 hours in IB1486-GA and LG1458-GA in T12 + 15 g/L glucose.
Cultures were carried out in 250 ml baffled shake flasks with the fill volume noted and 250 rpm shaking
at 30° C and 80% relative humidity. (B) Pfk activity at 24 hours after inoculation in T12 + 15 g/L glucose
with 30 ml fill volume in 250 ml flasks. Error bars represent triplicate mean ± SD.

Glucaric acid production was also very poor for LG1458-GA under batch conditions, with titers below the
limit of detection in T12 + 15 g/L glucose (30 ml fill volume). LG1458-GA showed incomplete glucose
consumption as well, with 3.0 ± 0.1 g/L remaining at 48 hours. Although titers in IB1486-GA showed
high variability, glucaric acid production was clear in all samples in T12 + 15 g/L glucose, with measured
titers of 0.9 ± 0.3 g/L glucaric acid in shakes flasks with 30 ml fill volume. Glucose was also completely
consumed in the cultures.

In contrast to the batch condition, under the starch hydrolysis (glucose feeding) condition, titers in
LG1458-GA were comparable to IB1468-GA and any acetate produced was fully consumed by the
conclusion of the experiment. One of the clear advantages of fed-batch condition is the elimination of
acetate buildup and carbon loss to acetate formation. Additional changes in metabolism, such as
upregulation of genes associated with sugar transport (Franchini and Egli, 2006; Raman et al., 2005),
could also be changing relative metabolite pools favorably. While a fed-batch production strategy
provides a significant benefit for LG1458-GA, IB1468-GA does not benefit as strongly from slow glucose
feeding, likely due to the fact that acetate production is already much lower in this strain. Pfk activity

may also be low enough in this strain that other changes in metabolism related to glucose limitation are not significant.

Although a static condition of low Pfk activity can clearly be tolerated in T12 medium and can provide a benefit in glucaric acid production under batch conditions, the previous screening work in Section 3.1 indicated that there is a limit to what could be gained in this manner, as further knockdown of Pfk activity by aTc addition at inoculation resulted in poor growth and eventual "escape" of the culture. A *pfkA pfkB* double knockout strain, IB2255, was tested to assess the productivity that could be expected in T12 medium under batch conditions with no Pfk activity. After 48 hours in T12 with 15 g/L glucose, 0.18 ± 0.01 g/L was produced, significantly lower than the amounts produced in IB1486-GA. To maximize productivity in a 48 hour batch, at least some time needs to be spent with higher Pfk activity in the culture.

3.4 Discussion

Results with IB1486-GA indicate that dynamic control of Pfk activity can be utilized to improve titers of glucaric acid, a product requiring several enzymatic conversions from G6P. The system was applicable for use with a semi-defined medium under both batch and simulated fed-batch conditions. While gains in titer were consistent across multiple conditions, the maximum gains were smaller than those observed previously for *myo*-inositol production in glucose minimal medium (Brockman and Prather, 2015). Previous work with *myo*-inositol production in glucose minimal medium showed that switching at low cell density was optimal for the largest gains in titer. In T12 medium, these earlier switching times resulted in more rapid escape and little time for conversion of glucose to glucaric acid, perhaps due to the greater expression burden of the complete glucaric acid pathway and the higher availability of nutrients in T12 that "escapers" could use to rapidly grow and overtake the population. The later switching times result in higher usage of glucose for biomass formation, so the amount of glucose processed after switching to production mode is relatively low. While genetic stability can be achieved out to at least 72 hours for aTc addition at 24 hours, future work may be needed to address genetic stability in longer fermentations and expand the usefulness of switching between growth and production modes.

Activity of the downstream enzymes in the glucaric acid pathway is another potential limitation, but in this particular medium, it does not appear that the activity of MIOX, a bottleneck under some other conditions, was limiting overall pathway yield, as minimal buildup of myo-inositol was observed in the cultures. However, balancing of expression between the three pathway enzymes could be an issue, since high level INO1 expression is required for any myo-inositol to be produced for further conversion (Moon et al., 2009). Reductions in INO1 expression upon expression of other enzymes in the glucaric acid pathway would be expected to limit maximum fluxes into the pathway, also limiting the glucose that could be effectively redirected in a given time period.

Importantly, IB1486-GA showed titers that were comparable with a wild-type control strain under fed-batch conditions and superior under batch conditions, indicating the genetic modifications required for control of Pfk activity were not detrimental to baseline GA production and could potentially be transferred into high-performing strains as well. Although the baseline Pfk activity was low in T12 medium, it was still sufficient for rapid growth without excessive overflow metabolism. More consistent success with chromosomal modifications in the K strains led to the initial construction of the Pfk-I control system in that background, but additional improvements in glucaric acid titer, both with and without Pfk knockdown, can likely be achieved by transferring the genetic modifications of IB1486 to an E. coli B strain. In previous work, wild-type BL21 has outperformed MG1655 containing the same pathway genes (Moon et al., 2009; Raman et al., 2014; Shiue et al., 2015).

3.5 Conclusions

GA titers and yields could be improved under multiple culture conditions through timed knockdown of Pfk activity, with maximum improvements of up to 42% observed. In the absence of aTc, the switchable strain IB1486 shows titers comparable to or above those observed with wild-type MG1655, indicating the genetic modifications in IB1486 do not result in degradation of baseline performance and could potentially be applied to high-performing strains for increases in titer. Optimization of strain background and pathway enzyme expression levels may lead to both higher baseline titers and to greater gains from dynamic control of Pfk activity.

Chapter 4: Cell-density based autonomous control of Pfk-I expression

Abstract

Dynamic control of native enzymes in cellular metabolism offers opportunities to better balance growth and small-molecule production, as well as to avoid buildup of intermediates. Currently, most dynamic systems rely on addition of an inducer to the culture medium in order to trigger alterations in enzyme level. Quorum sensing and nutrient-starvation systems have been successfully applied to autonomously trigger heterologous protein expression or control cell population dynamics, but applications in controlling metabolic fluxes have not been extensively developed. This work demonstrates that systems based on both nutrient starvation (phosphate starvation) and quorum sensing (*esa* system) can be used in *E. coli* to control expression levels of phosphofructokinase-I, a key enzyme in glycolysis. In these modified cells, Pfk activity drops and growth is automatically arrested upon reaching a critical cell density, without any addition of inducer. It was further demonstrated that yields and titers of a heterologous product, *myo*-inositol, could be improved through use of this system, without requiring any outside intervention during the course of the fermentation.

4.1 Introduction

Balancing native metabolism with newly introduced or overexpressed small-molecule production pathways is a significant challenge in the development of new bioprocesses. Improved steady-state flux distributions can be generated through combinatorial promoter replacement and gene knockouts (Santos and Stephanopoulos, 2008), but when the pathway of interest is in direct competition with growth, this may result in reductions in growth rate that ultimately limit productivity. In these cases, a dynamic strategy of switching between a growth mode with high biomass formation and a production mode with greater flux into product formation would be expected to maximize productivity in a fixed batch time (Anesiadis et al., 2008; Anesiadis et al., 2013; Gadkar et al., 2005). A number of recent studies have focused on experimental implementation of such systems in *E. coli* (Brockman and Prather, 2015; Solomon et al., 2012b; Soma et al., 2014; Torella et al., 2013). This strategy has proved especially successful for cases where the knockout or downregulation of the target enzyme would normally result in significant detrimental effects on growth.

With a similar motivation, our group has recently developed a system for dynamic control of phosphofructokinase-I (Pfk-I) levels in the cell, which can be used to increase yields and titers of products derived from glucose-6-phosphate (G6P) (Brockman and Prather, 2015). However, as in the case of the other studies mentioned, to achieve the maximum gain in product titers, a small molecule inducer had to be added to the cultures at a predetermined time during the fermentation. Typically, this time would represent an optimal tradeoff between carbon utilization for formation of biomass and carbon utilization to form product (Gadkar et al., 2005). As a result, rather than manually monitoring biomass and adding inducer, it should be possible to develop an automated trigger in the cell, where switching naturally occurs after formation of a target amount of biomass.

A number of systems based on nutrient starvation promoters such as *phoA* and *trp* have been used for applications requiring cell density-dependent or delayed protein expression in *E. coli* (Laird et al., 2005; Swartz, 2001; Yoon et al., 1996). In *Saccharomyces cerevisiae*, the *HXT1*, *HXT2*, and *GAL1/GAL10* promoters have been successfully used to link control of gene expression to glucose concentrations in the medium (Scalcinati et al., 2012; Xie et al., 2015). Limitation in a key nutrient can alter fluxes and inherently limit the amount of biomass that can be formed, and this strategy is often used for maximization of product titers in the absence of any additional starvation-based protein expression strategy (Johansson et al., 2005; Youngquist et al., 2013; Zhu et al., 2008). However, nutrient starvation

also induces a wide variety of regulatory responses in the cell, some of which may be undesirable for product formation. Linking nutrient starvation with a specific, desired outcome could provide a route to enhance positive effects on production and limit negative effects in the cell, but it may still be difficult to achieve general applicability.

As an alternative, quorum sensing (QS) systems are a well-known mechanism for carrying out cell-density dependent processes, and have been used synthetically for applications such as timed induction of recombinant proteins (Tsao et al., 2010), timed lysis (Saeidi et al., 2011), and balancing of different cell populations (Balagadde et al., 2008). The *esa* quorum sensing system from *Pantoea stewartii* offers an especially appealing platform for fine-tuning cell-density dependent gene expression, given previous work on identifying and engineering components of this QS system. Interestingly, two promoters with opposite responses to binding by the quorum sensing transcription factor EsaR are known. EsaR binds DNA in the absence of its cognate autoinducer, 3-oxohexanoyl-homoserine-lactone (3OC6HSL) (Minogue et al., 2002). The P_{esaS} promoter is activated by EsaR binding (Schu et al., 2009), while the P_{esaR} promoter is repressed by EsaR binding (Minogue et al., 2002). Additionally, a number of variants of the EsaR transcription factor have been developed by directed evolution, which show varying levels of binding affinity to 3OC6HSL (Shong et al., 2013), providing a secondary method to tune timing of promoter derepression or deactiviation, beyond only control of 3OC6HSL synthase (EsaI) expression level.

Utilizing components of the *esa* quorum sensing system, we have been able to develop a new autonomous system for control of Pfk-I levels. Uniquely, this system requires no outside intervention, but rather relies on the cells themselves for synthesis of the autoinducer 3OC6HSL, with Pfk activity knockdown and growth arrest occurring naturally when the threshold level of 3OC6HSL is reached. We have developed a series of host strains with varying levels of 3OC6HSL synthase expression, allowing a host strain to be selected with a desired time of Pfk-I switching. Utilizing this system for the previously tested application of *myo*-inositol production, an increase in titers of 30% over a host strain with a native *pfkA* promoter was achieved on glucose as a sole carbon source.

4.2 Materials and methods

4.2.1 Strains and plasmids

E. coli strains and plasmids used in this study are listed in Table 4.1. *E. coli* strain DH10B was used for molecular cloning and plasmid preparation. Strains IB531 and IB1643 were described in Chapter 2 (Brockman and Prather, 2015). Strain IB1624 was constructed using the previously described method for construction of IB1643. The *pfkA* cassette used for replacement of the native locus was identical to that used in IB1643, except that the constitutive promoter used to drive *pfkA* expression in IB1643 (apFAB114) was replaced with a different promoter from the BIOFAB library, apFAB104, which has a higher promoter strength (BIOFAB, 2012).

Table 4.1 | Strains and plasmids used in this study.

Strain / plasmid	Genotype	Reference/source
DH10B	F⁻ *mcrA Δ(mrr-hsdRMS-mcrBC) φ80lacZΔM15 ΔlacX74 recA1 endA1 araD139 Δ(ara, leu)7697 galU galK λ-rpsL nupG*	Life Technologies (Carlsbad, CA)
MG1655 parent strains		
IB531	MG1655 *ΔendA*	Prather Lab
IB1379	MG1655 *ΔendA Δzwf ΔpfkB*	(Brockman and Prather, 2015)
Biofab promoter replacments for pfkA		
IB1643	MG1655 *ΔendA Δzwf ΔpfkB ΔsspB pfkA::114-pfkA(DAS+4)*	(Brockman and Prather, 2015)
IB1624	MG1655 *ΔendA Δzwf ΔpfkB ΔsspB pfkA::104-pfkA(DAS+4)*	This study
P_tet-sspB integration		
IB1863	MG1655 *ΔendA Δzwf ΔpfkB ΔsspB pfkA::114-pfkA(DAS+4) HK022::TetR-P_LtetO-sspB*	(Brockman and Prather, 2015)
P_phoA-sspB integrations		
IB643	MG1655 *ΔendA Δzwf ΔpfkB ΔsspB pfkA::114-pfkA(DAS+4) HK022::P_phoA-sspB*	This study
IB1509	MG1655 *ΔendA Δzwf ΔpfkB ΔsspB pfkA::104-pfkA(DAS+4) HK022::P_phoA-sspB*	This study
P_BAD-sspB integrations		
IB1449	MG1655 *ΔendA Δzwf ΔpfkB ΔsspB pfkA::114-pfkA(DAS+4) HK022::AraC-P_BAD-sspB*	This study
IB1448	MG1655 *ΔendA Δzwf ΔpfkB ΔsspB pfkA::104-pfkA(DAS+4) HK022::AraC-P_BAD-sspB*	This study
P_esaR-sspB integreations and RBS tuning		
IB2265	MG1655 *ΔendA Δzwf ΔpfkB ΔsspB pfkA::114-pfkA(DAS+4)HK022::EsaR-P_EsaR-sspB*	This study
IB2250	MG1655 *ΔendA Δzwf ΔpfkB ΔsspB pfkA::104-pfkA(DAS+4)HK022::EsaR-P_EsaR-sspB*	This study
AG2349	MG1655 *ΔendA Δzwf ΔpfkB ΔsspB pfkA::114pfkA(DAS+4) HK022::EsaR-P_EsaR-RBS157-sspB*	This study
AG2350	MG1655 *ΔendA Δzwf ΔpfkB ΔsspB pfkA::114pfkA(DAS+4)*	This study

	HK022::EsaR-P$_{EsaR}$-RBS422-sspB	
AG2349+L25	MG1655 ΔendA Δzwf ΔpfkB ΔsspB pfkA::114pfkA(DAS+4) HK022::EsaR-P$_{EsaR}$-RBS157-sspB 186::L25-EsaI	This study
AG2349+L31	MG1655 ΔendA Δzwf ΔpfkB ΔsspB pfkA::114pfkA(DAS+4) HK022::EsaR-P$_{EsaR}$-RBS157-sspB 186::L31-EsaI	This study

P$_{esaS}$-pfkA promoter replacements and RBS tuning

IB1897	MG1655 ΔendA Δzwf ΔpfkB pfkA::P$_{EsaS}$-pfkA(DAS+4)	This study
IB1898	MG1655 ΔendA Δzwf ΔpfkB pfkA::P$_{EsaS}$-pfkA(LAA)	This study
IB646	MG1655 ΔendA Δzwf ΔpfkB pfkA::P$_{EsaS}$-pfkA(DAS+4) HK022::104-EsaR	This study
IB2275	MG1655 ΔendA Δzwf ΔpfkB pfkA::P$_{EsaS}$-pfkA(LAA) HK022::104-EsaRI170V	This study
IB2351	MG1655 ΔendA Δzwf ΔpfkB pfkA::P$_{EsaS}$-RBS1087-pfkA(LAA) HK022::104-EsaRI170V	This study
IB2352	MG1655 ΔendA Δzwf ΔpfkB pfkA::P$_{EsaS}$-RBS468-pfkA(LAA) HK022::104-EsaRI170V	This study
IB2353	MG1655 ΔendA Δzwf ΔpfkB pfkA::P$_{EsaS}$-RBS3096-pfkA(LAA) HK022::104-EsaRI170V	This study
IB646+L18	MG1655 ΔendA Δzwf ΔpfkB pfkA::P$_{EsaS}$-pfkA(DAS+4) HK022::104-EsaR 186::L18-EsaI	This study
IB646+L19	MG1655 ΔendA Δzwf ΔpfkB pfkA::P$_{EsaS}$-pfkA(DAS+4) HK022::104-EsaR 186::L19-EsaI	This study
IB646+L25	MG1655 ΔendA Δzwf ΔpfkB pfkA::P$_{EsaS}$-pfkA(DAS+4) HK022::104-EsaR 186::L25-EsaI	This study
IB646+L31	MG1655 ΔendA Δzwf ΔpfkB pfkA::P$_{EsaS}$-pfkA(DAS+4) HK022::104-EsaR 186::L31-EsaI	This study
IB2275+L18	MG1655 ΔendA Δzwf ΔpfkB pfkA::P$_{EsaS}$-pfkA(LAA) HK022::104-EsaRI170V 186::L18-EsaI	This study
IB2275+L19	MG1655 ΔendA Δzwf ΔpfkB pfkA::P$_{EsaS}$-pfkA(LAA) HK022::104-EsaRI170V 186::L19-EsaI	This study

Strains transformed with pTrc-INO1 are denoted by -I

Plasmids

pAC-EsaR	pACYC184 with *lac* promoter, *esaR* gene, and transcriptional terminator	(Shong et al., 2013)
pBAD30	p15A, Amp^R, *araC*, P$_{BAD}$	(Guzman et al., 1995)
pBAD-SspB	p15A, Amp^R, *araC*, P$_{BAD}$-RBS B0034-sspB	This study
pCas9-CR4	P$_{tet}$- Cas9 (S. pyogenes), Spec^R	(Reisch and Prather, in preparation)
pCP20	Rep^a, Amp^R, Cm^R, FLP recombinase expressed by λ p$_r$ under control of λ cI857	CGSC #7629
pCS-P$_{EsaR}$-lux	pCS26 with P$_{esaR}$ promoter controlling expression of luxCDABE	(Shong et al., 2013)
pCS-P$_{EsaS}$-lux	pCS26 with P$_{esaS}$ promoter controlling expression of luxCDABE	(Shong et al., 2013)
pE-FLP	oriR101, repA101ts, Amp^R, FLP recombinase expressed by pE	(St-Pierre et al., 2013), Addgene Plasmid #45978
pKD-sgRNA-pfkARBS	oriR101, repA101ts, Amp^R, araC, araBp-λ$_γ$-λ$_β$-λ$_{exo}$, sgRNA targeting *pfkA*	(Reisch and Prather, in preparation)
pKD-sgRNA-sspBRBS	oriR101, repA101ts, Amp^R, araC, araBp-λ$_γ$-λ$_β$-λ$_{exo}$, sgRNA targeting RBS for *sspB*	
pKVS45	p15A, Amp^R, *tetR*, P$_{Tet}$	(Solomon et al., 2012b)
pKVS-B0034-EsaI	pKVS45 with RBS B0034-EsaI	This study

74

pMMB206	IncQ, Cm^R, *lacI*, P_{tac}	(Morales et al., 1991)
pMMB-B0034-EsaI	pMMB206 with RBS B0034-EsaI	This study
pOSIP-CH	pUC *ori*, RK6γ *ori*, Cm^R, *attP* HK022, ccdB, HK022 integrase expressed by λ p_r under control of λ cI857	(St-Pierre et al., 2013), Addgene Plasmid #45980
pSB3K3	p15A, Kan^R	(Shetty et al., 2008)
pSB3K3-EsaR-P_{EsaR}-SspB	pSB3K3 with $P_{BIOFAB104}$-*esaR*, P_{esaR}-*sspB*	This study
pTrc-INO1	pTrc99A with *S. cerevisiae* INO1 inserted at the EcoRI and HindIII sites	(Moon et al., 2009)
pTKIP-neo	ColE1(pBR322) *ori*, Amp^R, Kan^R	(Kuhlman and Cox, 2010)
pTKS/CS	p15A, Cm^R, P_{lacIq} *tetA*	(Kuhlman and Cox, 2010)
pTKRED	*ori*R101, *repA*101ts, $Spec^R$, *araC*, P_{lac} $λ_γ$ $λ_β$ $λ_{exo}$ *lacI*, P_{araB} I-SceI	(Kuhlman and Cox, 2010)
pTKIP-P_{EsaS}-PfkA(DAS+4)	pTKIP-neo with P_{EsaS}-*pfkA(DAS+4)*	This study
pTKIP-P_{EsaS}-PfkA(LAA)	pTKIP-neo with P_{EsaS}-*pfkA(LAA)*	This study

4.2.2 Construction of P_{phoA}, P_{BAD}, and P_{EsaR}-based SspB expression cassettes

For construction of the P_{phoA}-sspB expression cassette, the *phoA* promoter and a synthetic 5′ UTR were appended to *sspB* using an extended 5′ overhang on the PCR primer for amplification of the *sspB* sequence from the *E. coli* genome. The AraC-P_{BAD}-sspB cassette was generated by cloning of the *sspB* sequence, preceded by RBS B0034 (http://partsregistry.org), into pBAD30 between the EcoRI and BamHI restriction sites, followed by amplification of the entire arabinose-inducible expression cassette by PCR. The EsaR-P_{EsaR}-sspB cassette was originally constructed using overlap extension PCR and cloned into the plasmid pSB3K3 to yield pSB3K3-EsaR-P_{esaR}-sspB. The EsaR coding sequence was amplified from pAC-EsaR (Shong et al., 2013) and the constitutive promoter apFAB104 was appended to drive EsaR expression. The P_{EsaR} sequence was amplified from pCS-P_{esaR}-lux (Shong et al., 2013). The entire EsaR-P_{EsaR}-SspB expression cassette was then PCR amplified from pSB3K3-EsaR-P_{esaR}-sspB for use in integration steps. Restriction sites were also appended as needed during PCR amplification of all cassettes to allow for ligation into the integration vector. Integration of the SspB expression cassettes into the genome was carried out via "clonetegration" (St-Pierre et al., 2013). The pOSIP-CH backbone and the desired SspB expression cassettes were digested with KpnI and PstI and ligated overnight. The ligation product was used to transform strains IB1624 and IB1643 for integration at the HK022 locus. The phage integration genes and antibiotic resistance cassette were cured with pE-FLP, yielding the corresponding strains listed in Table 4.1.

4.2.3 Construction of RBS library for P_{esaR}-SspB

To adjust the expression level of SspB from the P_{esaR} promoter and reduce leaky expression, an RBS library was constructed using strain IB2265 as a basis. The original 5' UTR consisted of the following sequence: "caattcattaaagaggagaaaggatcc". The start of the SspB coding sequence contains a protospacer adjacent motif (PAM, underlined) "atggattgt", allowing a Cas9-based targeting method to be used for construction of the RBS library (Reisch and Prather, in preparation). Briefly, the sgRNA targeting the 20 bp upstream from the PAM, which included the RBS sequence, was inserted into plasmid pKD-sgRNA-sspBRBS via circular polymerase extension cloning. Strain IB2265 was transformed with this plasmid, along with plasmid pCas9-CR4 for inducible expression of Cas9. An 80 bp oligonucleotide with two degenerate nucleotides in the RBS and an additional degenerate nucleotide adjacent to the PAM was then transformed into the strain, and cell survival after Cas9 cleavage of the genome was used to select for cells that integrated the genomic changes encoded in the oligonucleotide. Surviving colonies were screened for growth on glucose minimal medium, and several were isolated with restored growth. Among the successful colonies tested, two were saved for further characterization and testing. The first contained 5' UTR sequence "caattcattaaagagctgaaaggatca" (base changes underlined) and was designated AG2349. The second contained the 5' UTR sequence "caattcattaaagagtcgaaaggatca" (base changes underlined) and was designated AG2350.

4.2.4 Construction of P_{esaS}-pfkA variants

The replacement of the native pfkA locus with P_{EsaS}-pfkA(degradation tagged) was carried out via a "landing pad" method (Kuhlman and Cox, 2010). Overlap extension PCR was used to append the P_{EsaS} promoter, amplified from pCS-P_{EsaS}-lux, to the 5' UTR from the BIOFAB library and the pfkA coding sequence. Either the native SsrA tag (AADENYALAA, "LAA") or a modified version (AADENYSENYADAS, "DAS+4") was also appended to the pfkA coding sequence using primer overhangs. The products were cloned into the vector pTKIP-neo by restriction digest with HindIII and KpnI, yielding pTKIP-P_{esaS}-pfkA(LAA) and pTKIP-P_{esaS}-pfkA(DAS+4). Lambda-red mediated recombination was used to introduce the tetracycline resistance marker and "landing pad" sequences amplified from pTKS/CS into the genome at the pfkA locus. The resultant strain was then transformed with pTKRED and either pTKIP-P_{esaS}-pfkA(LAA) and pTKIP-P_{esaS}-pfkA(DAS+4). Integration of the construct from the pTKIP plasmid into the genome was achieved as described previously (Kuhlman and Cox, 2010). The kanamycin resistance cassette remaining after integration was cured by expression of FLP recombinase from pCP20 to yield strains IB1897 and IB898. For activation of the P_{EsaS} promoter, EsaR is required. A cassette containing the

apFAB104 promoter driving expression of EsaR was integrated into the genome using the "clonetegration" method described in Section 4.2.2. Additionally, an alternative expression cassette with previously described EsaR variant, EsaRI170V, that is less sensitive to its cognate autoinducer (Shong et al., 2013), was prepared. IB1897 and IB1898 were both separately transformed with ligation mixtures containing the clonetegration plasmid pOSIP-CH and either the EsaR and EsaRI170V cassette. The successful integration events were integration of EsaR into IB1897 and integration of EsaRI170V into IB1898. Those strains were designated IB646 and IB2275 respectively.

4.2.5 Construction of an RBS library for P_{esaS}-$pfkA$

The expression level of Pfk-I from the intial P_{esaS} promoter –RBS construct was much higher than the wild type expression of Pfk-I. To adjust expression of Pfk-I, an RBS library was constructed in strain IB646 using the same Cas9 counterselection method described in Section 4.2.3 for adjustment of SspB expression from the P_{esaR} promoter (Reisch and Prather, in preparation). In this case, the useable PAM sequence for Cas9 recognition was contained within the coding sequence of $pfkA$. For selection, two silent mutations were made to the coding sequence of $pfkA$, and then an additional two degenerate nucleotides were included in the RBS sequence to create the RBS library. The library members were screened for improved growth in minimal medium relative to the parent strain. One strain was isolated with improved growth and the RBS sequence "caattcattaaagaggcgaaaggatcc" (base change underlined). This strain was designated IB2353. Two strains that did not show growth on glucose minimal medium were also retained for analysis, IB2351 ("caattcattaaagagttgaaaggatcc") and IB2352 ("caattcattaaagagtggaaaggatcc").

4.2.6 Integration of EsaI expression cassettes

Plasmid-based constructs for EsaI expression were constructed by PCR amplification of the *esaI* coding sequence from pAC-EsaR-EsaI (Shong and Collins, 2013) with addition of RBS B0034 on the primer, and cloning into the pKVS45 or pMMB206 backbones at the EcoRI and HindIII restriction sites.

For genomic integration of EsaI constructs with varying expression levels, a series of EsaI expression cassettes were generated via PCR. The promoter and 5′ UTR combinations for these cassettes were taken from those evaluated by Mutalik et. al. to give a range of expression levels (Mutalik et al., 2013). The EsaI expression cassettes with digested with KpnI and SphI, as was the clonetegration vector pOSIP-KO. The target strain was then transformed with the ligation mixture and screened via the standard procedure for one step cloning and integration (St-Pierre et al., 2013). Use of the pOSIP-KO vector can

result in integration at one of two 186 attachment sites. Strains were screened for integration at the primary site, and only those with primary site integration were used. Table 4.2 lists the set of promoter and 5' UTR sequences that resulted in moderate accumulation of 3OC6HSL and were appropriate for further testing. These were integrated into the strain backgrounds IB646, IB2275, and AG2349, and the resulting strains are denoted by their parent strain number and the EsaI expression cassette notation (e.g. IB646-L18).

During all integration steps, colonies were screened via colony PCR with OneTaq master mix. PCR amplifications for cloning or genomic integration were carried out with Q5 polymerase. Enzymes utilized for PCR amplification, restriction digests, and ligation were obtained from New England Biolabs (Ipswich, MA). Oligonucleotides were obtained from Sigma-Genosys (St. Louis, MO) or Integrated DNA Technologies (Coralville, Iowa).

Table 4.2 | Promoter and UTR sequences for integrated expression cassettes.
RBS sequences are highlighted in red. Changes in the RBS selected during RBS library screening are underlined. The sequence of the protein degradation tag is given if applicable.

Construct	Promoter	5' UTR / RBS	Degradation tag, DNA sequence	Integration site
SspB expression cassettes				
P_tet-sspB	tccctatcagtgatagagattgacatccctatcagtg atagagatactgagcac	ctaggtttctccatacccgttttt ttgggctagcgaattcaaaga ggagaaatactag		HK022
P_phoA-sspB	ctgtcataaagttgtcacggccgagacttatagtcg cttt	caattcattaaagaggagaag gatcc		HK022
P_BAD-sspB	ccataagattagcggatcctacctgacgctttttatc gcaactctctactgtttctccat	acccgttttttttgggctagcgaa ttcaaagaggagaaatactag		HK022
P_esaR-sspB	gcagattgagtaaccgtgaatgtttgtacaaatgttt caaagatgttactatgagtgtcccggccagcatcac tttatattttgtgacgtctggccggacgttttccctagt gttggctgttttagcgacctggccgtacaggtcagg ttttttttttaccgctaaacaactgaagccattgtaacct ctgaatgattcattgtaagttactcttaagtatcatctt gcctgtactatagtgcaggttaagtccacgttaagta aaagaagcagc	caattcattaaagaggagaaa ggatcc		HK022
P_esaR-RBS157-sspB (AG2349)	gcagattgagtaaccgtgaatgtttgtacaaatgttt caaagatgttactatgagtgtcccggccagcatcac tttatattttgtgacgtctggccggacgttttccctagt gttggctgttttagcgacctggccgtacaggtcagg ttttttttttaccgctaaacaactgaagccattgtaacct ctgaatgattcattgtaagttactcttaagtatcatctt gcctgtactatagtgcaggttaagtccacgttaagta aaagaagcagc	caattcattaaagagctgaaag gatca		HK022

P_{esaR}-RBS422-sspB (AG2350)	gcagattgagtaaccgtgaatgtttgtacaaatgttt caaagatgttactatgagtgtcccggccagcatcac tttatattttgtgacgtctggccggacgttttccctagt gttggctgttttagcgacctggccgtacaggtcagg ttttttttttaccgctaaacaactgaagccattgtaacct ctgaatgattcattgtaagttactcttaagtatcatctt gcctgtactatagtgcaggttaagtccacgttaagta aaagaagcagc	caattcattaaagagtcgaaag gatca		HK022

PfkA expression cassettes

114-pfkA (DAS+4)	tcgacatcaggaaaattttctgatacttacagccat	caattcattaaagaggagaaa ggatcc	gcggcgaacgatgaaa actatagcgaaaactat gcggatgcgagc	*pfkA* native locus
104-pfkA (DAS+4)	tcgacataaagtctaacctataggatacttacagccat	caattcattaaagaggagaaa ggatcc	gcggcgaacgatgaaa actatagcgaaaactat gcggatgcgagc	*pfkA* native locus
P_{esaS}-pfkA (LAA)	gctcacaacagtgtaagcgtatccgttattgtttgatttt caaggaaaaaagaaaacattcaggctccatgctgct tcttttacttaacgtggacttaacctgcactatagtaca ggcaagatgatacttaagagtaacttacaatgaatca ttcagaggttacaatggcttcagttgtttagc	caattcattaaagaggagaaa ggatcc	gctgctaacgacgaaaa ctacgctctggctgct	*pfkA* native locus
P_{esaS}-pfkA (DAS+4)	gctcacaacagtgtaagcgtatccgttattgtttgatttt caaggaaaaaagaaaacattcaggctccatgctgct tcttttacttaacgtggacttaacctgcactatagtaca ggcaagatgatacttaagagtaacttacaatgaatca ttcagaggttacaatggcttcagttgtttagc	caattcattaaagaggagaaa ggatcc	gcggcgaacgatgaaa actatagcgaaaactat gcggatgcgagc	*pfkA* native locus
P_{esaS}-RBS3096-pfkA (DAS+4) (IB2353)	gctcacaacagtgtaagcgtatccgttattgtttgatttt caaggaaaaaagaaaacattcaggctccatgctgct tcttttacttaacgtggacttaacctgcactatagtaca ggcaagatgatacttaagagtaacttacaatgaatca ttcagaggttacaatggcttcagttgtttagc	caattcattaaagaggcgaaa ggatcc	gcggcgaacgatgaaa actatagcgaaaactat gcggatgcgagc	*pfkA* native locus
P_{esaS}-RBS1087-pfkA (DAS+4) (IB2351)	gctcacaacagtgtaagcgtatccgttattgtttgatttt caaggaaaaaagaaaacattcaggctccatgctgct tcttttacttaacgtggacttaacctgcactatagtaca ggcaagatgatacttaagagtaacttacaatgaatca ttcagaggttacaatggcttcagttgtttagc	caattcattaaagagttgaaag gatcc	gcggcgaacgatgaaa actatagcgaaaactat gcggatgcgagc	*pfkA* native locus
P_{esaS}-RBS468-pfkA (DAS+4) (IB2352)	gctcacaacagtgtaagcgtatccgttattgtttgatttt caaggaaaaaagaaaacattcaggctccatgctgct tcttttacttaacgtggacttaacctgcactatagtaca ggcaagatgatacttaagagtaacttacaatgaatca ttcagaggttacaatggcttcagttgtttagc	caattcattaaagagtggaaag gatcc	gcggcgaacgatgaaa actatagcgaaaactat gcggatgcgagc	*pfkA* native locus

EsaR expression cassette

104-esaR	tcgacataaagtctaacctataggatacttacagccat	caattcattaaagaggagaaa ggatcc		HK022

EsaI expression cassettes

L18-esaI (P8 / BCD21)	ttcacttttaatcatccggctcgtataatgtgtgga	gggcccaagttcacttaaaaa ggagatcaacaatgaaagcaa ttttcgtactgaaacatcttaatc atgcgagggatggtttcta		P186 primary
L19-esaI (P8 / BCD22)	ttcacttttaatcatccggctcgtataatgtgtgga	gggcccaagttcacttaaaaa ggagatcaacaatgaaagcaa ttttcgtactgaaacatcttaatc atgcctaggaagttttcta		P186 primary

L25-esaI (P9 / BCD22)	ttgcctcttaatcatcggctcgtataatgtgtgga	gggcccaagttcacttaaaaa ggagatcaacaatgaaagcaa ttttcgtactgaaacatcttaatc atgcctaggaagtttcta		P186 primary
L31-esaI (P4 / BCD22)	ttgacatcaggaaaatttttctgtataatgtgtgga	gggcccaagttcacttaaaaa ggagatcaacaatgaaagcaa ttttcgtactgaaacatcttaatc atgcctaggaagtttcta		P186 primary

4.2.7 Culture medium and conditions

For plasmid preparation and genetic manipulations, strains were cultured in Luria-Bertani (LB) medium at either 30° or 37° C. Temperature sensitive plasmids were cured at 42° C.

Except where noted, growth and production experiments were carried out at 30°C in a modified MOPS medium containing 10 g/L D-glucose, 3 g/L NH_4Cl, 2 mM $MgSO_4$, 0.1 mM $CaCl_2$, 40 mM MOPS, 4 mM tricine, 50 mM NaCl, 100 mM Bis-Tris, 134 µM EDTA, 31 µM $FeCl_3$, 6.2 µM $ZnCl_3$, 0.76 µM $CuCl_2$, 0.42 µM $CoCl_2$, 1.62 µM H_3BO_3, and 0.081 µM $MnCl_2$. Dibasic potassium phosphate (K_2HPO_4) was supplemented into this medium at 1 g/L, except under phosphate limitation conditions, where it was added at the concentrations specified in the Results section. For strains containing pTrc-INO1, carbenicillin (100 µg/mL) was added for plasmid maintenance. Seed cultures were initiated using a 1:100 – 1:500 dilution from LB cultures and were grown at 30°C for 18 - 24 hours in modified MOPS with 1 g/L K_2HPO_4, until mid-exponential phase was reached. The seed cultures were then used for inoculation of working cultures for growth, activity, and production experiments.

For myo-inositol production experiments, working cultures of 50 ml in 250 ml baffled shake flasks were inoculated to OD = 0.05 from seed cultures, and 50 µM β-D-1-thiogalactopyranoside (IPTG) was added at inoculation. Flasks were incubated at 30° C with 250 rpm shaking and 80% humidity. Samples were taken periodically for measurement of enzyme activity, protein levels, and extracellular metabolites. For growth screening experiments during RBS library construction, working cultures were inoculated into in 48-well flower plates for OD monitoring in a BioLector (m2p labs, Baseweiler, Germany) and incubated at 30°C, 1200 rpm, and 80% humidity.

4.2.8 Phosphofructokinase activity assays

Phosphofructokinase activity assays were carried out as described in Chapter 2.

4.2.9 Measurement of *myo*-inositol titers and yields

Glucose and *myo*-inositol levels were quantified by high performance liquid chromatography (HPLC) on an Agilent 1100 or 1200 series instrument (Santa Clara, CA) with an Aminex HPX-87H anion exchange column (300 mm by 7.8 mm; Bio-Rad Laboratories, Hercules, CA). Sulfuric acid (5 mM) at a flow rate of 0.6 mL/min was used as the mobile phase. Compounds were quantified from 10 μL sample injections using a refractive index detector. Column and refractive index detector temperatures were held at 55° C.

4.3 Results

4.3.1 Phosphate starvation-inducible knockdown of Pfk activity

The use of phosphate starvation to drive SspB expression, and correspondingly drive a reduction in Pfk activity, is an interesting strategy for a number of reasons. Phosphate is an essential nutrient and phosphate starvation strategies have already been demonstrated to improve yields for a number of products, such as shikimic acid and fatty acids (Johansson et al., 2005; Youngquist et al., 2013). Additionally, phosphate feeding could be used to achieve cycling in the Pfk activity level, unlike in the case of inducer addition, where once added, the inducer cannot be easily removed to stop SspB expression and allow recovery of Pfk activity. Thus, phosphate starvation provides an autonomous, reversible method for controlling the shift between growth (high Pfk activity) and production (low Pfk activity) modes. The *phoA* promoter has previously been shown in the literature to exhibit strong induction upon phosphate starvation (Shin and Seo, 1990) and was initially selected for evaluation.

To verify that the *phoA* promoter amplified from the *E. coli* genome would exhibit the desired induction behavior in media of interest, the promoter construct was used to drive GFP expression from a plasmid, and strong induction was seen in glucose minimal medium under phosphate starvation conditions (data not shown). Given the promising results with GFP, strains IB643 and IB1509 were constructed to test the potential applicability of this strategy for SspB expression. Each strain has a genomically-integrated cassette for expression of *sspB* driven by the *phoA* promoter. The strain backgrounds are identical except for the constitutive promoter driving Pfk expression. Two promoter variants were tested (apFAB 114 and apFAB104). In Chapter 2, it was shown that apFAB104 resulted in higher expression of Pfk than apFAB114, and so this might provide a route to balance Pfk expression when expressing SspB from promoters which were leakier than the tet promoter. The growth of IB643 and IB1509 was measured in

modified MOPS minimal medium with 10 g/L glucose and excess phosphate. The growth rate of IB1509 was similar to IB1863, where SspB expression is driven by the tet promoter, while IB643 was slightly slower (Fig 4.1A). To test the effect of phosphate starvation on Pfk activity, cultures were spun down and transferred from the excess phosphate condition to phosphate-free modified MOPS minimal medium with 10 g/L glucose. Pfk activity was measured after one hour in phosphate starvation. As expected IB1509 and IB643 showed a strong decline in activity in response to phosphate starvation, while the wild-type and P_{tet}-sspB controls did not (Fig 4.1B). IB1509 showed baseline activity and growth closest to the IB531 control and was selected for further testing.
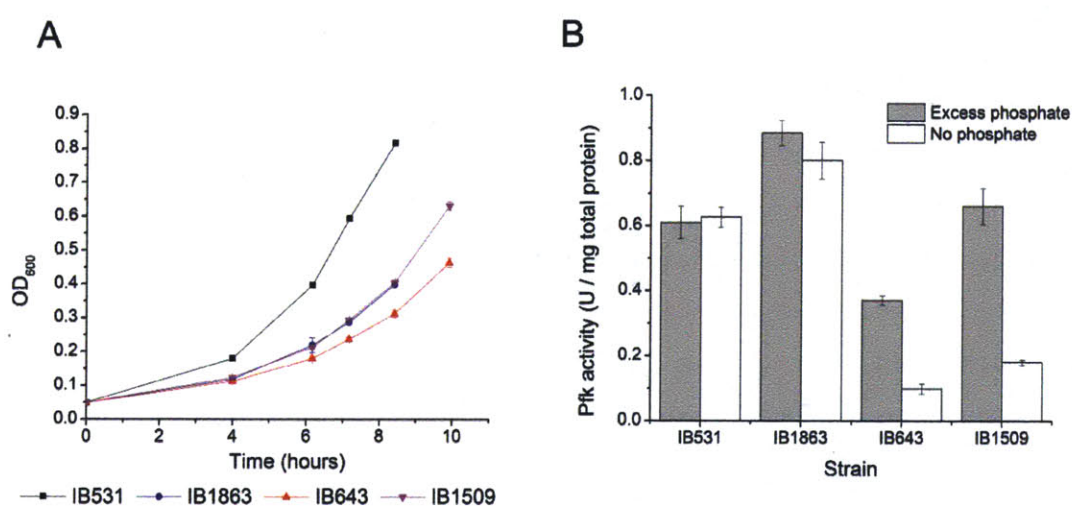
Fig. 4.1 | Characterization of strains IB643 and IB1509 with phosphate-starvation controlled SspB expression.
(A) Growth of IB643 and IB1509 on modified MOPS minimal medium with 10 g/L glucose and excess phosphate at 30° C, compared to the original parent IB531 (MG1655 $\Delta endA$) and IB1863, with aTc inducible control of SspB expression. (B) Pfk activity in these strains. All cultures were initially growth in modified MOPS minimal medium with excess phosphate. The "no phosphate" samples were taken after cultures were spun down and re-suspended in phosphate-free modified MOPS for 1 hour. Error bars represent triplicate mean ± SD.

To test whether the decline in Pfk activity upon phosphate starvation could be used to improve yields of MI, strain IB1509 was transformed with pTrc-INO1. MI production in this strain was compared to MI production in the wild-type strain, IB531-I, in modified MOPS minimal medium, supplemented with 10 g/L glucose and 0.1, 0.2, or 1 g/L K_2HPO_4. At 0.1 or 0.2 g/L K_2HPO_4, the available phosphate in the medium is exhausted before the glucose is fully consumed, limiting the formation of biomass. While the

excess glucose cannot be used to form biomass, it can still be consumed and converted into other products as long as the cells remain viable under the nutrient limited condition.

The growth profiles for IB531-I and IB1509-I (Fig. 4.2A) show that biomass formation is limited in both strains at 0.1 g/L and 0.2 g/L K_2HPO_4, as expected. The growth profile for IB1509-I shows an earlier plateau in biomass formation under phosphate starvation conditions, and then slow formation of biomass up to wild-type levels. This corresponds with expected behavior for the strain: as phosphate levels fall below the threshold of *phoA* induction, SspB is expressed and Pfk activity declines, limiting glycolytic flux and the ability to form biomass.   Activity measurements in samples taken from the cultures support this (Fig. 4.2B), showing that Pfk activity in the cultures with 0.1 g/L K_2HPO_4 had already fallen below the wild-type levels by 24 hours. At 48 hours, some recovery of Pfk activity is observed in the cultures with the lowest phosphate level; however all IB1509-I cultures still showed activity below the wild-type.
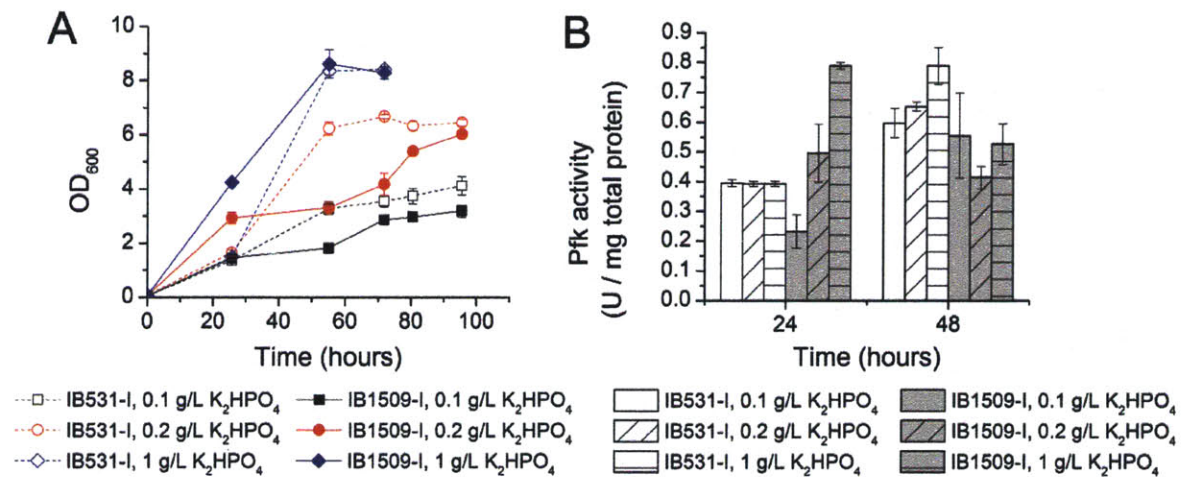
Fig 4.2 | Growth and Pfk activity in IB531-I (open) and IB1509-I (filled).
(A) Growth curves for strains in modified MOPS minimal medium with 0.1 (square), 0.2 (circle), or 1 (diamond) g/L K_2HPO_4 and 10 g/L glucose in the medium. (B) Pfk activity of both strains in each of the culture conditions, measured at 24 and 48 hours. Error bars represent triplicate mean ± SD.

Fig. 4.3A shows the titers and Fig. 4.3B the yields of MI observed in IB1509-I and IB531-I at the conclusion of the experiment (96 hours). Interestingly, titers of MI were improved by phosphate starvation in both strains, not just in IB1509-I. The reasons for this have not yet been fully investigated, but could include natural limitation of glycolytic flux during phosphate starvation or upregulation of

endogenous phosphatases that dephosphorylate myo-inositol-1-phosphate to MI more rapidly, helping to pull flux through INO1. IB1509-I did show improved yields and titers over IB531-I; however this was true under conditions of excess phosphate as well as phosphate starvation.
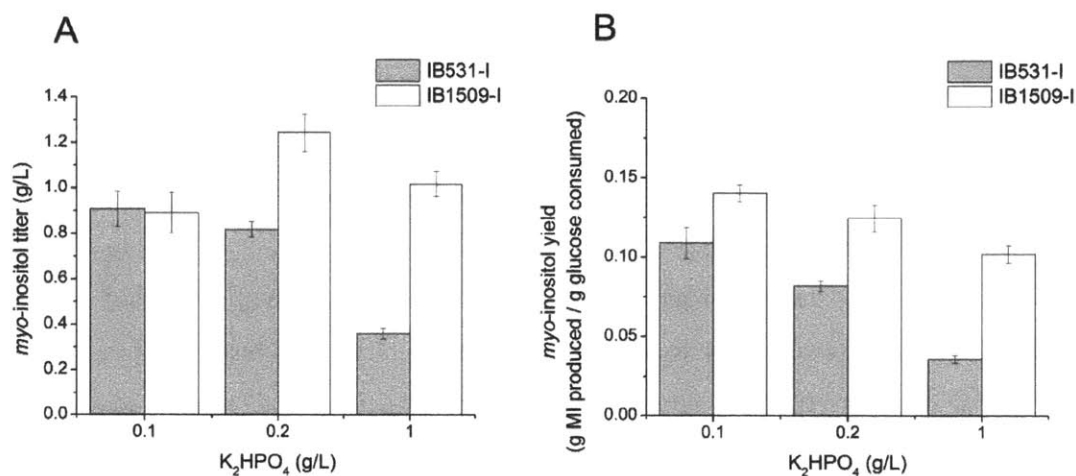
Fig. 4.3 | Titers (A) and yields (B) of MI in IB531-I and IB1509-I at 72 hours in modified MOPS minimal medium containing the specified amount of phosphate. Error bars represent triplicate mean ± SD.

Realizing that the improvement in titers could be driven at least partially by the deletion of *zwf* in IB1509-I, which is not present in IB531-I, MI production IB1509-I was also compared to that in IB1863-I under phosphate starvation. IB1863-I has the same genetic modifications as IB1509-I, except that expression of SspB is driven by a tet promoter rather than the *phoA* promoter. Titers (Fig. 4.4A) and yields (Fig. 4.4B) were very similar between the two strains across all conditions, indicating the effect of Pfk knockdown at phosphate starvation on MI titer was weak compared to the broader effect of phosphate starvation alone. This may be due to the fact that flux into glycolysis is already relatively low under phosphate starvation conditions.
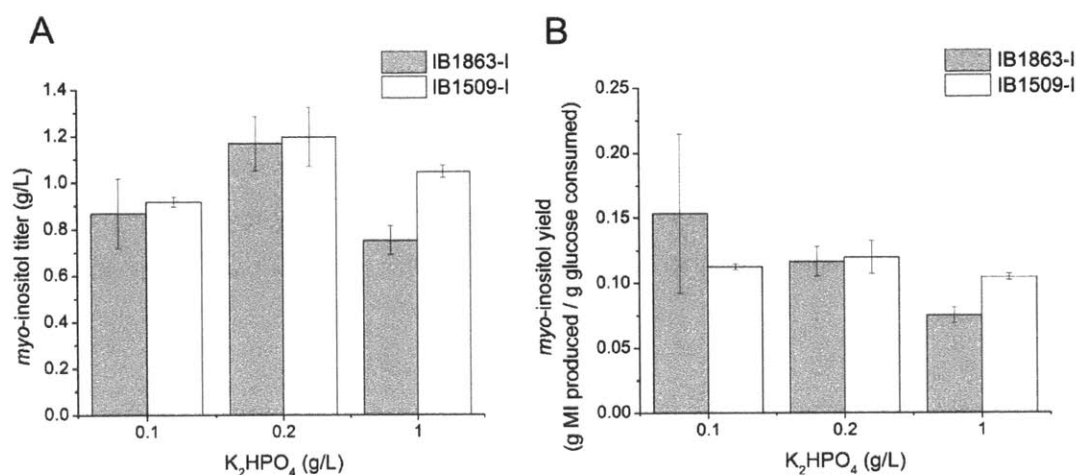
Fig. 4.4 | Titers (A) and yields (B) of MI in IB1863-I and IB1509-I at 72 hours in modified MOPS minimal medium containing the specified amount of phosphate. Error bars represent triplicate mean ± SD.

While phosphate-starvation based SspB induction did not show significant impact on MI production in a batch system, it may still be interesting for fed-batch applications. Use of the P_{phoA}-based system creates an inherent lag in recovery of Pfk activity, due to the fact even when phosphate is again added to the system to shut off SspB expression, the SspB protein already present in the cell must be diluted before Pfk degradation ceases. Thus while wild-type cells can rapidly return to full metabolism upon phosphate addition after starvation, there will be a slower transition for IB1509. This could be further explored as a potential method to restrict metabolism but maintain viability when phosphate is fed along with glucose or is fed in cycles.

4.3.2 Arabinose-inducible knockdown of Pfk activity

As an alternative variant of the system, arabinose-inducible expression of SspB was explored. This system was envisioned for processing of sugar mixtures derived from cellulosic biomass. In those mixtures, glucose will be present, along with pentoses such as arabinose and xylose. Ideally, catabolite repression from glucose would prevent induction of SspB until that sugar was fully consumed. Glucose would be consumed rapidly for biomass formation, and upon glucose exhaustion, SspB would be induced and Pfk knockdown would redirect carbon flux from xylose and arabinose consumption into glucaric acid production.

In the absence of arabinose, the newly constructed strains, IB1448 and IB1449, had growth rates similar to the previously constructed strain IB1863, with expression of SspB controlled by the tet promoter. Pfk activity was dependent upon arabinose addition, as expected; however even in the presence of excess glucose, arabinose addition still resulted in a decline in Pfk activity after one hour (Fig. 4.5A) and eventual growth arrest (Fig. 4.5B). Although this system could be interesting for sequential feeding of sugar mixtures, it was not pursued further, due to the lack of applicability for batch processing of mixed substrates.
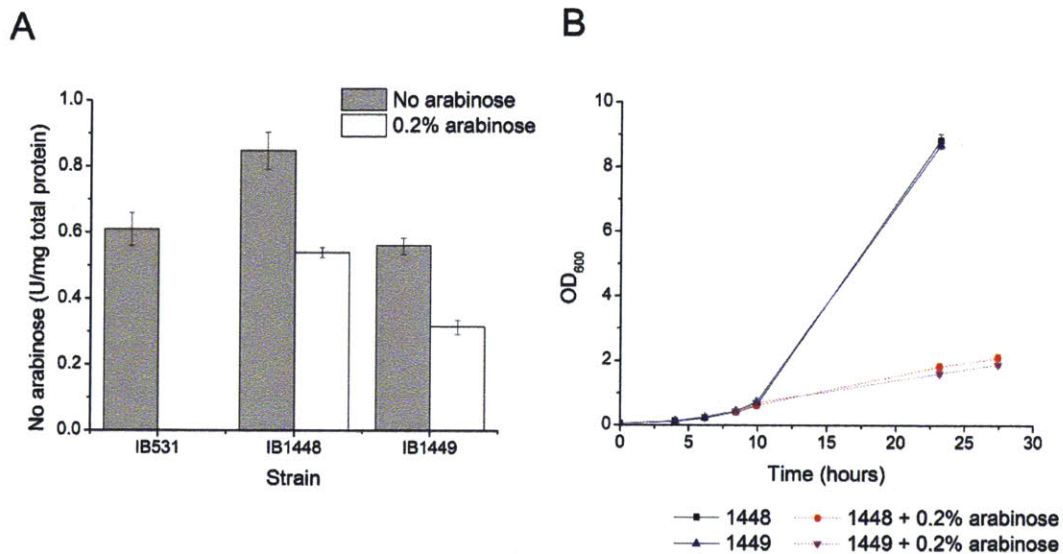
Fig. 4.5 | Activity and growth of strains IB1448 and IB1449 with arabinose-inducible SspB.
(A) Pfk activity in IB531, IB1448, and IB1449 in modified MOPS minimal medium with 10 g/L glucose at 30° C. Measurements with 0.2% arabinose addition were taken one hour after addition of arabinose to the medium, in the presence of excess glucose. (B) Growth of IB1448 and IB1449 at 30° C in modified MOPS minimal medium with 10 g/L glucose and addition of 0.2% arabinose at OD = 0.4 for the cultures indicated. Error bars represent triplicate mean ± SD.

4.3.3 Acyl-homoserine lactone-inducible knockdown of Pfk activity

A system based on bacterial quorum sensing was also developed, which would allow autonomous switching based on acyl-homoserine lactone (AHL) buildup during biomass formation, but without requiring nutrient depletion. The system selected for testing was based on the *esa* QS system from *P. stewartii*. The two known promoter architectures for this system (EsaR activation, EsaR repression), allow two different configurations of the system to be tested: post-translational control and transcriptional control. The post-translational control system functions by the same principles described

for the P_{phoA} and P_{BAD} systems, with SspB expression controlled by an inducible promoter. In this case the P_{esaR} promoter was used to drive SspB expression, resulting in induction of SspB upon buildup of 3OC6HSL. The presence of a characterized promoter, $P_{esaS,}$ with the opposite response (e.g. activated only in the *absence* of 3OC6HSL) also allowed for testing of direct transcriptional control of Pfk-I. The SsrA degradation tag was still appended to the coding sequence of *pfkA* to facilitate rapid depletion of the enzyme after cessation of transcription. The potential complication of transcriptional control is that it could require re-tuning of Pfk expression levels, as the strength of the P_{esaS} promoter was not likely to match that of the native *pfkA* promoter.

There are two main points for controlling the timing of the switch from high Pfk activity (growth) to low Pfk activity (production). The first is through control of expression level of the AHL synthase EsaI. This directly controls the rate of 3OC6HSL accumulation in the system. The other control point comes through utilization of EsaR variants, which have been evolved for increased or reduced sensitivity to 3OC6HSL and show changes in the binding affinity to this molecule (Shong et al., 2013). Thus, with the same rate of 3OC6HSL accumulation, different EsaR variants would be expected to show different binding response and different times of promoter derepression or deactivation.

4.3.4 Post-translational control through use of P_{EsaR} to control SspB expression

For initial testing, strains were constructed based on the P_{esaR}-SspB system, as it was most similar to the autonomous systems previously tested and would not require additional tuning of Pfk expression, since the previously characterized constitutive promoters for *pfkA* could be used. The preliminary strains constructed in this manner, IB2250 and IB2265, showed disappointing results, as neither strain was capable of growth on glucose minimal medium. Pfk activity levels were measured after growth on LB and found to very low, indicating the leaky expression of SspB was likely resulting in low Pfk-I levels, even without induction by addition of 3OC6HSL. An RBS library for P_{EsaR}-*sspB* was constructed as described in Section 4.2.3. Several colonies were isolated which then showed the expected behavior: growth on glucose minimal medium in the absence of 3OC6HSL and a strong reduction in growth upon 3OC6HSL addition. Several of the functional strains were sequenced, and the sequences were also analyzed using the RBS calculator (Salis, 2011). All of the functional strains sequenced showed a lower predicted translation initiation rate than the parent strain, indicating that reduction in baseline expression of SspB likely restored the desired behavior of the strains.

Two of the isolated strains, AG2349 and AG2350, were retained for further testing and development, and the RBS sequences for these strains can be found in Table 4.2. Fig. 4.6A and 4.6B illustrate the response in growth and Pfk activity respectively to exogenous addition of 3OC6HSL in AG2350. As expected, a decline in Pfk activity was observed, along with growth arrest. AG2350 still showed somewhat lowered baseline Pfk activity when compared to the wild-type control IB531, but growth on glucose was not significantly impaired.
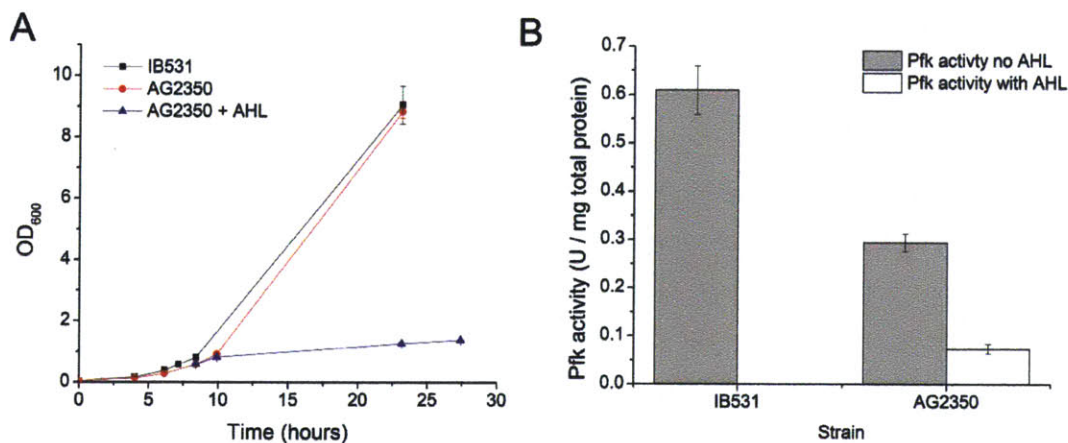
Fig. 4.6 | Growth and activity of strain AG2350, with AHL-inducible SspB expression.
(A) Growth of AG2350 and the original parent strain IB531 in modified MOPS minimal medium with 10 g/L glucose at 30° C, and AHL addition at OD = 0.6 for indicated cultures. (B) Pfk activity in AG2350 in the same medium. For the "with AHL" case, activity was sampled one hour after AHL addition. Error bars represent triplicate mean ± SD.

4.3.5 Transcriptional control through use of P_{EsaS} to control Pfk-I expression

In conjunction with development of post-translational control based on SspB expression, direct transcriptional control of Pfk-I expression via the P_{esaS} promoter was also explored. IB646 and IB2275 were initially constructed to test the potential of this strategy. The two strains both contained degradation tagged *pfkA* drive by the P_{esaS} promoter, but each utilized a different variant of EsaR for promoter activation, integrated as described in Section 4.2.4. IB646 contained an expression cassette for wild-type EsaR, while IB2275 expressed the variant EsaRI170V, which shows reduced binding affinity for 3OC6HSL (Shong et al., 2013). Construction of both these parent strains was designed to allow comparisons of the EsaR variants to be made, as well as to confirm that both variants worked as expected *in vivo*.

As expected, the Pfk-I expression levels in both strains were poorly matched to the wild-type levels. Pfk activity was measured in these strains and was shown to be up to 40x wild-type levels. Growth was also impaired on glucose minimal medium and final biomass levels were substantially lower than observed in the wild type; however growth arrest could still be observed upon exogenous 3OC6HSL addition, indicating control over Pfk activity was likely still being achieved (Fig 4.7A). Preliminary tests of IB646 indicated a large drop in Pfk activity occurred upon addition of 3OC6HSL, with the activity falling below wild-type levels (Fig 4.7B). Additional testing with expression of the AHL synthase EsaI (described in more detail in Section 4.3.5) confirmed very strong control of Pfk activity in both IB646 and IB2275, and activity repression to below wild type levels.
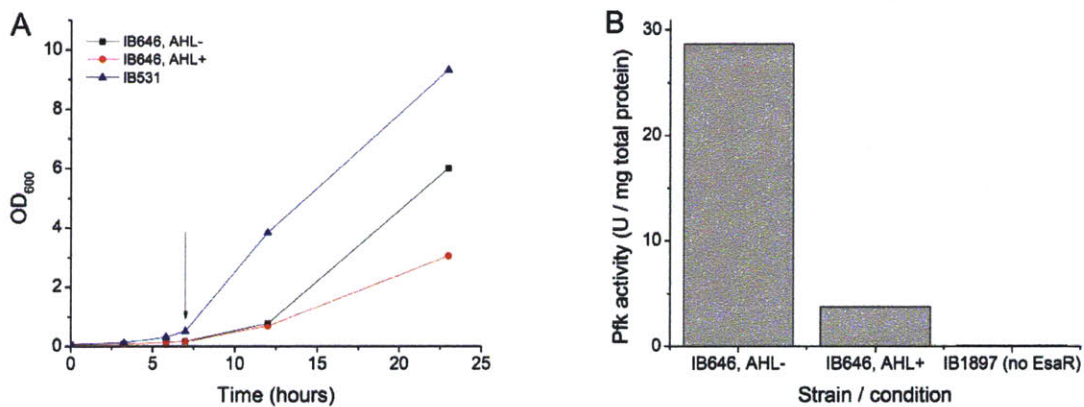
Fig. 4.7 | Preliminary tests of growth and Pfk activity in strain IB646.
(A) Growth of IB646 in modified MOPS + 10 g/L glucose with and without AHL addition at the time indicated by the arrow. Final OD_{600} for IB646 remains at approximately 6, while the wild-type strain IB531 reaches final OD_{600} values of 9-10. (B) Pfk activity of IB646 with and without AHL addition in LB. IB1897, the parent strain without integrated EsaR is also shown, indicating that EsaR expression is required for activation of Pfk expression. Expected Pfk activity with wild-type *pfkA* promoter in this medium is approximately 0.8 U / mg total protein.

While the results were promising, the reduction in final OD due to high Pfk activity in IB646 and IB2275 was undesirable. As the initial promoter construct utilized a strong RBS, an RBS library was constructed for IB646 to try to reduce baseline Pfk activity via the protocol outlined in Section 4.2.5. Several colonies were screened from the library. Some exhibited no growth on glucose minimal medium even in the absence of 3OC6HSL, but two colonies were isolated that showed improved growth on glucose minimal medium relative to IB646 and that were responsive to 3OC6HSL. Sequencing of colony PCR products

and analysis of the predicted RBS strength via the RBS calculator (Salis, 2011) revealed that colonies that did not grow on glucose had predicted translation initiation rates 20 – 50x lower than the original RBS. The colonies showing improved growth both had the same RBS, with a predicted translation initiation rate of 3096, 7.3x lower than the original RBS. Two of the strains incapable of growth on glucose, IB2351 and IB2352, were selected for further analysis, along with the improved strain IB2353. Pfk activity was measured in these three strains during growth on M9 + 0.4% glycerol and found to be consistent with the observed phenotype. IB2351 and IB2352 showed activity lower than the wild-type control, IB531, while IB2353 showed intermediate activity between the wild-type and the parent, IB646 (Fig.4.8A). While IB2353 does not show complete recovery of wild-type growth and final OD, it does show improvement over the parent strain IB646 (Fig. 4.8B).
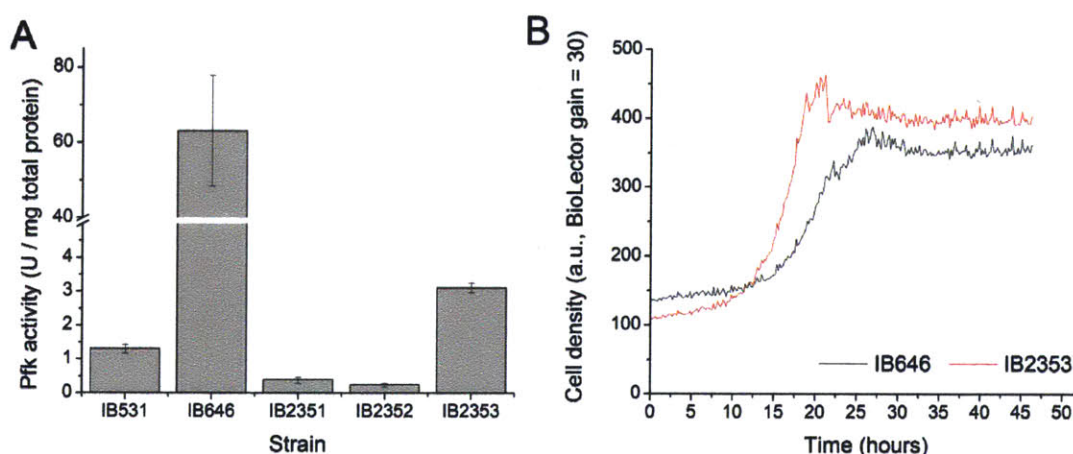
Fig. 4.8 | Growth and activity of strains derived from IB646 RBS library.
(A) Pfk activity in IB646, IB531, and RBS library strains IB2351-2353 in M9 + 0.4% glycerol. Strains IB2351 and IB2352 with activity lower than that of IB531 did not show growth on glucose minimal medium. Error bars represent duplicate mean ± SD. (B) Representative growth curves of IB646 and IB2353 in modified MOPS minimal medium + 1% glucose at 30 C. Final OD_{600} values measured by spectrophotometer were 6.58 ± 0.09 (IB646) and 7.98 ± 0.11 (IB2353).

4.3.6 Linking to EsaI expression for autonomous control

In order for either of these systems to function autonomously in a fermentation, without exogenous AHL addition, the expression of EsaI was also required. The expression level of EsaI is expected to affect the rate of 3OC6HSL synthesis, with lower expression levels expected to result in slow 3OC6HSL accumulation, resulting in knockdown of Pfk-I expression later in the fermentation, when more biomass

is present. For an initial test of timing through EsaI expression level, EsaI was expressed from a plasmid in strains IB646 (Fig. 4.9A) and IB2275 (Fig. 4.9B). The medium copy plasmid pKVS-B0034-EsaI has very tight control of expression through use of the tet promoter. Relying only on leaky expression of EsaI, switching of Pfk activity to the "off" state occurred much later than if EsaI was expressed at high levels from inoculation. A similar trend can be seen for expression from the plasmid pMMB-B0034-EsaI; however, as the lac promoter has higher leaky expression, there is a smaller difference in the time of switching. It is also clear that there is a difference in behavior between the strain with wild-type EsaR (IB646) and the strain with the less sensitive EsaR variant EsaRI170V (IB2275). With the less sensitive EsaR variant, higher Pfk activity levels are reached before AHL buildup starts to result in a decline in *pfkA* expression. This also alters the time at which Pfk activity falls below the critical threshold for a given expression level of EsaI, providing another route for modulation of switching time.
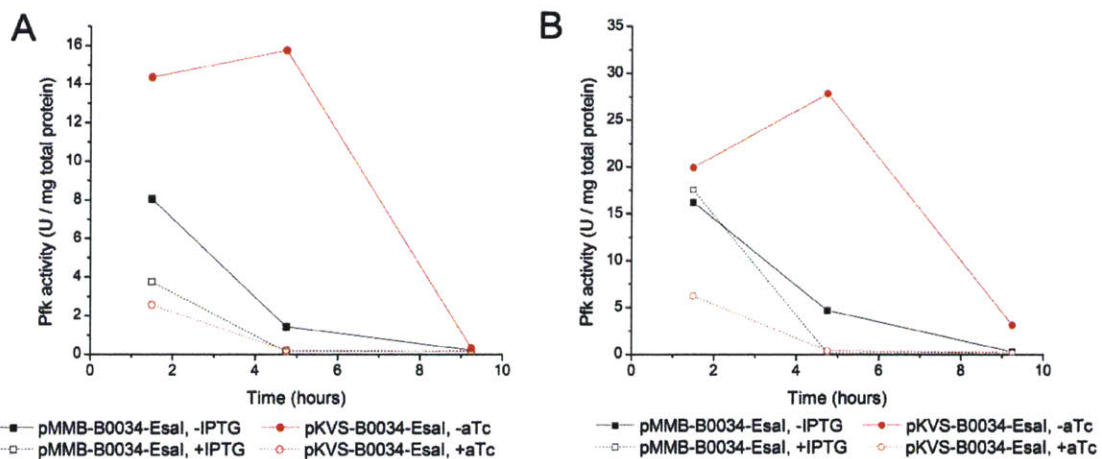
Fig. 4.9 | Pfk activity in IB646 and IB2275 with plasmid-based EsaI expression.
(A) IB646 with EsaI expression induced from pMMB-B0034-EsaI and pKVS-B0034-EsaI (filled symbols) or leaky expression (open symbols). (B) IB2275 with EsaI expression induced from pMMB-B0034-EsaI and pKVS-B0034-EsaI (filled symbols) or leaky expression (open symbols).

Control through plasmid-based expression of EsaI required both an additional antibiotic selection as well as tuning of inducer addition. To make the system entirely autonomous, a variety of constitutive EsaI expression cassettes were integrated into the genome, to generate a series of strains that automatically turn off Pfk-I expression at the desired cell density, without any outside intervention. As described in Section 4.2.6, an existing promoter and 5' UTR library was used to guide the design of EsaI expression cassettes of different strengths (Mutalik et al., 2013). These EsaI expression cassettes were integrated

both into strains utilizing direct transcriptional control of *pfkA* (IB6464, IB2275), as well as one relying on controlled degradation of Pfk-I through SspB expression (AG2349). The promoter and 5' UTR sequences integrated into each strain can be found in Table 4.2 with the strains containing each integrated cassette denoted by parent strain number followed by the promoter / RBS pair designation (e.g. IB646 + L18).

The varying EsaI expression levels resulted in strains with a variety of growth profiles in glucose minimal medium (Fig. 4.10A). As expected, the OD of the cultures at 36 hours corresponded inversely with the predicted strength of the promoter / 5' UTR combination (Fig. 4.10B). Time course activity measurements in strain IB646+L18 and IB646+L19 in LB showed that, as expected, Pfk activity declined over the course of the culture (Fig. 4.10C). The time at which Pfk activity fell below wild-type levels also followed the expected trend, with that switch occurring around 4 hours for the stronger L18 expression cassette and around 8 hours for the weaker L19 one.

Switching time could also be altered by integration of the EsaI expression cassettes into IB2275. Using the same expression cassette, arrest of growth was delayed in the IB2275 background relative to the IB646 background (Fig. 10D), as it likely takes longer to build up enough 3OC6HSL for binding to EsaRI170V.

Several EsaI expression cassettes were also integrated into AG2349, which relies on expression of SspB from P_{esaR} to increase the rate of Pfk-I degradation and reduce the Pfk activity. In those strains, a long lag time was observed in glucose minimal medium after inoculating working cultures from a starter culture. This lag is likely related to the need to dilute out existing SspB in the cells from the starter before Pfk-I can build up and growth can resume. In contrast, with direct transcriptional control of *pfkA*, production of the enzyme can immediately resume upon dilution of 3OC6HSL by inoculation into fresh medium. Addition of 0.2% casamino acids to the medium when growing strains based on AG2349 improved their growth behavior, allowing several divisions to occur independent of glucose utilization. Once growth did occur, the rate was very similar to that of IB1379.
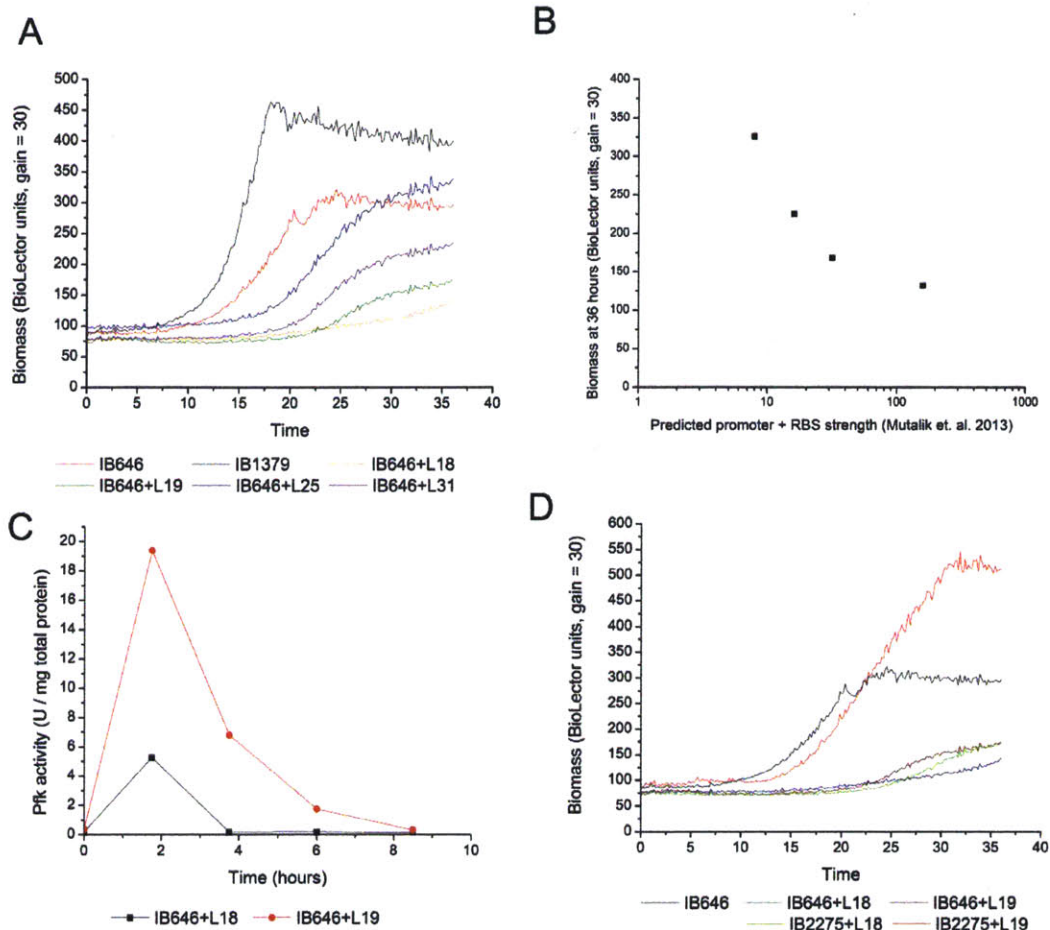
Fig. 4.10 | Growth and activity in IB646 and IB2275 with integrated EsaI expression cassettes.
(A) Growth of IB646 and IB1379 (native *pfkA* promoter) in comparison with IB646 variants containing various integrated EsaI expression cassettes. (B) Biomass density at 36 hours as a function of predicted strength of promoter/RBS combination driving expression in IB646 background. (C) Time course of Pfk activity measured in IB646+L18 and IB646+L19 cultures in LB. Activity at t=0 is activity in stationary phase starter cultures. (D) Comparison of growth in IB646 and IB2275 with L18 and L19 EsaI expression cassettes.

Through varied constitutive expression of EsaI, a set of strains have been developed for which switching from "growth mode" (high Pfk activity) to "production mode" (low Pfk activity) is completely autonomous, requiring no intervention via inducer addition to the medium or limitation of oxygen supply. These strains can potentially be used for production of *myo*-inositol, glucaric acid, or other metabolites derived from G6P and F6P. The creation of a series of strains allows the optimal strain to be selected for each application, as later switching may be more desirable for cases where intensive growth

and protein expression is initially required. The strains can be used to explore trade-offs between yield and titers, allowing the point of maximum productivity to be achieved.

4.3.7 *Myo*-inositol production in autonomous strains

Given the success in achieving autonomous control of growth utilizing components of the *esa* quorum sensing system, several of the strains were transformed with pTrc-INO1 and tested to determine if the switching could successfully be used to increase *myo*-inostiol (MI) production. Strains based on IB646 and IB2275 were tested in modified MOPS minimal medium + 10 g/L glucose, while strains based on AG2349 were tested in that medium supplemented with an additional 0.2% casamino acids. The results for both conditions are shown in Figs. 4.11A and 4.11B.

Not surprisingly, MI production was very poor in IB646-I, given its poor growth profile and high Pfk activity. However, through EsaI expression and control of Pfk activity, MI production could be recovered back to levels at or above that in IB1379-I, with native *pfkA* expression. Strain IB2275+L19-I showed the greatest improvement over IB1379-I, with 30% higher titers. This was validated in a second run, and also in casamino acid supplemented medium (Fig. 4.11B), where a 43% improvement in titers was achieved. The growth profiles aslo showed the expected shape, with a clear period of growth arrest (Fig. 4.11C). The results for strains based on AG2349 were not as promising. Although the parent strain performed better than IB646 under plasmid-free conditions, its growth was more severely impaired by pTrc-INO1 expression than expected, given the close match to IB1379 under plasmid-free conditions (Fig. 4.11D). Activity profiles (data not shown) showed a decline in AG2349-I activity over the course of the fermentation in the absence of EsaI, likely due to leaky SspB expression, and decreased activity of the BioFab promoter in stationary phase.

For future work, integration of EsaI into versions of IB646 and IB2275 with optimized *pfkA* expression (one of which has already been generated, IB2353) seems likely to yield the greatest improvements in titer, as poor characteristics of these host strains may be depressing performance in the "growth" phase of the fermentation.
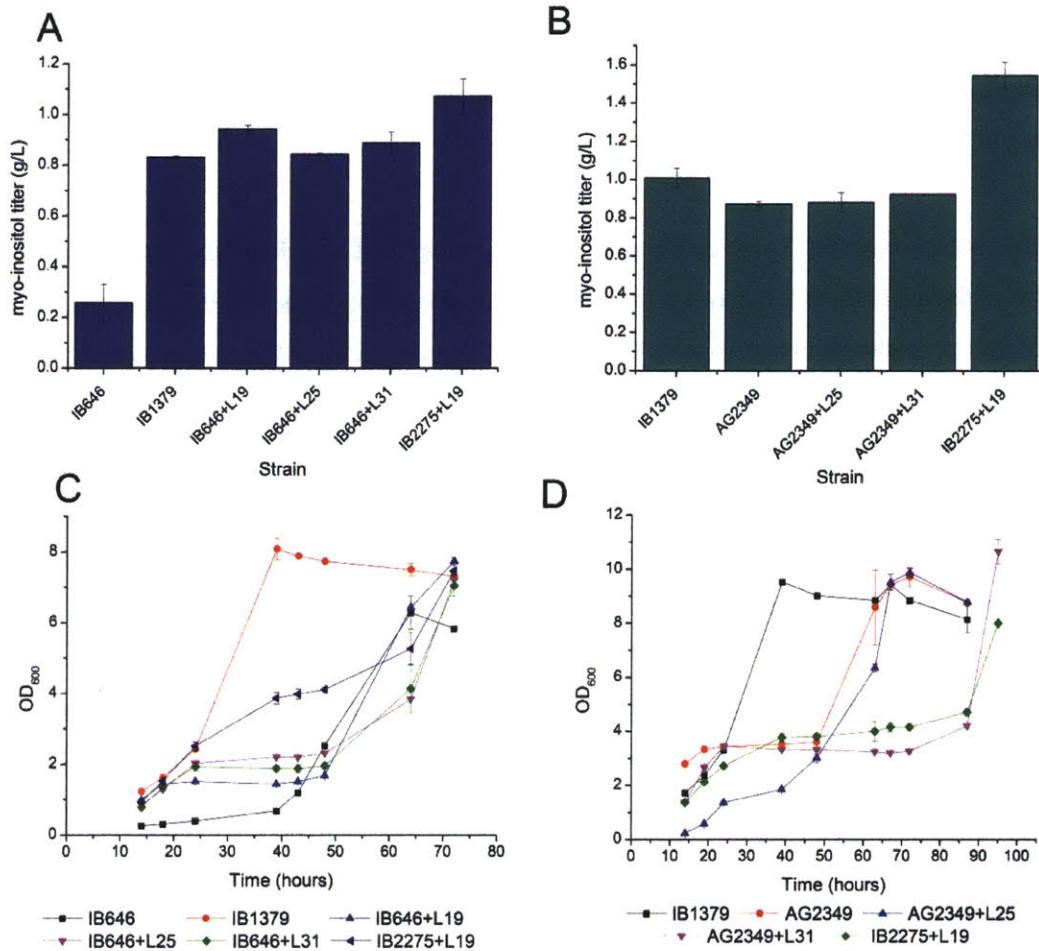
Fig. 4.11 | Growth and MI production in strains with autonomous *pfkA* switching.
(A) MI titers at 72 hours in modified MOPS minimal medium + 10 g/L glucose for strains based on IB646 and IB2275. IB1379 contains the native *pfkA* promoter. (B) MI titers at glucose exhaustion (72-114 hours) in modified MOPS minimal medium + 10 g/L glucose + 0.2% casamino acids. Strains based on AG2349 were tested, along with the top performing strain from the previous test, IB2275+L19, and the control strain IB1379. (C) Growth profiles in modified MOPS minimal medium + 10 g/L glucose for the strains with titers given in (A). (D) Growth profiles in modified MOPS minimal medium + 10 g/L glucose + 0.2% casamino acids for the strains with titers given in (B). Error bars represent duplicate mean ± SD.

4. Discussion

This work has illustrated that the SspB expression module can be adapted for multiple modes of autonomous control, including nutrient starvation and quorum sensing. Leaky baseline expression of SspB can be tuned by modulation of the RBS sequence, allowing a variety of promoter systems with

differing baseline expression and induction behaviors to be utilized. In addition to control through a single inducible promoter, the expression of SspB could also be coupled with multi-input cellular logic functions, such as AND gates (Anderson et al., 2007), allowing multiple factors to be used in determining switching behavior.

While the control strategies based on the *phoA* and P_{BAD} promoters both functioned with respect to induction of SspB and modulation of Pfk activity, they did not appear to be feasible strategies for generating improvements in *myo*-inositol production. Careful selection of promoter systems is required with respect to external conditions, as well as changes in cell physiology associated with the induction signal. Generally, use of nutrient starvation promoters may suffer from the inability to control the effect of broad changes in cell physiology associated with starvation. Use of targeted signals (e.g. buildup of a pathway intermediate) or non-native signals may provide a more robust basis for manipulation of individual nodes in metabolism.

The quorum sensing-based strategy explored in this work offers one example of utilization of a non-native signal, 3OC6HSL. The rate of accumulation of this molecule can be artificially controlled through varying the expression of the cognate AHL synthase or use of transcription factor variants with differing affinity for AHL. Build-up of this non-native signal was effectively used to trigger SspB expression in a completely autonomous manner, dependent only on the properties of the cell itself. This offers a powerful strategy for controlling the period of biomass accumulation, independent of medium formulation, inducer addition, and process conditions. As a result, cells can be continuously maintained in medium and process conditions favoring rapid growth and high accumulation of heterologous pathway enzymes, but after a period of growth, they will still switch physiological states to one more favorable to production of a desired small molecule, and this will occur at a point pre-determined by the genetics of the strain utilized.

An additional benefit of utilizing the *esa* quorum sensing system is that it offered an opportunity to explore direct transcriptional control of *pfkA* expression, as well as Pfk-I degradation through SspB expression. The P_{esaS} promoter differs from typically utilized quorum sensing promoters like P_{las} and P_{lux}, in that its default state is "on" in the absence of AHL, allowing accumulation of 3OC6HSL to be used to turn off expression of the target gene (Schu et al., 2009). Both this system and the P_{esaR}-sspB expression system could be coupled with expression of the AHL synthase EsaI to result in autonomous knockdown

of Pfk activity and growth arrest at relevant cell densities. More detailed time course and physiological analysis of the cell in future work could be used to determine the relative advantages, disadvantages, and response times of each system. One already apparent limitation of the SspB-based system for autonomous control is that, if SspB becomes induced during the starter culture, it must be diluted out through several doublings in the working culture before normal growth can resume. In contrast, with transcriptional control, Pfk activity can recover more quickly upon transfer from starter to working culture, because expression of the enzyme starts immediately upon inoculation in fresh medium without 3OC6HSL.

Initial results indicate the quorum sensing based strategy can be utilized to achieve increases in production of a heterologous product, *myo*-inositol. Increases in MI titer up to 30% could be achieved on glucose as a sole carbon source when compared to a strain with native *pfkA* expression in a 72 hour batch, without any intervention or addition of inducer. Further optimization of Pfk-I levels in the autonomous strains could result in larger increases in yield and titer.

5. Conclusions

The strains harboring the *esa*-based autonomous induction system will continue to be tested to determine if larger improvements in *myo*-inositol production can be attained. Manual timing of Pfk knockdown resulted in maximum two-fold improvement in yields and titers (Brockman and Prather, 2015), and a similar improvement could likely be expected from an optimized quorum sensing system. Additionally, as a series of strains have been developed with growth arrest at different cell densities, it should be possible to look for the expected trends in yield and titer, with increasing yield for earlier growth arrest.

More broadly, it will be interesting to add multiple points of control; for example, expression of glucose-6-phosphate dehydrogenase could be actively controlled, rather than relying on a gene knockout, or expression of INO1 could also be delayed, to reduce expression stress early in the fermentation. Differences in timing between expression of the different genes could potentially be achieved by utilizing previously developed variants of the P_{esaR} promoter with varied induction profiles in response to AHL accumulation (Shong and Collins, 2013) or by utilizing secondary signals.

Chapter 5: Conclusions and future directions

Abstract

The aims of this thesis were focused on the development of strategies for dynamic control of phosphofructokinase-I activity, and the application of these strategies for improving production of *myo*-inositol and glucaric acid. This chapter summarizes the major finding in this thesis work and suggests directions for future exploration.

5.1 Thesis summary

In this thesis, a system for dynamic control of phosphofructokinase-I (Pfk-I) activity has been constructed. Pfk-I was identified as a relevant target enzyme for controlling the pools of G6P and F6P, which could then be redirected into heterologous products of interest, such as *myo*-inositol and glucaric acid. This system could be applied to other molecules derived from G6P and F6P, and more broadly, the techniques demonstrated could be used to construct "metabolite valves" at alternative control points in metabolism, allowing intracellular pools of other important building blocks, such as acetyl-CoA, to be altered. The key findings and accomplishments in this thesis work are summarized below.

5.1.1 Initial development of a Pfk-I valve and application to *myo*-inositol production

A protein degradation strategy for dynamic control of Pfk-I levels is presented in Chapter 2. A degradation-tagged variant of *pfkA* with a synthetic promoter was integrated into the *E. coli* genome. Expression of SspB from an inducible promoter was successfully used to increase the degradation rate of Pfk-I and reduce Pfk activity. This resulted in a reduction in growth rate, as well as an increase in the pool of intracellular G6P, which could potentially be redirected into formation of other products. Testing with INO1 expression for conversion of G6P to *myo*-inositol showed that appropriately timed switching from growth (high Pfk activity) to production (low Pfk activity) mode resulted in a two-fold improvement in *myo*-inositol yields and titers from glucose. While the specific application demonstrated relies on degradation of Pfk-I and buildup of G6P, the development strategy presented for metabolite valves is more general. The main steps are (1) identification of the enzyme acting as a flux control point; (2) disruption of native regulation and tuning of baseline expression; (3) implementation of the strategy for activity knockdown; (4) combination with a heterologous pathway.

5.1.2 Application to glucaric acid production

In Chapter 3, the application of the Pfk-I degradation system is expanded to glucaric acid production. Additional medium conditions were explored, with the addition of supplemental carbon sources, as well as new feeding strategies, based on slow release of glucose by starch hydrolysis. In T12 medium (supplemented with soytone and peptone), glucaric acid yields and titers could be improved by 18% under batch conditions and 42% under starch hydrolysis (fed-batch) conditions. The yield and titer improvements were smaller than what was observed in Chapter 2, but activity measurements showed that the baseline Pfk activity level in the metabolite valve strain is low in T12 medium in comparison to wild-type *E. coli*, so the relative changes achieved during activity knockdown were also smaller. Analysis

of a *pfkAB* knockout indicated that glucaric acid productivity is limited in T12 medium as Pfk activity declines to zero, so switching between growth and production modes still provides an important advantage.

5.1.3 Autonomous control of Pfk activity

The system for control of Pfk-I levels developed in Chapter 2 and 3 requires carefully timed addition of inducer during the fermentation in order to achieve the highest titers in a given batch. The optimal switching time for any given batch time represents a tradeoff between utilization of substrate to produce sufficient biomass to serve as biocatalyst and utilization of substrate to form the product of interest. Thus, it should be possible to use cell density as a signal, with the switch to production mode automatically occurring when a desired amount of biomass has been formed. Initially, nutrient limitation (phosphate limitation) was explored as a proxy for cell density, given that consumption of a fixed amount of phosphate should yield a fixed amount of biomass in minimal medium. In studies of *myo*-inositol production, it was difficult to separate the general effect of phosphate starvation on MI production levels from the specific effect of Pfk-I knockdown.

As an alternative system not connected to broader metabolic responses in *E. coli*, components of the *esa* quorum sensing system from *P. stewartii* were evaluated. A set of strains was successfully developed where buildup of the autoinducer 3OC6HSL resulted in either decreased transcription or increased degradation of Pfk-I. The switching time in these strains is determined by (1) the expression level of the AHL synthase EsaI and (2) the variant of the EsaR transcription factor integrated in the strain. The switching in these strains is completely autonomous, not requiring any addition of inducer during the course of the fermentation to change the cellular phenotype. Preliminary results indicate this can also be used for increasing yields and titers of *myo*-inositol.

5.2 Future directions

The metabolite valve concept has been developed significantly in the thesis, and previous limitations related to response time and strength of response have been overcome. The controlled protein degradation results in very rapid declines in Pfk activity (<1 hour) and very low residual activity. This work also represents the first integration of a metabolite valve with the glucaric acid pathway and has shown that the strategy can be useful in improving yields and titers of this product. Future work will be

required to further develop autonomous control strategies, to address the genetic stability of the system, and to couple the Pfk-I valve with other useful dynamic controls.

5.2.1 Improving genetic stability of "metabolite valves"

As discussed in Chapters 2 and 3, the phenomenon of "escape" can limit full exploration of early Pfk knockdown times. In the case of inducible SspB expression, disruption of the inducible promoter by insertion of a mobile genetic element was one mode of escape. Coupling the function of the metabolite valve system to essential cellular functions could provide one route for increased stability. For example, the use of an auxotrophic strain could be coupled with addition of a limited amount of amino acid into the medium. Exhaustion of the amino acid could be used to trigger SspB induction, knocking down a gene of interest, but also inducing expression of the genes required to relieve the auxotrophy. While this can prevent larger disruptions of the artificial operon for SspB induction, it would not solve the problem of point mutations in SspB or ClpXP. Conversely, a low-level (DAS+4)-tagged toxin could be expressed along with SspB, making SspB a requirement to keep the toxin depleted. In that case, large insertions that delete both the toxin and SspB could occur, but not point mutations in SspB. Another option is the use of a more stable host strain. Reduced genome *E. coli* strains have been shown to have higher genetic stability with respect to mobile insertion elements (Pósfai et al., 2006), but other modes of genetic change (deletions, mismatches) did still occur at similar frequency.

Activator based-control of *pfkA* expression from P_{esaS} could be more robust, as in the absence of EsaR binding, promoter mutations that strongly upregulate Pfk-I are unlikely, and changes in EsaR that disrupt AHL binding are also likely to disrupt DNA binding and activation of Pfk-I. However, autonomous switching of the system relies on the expression of the AHL synthase, EsaI. This creates the same issues encountered with SspB expression, in that any inactivation of EsaI expression will allow escape, since accumulated AHL breaks down rather quickly. However, as EsaI expression is constitutive, there may be more options for coupling its expression with an essential gene or toxin / antitoxin systems to try to keep the expression cassette intact.

More work could also be done to examine the genetic stability in phosphate starvation-based control of Pfk activity. As new biomass cannot be formed without phosphate, escapers do not have a route to divide and take over the culture. There may still be differences in viability with and without Pfk knockdown that could lead to changes in the genetic composition of the culture, and the ability to

maintain Pfk degradation during cycles of phosphate feeding. In general, depletion of a small molecule is an interesting strategy for improving stability. If it is a nutrient, this will limit growth of escapers, but even if it is not, and is just used for autonomous signaling, there will not be selective pressure to lose the enzymes related to degradation after the molecule is already fully depleted. Secondary additions of the molecule are then likely to still remain effective.

In general, the greatest stability of these genetic systems will come with the following implementations:
(1) Use of an activated state for "on", as loss-of-function mutations in associated transcription factors will default to a non-growing cell state ("off"), rather than escape
(2) Use of a signal based on degradation of a small molecule or protein, as there will not be a strong selective pressure of loss of function of the degradation capacity after switching, leaving the system intact for possible feeding of the small molecule of interest to cycle between "on" and "off" states
(3) Redundancy of system parts (e.g. multiple integrations, combined transcriptional and post-translational control)
(4) Coupling of dynamic systems with essential cellular functions

5.2.2 Improved host strains for glucaric acid production

Glucaric acid production experiments were carried out in strain IB1486, which is based on the parent strain MG1655, an *E. coli* K strain. Previous work on the glucaric acid pathway has shown that BL21(DE3), an *E. coli* B strain, consistently outperforms MG1655 (Moon et al., 2009; Raman et al., 2014; Shiue et al., 2015). The genetic manipulations required for construction of the metabolite valve were initially more rapidly carried out in the K strain background. After some modifications to the lambda-red integration and clonetegration protocols, a variant of BL21(DE3) containing the modifications necessary for the Pfk valve to function has been generated and shows the expected knockdown in Pfk activity in response to aTc addition. Future work could focus on exploring the potential of this host strain and the function of the metabolite valve in BL21. Measurements of G6P and F6P pools may provide useful insights not only into whether the Pfk valve functions as expected in this strain, but perhaps also some of the underlying reasons why it outperforms the K strain. In addition to transferring the valve to a B strain, improvements in balancing the expression of the various pathway enzymes (INO1, MIOX, Udh) could be expected to produce improvements in yield and titer.

5.2.3 Development of autonomous control

Further development of autonomous control methods offers a very interesting area for future work. In the short term, better matching of Pfk expression levels with those found in wild-type cells could be expected to yield more normal growth patterns, and likely also larger improvements in *myo*-inositol production. In initial experiments, INO1 expression was induced by addition of IPTG, but the induction of this gene could also be tied to AHL buildup, though the use of the P_{esaR} promoter. Variants of this promoter have been developed with altered response profiles upon 3OC6HSL buildup, and those may be useful for controlling timing of INO1 expression separately from the timing of Pfk knockdown (Shong and Collins, 2013). In glucaric acid production, MIOX could also benefit from timed expression, due to the low stability of the enzyme, and the apparent activation by buildup of its substrate *myo*-inositol (Moon et al., 2009).

The EsaI expression cassettes developed in this study will also be generally useful for understanding timing of pathway expression and timed genetic knockdown, as they have already been tuned for threshold AHL buildup at a variety of different times. For example, these cassettes could be used in timed induction of sRNA constructs which could be used for knockdown of multiple genes at once, allowing redirection of a large number of pathway fluxes. The developed *esa* QS modules can also be used for inducer-free timed pathway or recombinant protein expression, similar to previous applications utilizing the *lux* or native *E. coli* QS systems (Liu and Lu, 2015; Tsao et al., 2010).

When adjusting only steady-state fluxes, the optimal condition represents a time and space average, and does not represent the maximum productivity that could be achieved by making changes in flux over time. Dynamic control based on cell density is an improvement, as it allows adjustments to be made over time; however, it does not account for changes in space within the fermenter, which can be quite significant at large scale. Moving to the next level, in future work, it will be useful to explore autonomous control systems which allow cells to adjust to heterogeneity in fermentation conditions, such as changes in dissolved oxygen or pH, or systems that permit internal metabolite pools to be monitored and actively balanced. Allowing each cell to individually adjust, based on its local condition in the fermenter, could provide the greatest fine tuning of control in both time and space.

5.3 Concluding remarks

Dynamic control of cellular systems can offer a number of advantages in a metabolic engineering context. Rather than fixing cellular phenotype at a steady state condition, dynamic responses can be used to limit buildup of intermediates and to better manage trade-offs between growth and production, which are required in typical batch and fed-batch fermentations. Building on advances in synthetic biology, multi-input responsive systems can be constructed, allowing several aspects of cell physiology or medium composition to determine the desired output response. Both metabolic models and experimental approaches will be valuable in advancing this field. The modeling approaches can provide information on the general types of systems that will benefit from dynamic control, and what increases in productivity might be expected. On the experimental side, continued development of strategies for rapidly assembling and testing combinatorial genetic constructs will be necessary. As control of native metabolic enzymes requires fine tuning of expression levels within a rather narrow range, the ability to predictably upregulate or downregulate expression through RBS and promoter libraries is required for success in this area.

The work in this thesis presents a new application of dynamic control for improvement of glucaric acid production, from concept development and selection of an appropriate control point based on metabolic modeling to experimental implementation. Some of the challenges in experimental implementation are discussed, underscoring areas for future development. Finally, a unique strategy for autonomous induction of metabolic switching is presented, which could be used a platform for a number of inducer-free dynamic control systems.

References

Alper, H., Miyaoku, K., Stephanopoulos, G., 2005. Construction of lycopene-overproducing E. coli strains by combining systematic and combinatorial gene knockout targets. Nat Biotechnol. 23, 612-6.

Andersen, J. B., Sternberg, C., Poulsen, L. K., Bjorn, S. P., Givskov, M., Molin, S., 1998. New unstable variants of green fluorescent protein for studies of transient gene expression in bacteria. Appl Environ Microbiol. 64, 2240-6.

Anderson, J. C., Voigt, C. A., Arkin, A. P., 2007. Environmental signal integration by a modular AND gate. Molecular Systems Biology. 3, n/a-n/a.

Anesiadis, N., Cluett, W. R., Mahadevan, R., 2008. Dynamic metabolic engineering for increasing bioprocess productivity. Metab Eng. 10, 255-66.

Anesiadis, N., Kobayashi, H., Cluett, W. R., Mahadevan, R., 2013. Analysis and design of a genetic circuit for dynamic metabolic engineering. ACS Synth Biol. 2, 442-52.

Baba, T., Ara, T., Hasegawa, M., Takai, Y., Okumura, Y., Baba, M., Datsenko, K. A., Tomita, M., Wanner, B. L., Mori, H., 2006. Construction of Escherichia coli K-12 in-frame, single-gene knockout mutants: the Keio collection. Mol Syst Biol. 2, 2006 0008.

Balagadde, F. K., Song, H., Ozaki, J., Collins, C. H., Barnet, M., Arnold, F. H., Quake, S. R., You, L., 2008. A synthetic Escherichia coli predator-prey ecosystem. Mol Syst Biol. 4.

Balleza, E., López-Bojorquez, L. N., Martínez-Antonio, A., Resendis-Antonio, O., Lozada-Chávez, I., Balderas-Martínez, Y. I., Encarnación, S., Collado-Vides, J., 2009. Regulation by transcription factors in bacteria: beyond description. FEMS Microbiology Reviews. 33, 133-151.

Bar-Even, A., Noor, E., Savir, Y., Liebermeister, W., Davidi, D., Tawfik, D. S., Milo, R., 2011. The Moderately Efficient Enzyme: Evolutionary and Physicochemical Trends Shaping Enzyme Parameters. Biochemistry. 50, 4402-4410.

Bayer, T. S., Smolke, C. D., 2005. Programmable ligand-controlled riboregulators of eukaryotic gene expression. Nat Biotech. 23, 337-343.

Bennett, B. D., Kimball, E. H., Gao, M., Osterhout, R., Van Dien, S. J., Rabinowitz, J. D., 2009. Absolute metabolite concentrations and implied enzyme active site occupancy in Escherichia coli. Nat Chem Biol. 5, 593-9.

Berger, S. A., Evans, P. R., 1991. Steady-state fluorescence of Escherichia coli phosphofructokinase reveals a regulatory role for ATP. Biochemistry. 30, 8477-80.

Bergmeyer, H. U., Bergmeyer, J., Grassl, M., 1983. Methods of enzymatic analysis / editor-in-chief, Hans Ulrich Bergmeyer ; editors, Jürgen Bergmeyer and Marianne Grassl. Weinheim ; Deerfield Beach, Fla. : Verlag Chemie, c1983-
3rd ed.

Biggs, B. W., De Paepe, B., Santos, C. N. S., De Mey, M., Kumaran Ajikumar, P., 2014. Multivariate modular metabolic engineering for pathway and strain optimization. Current Opinion in Biotechnology. 29, 156-162.

BIOFAB, BIOFAB Data Access Client. 2012.

Blangy, D., Buc, H., Monod, J., 1968. Kinetics of the allosteric interactions of phosphofructokinase from Escherichia coli. J Mol Biol. 31, 13-35.

Bremer, H., Dennis, P. P., 1996. Escherichia coli and Salmonella typhimurium. In: Neidhardt F.C., C. R. I., Ingraham J.L., Lin E.C.C., Low K.B., et al., (Ed.), Cellular and Molecular Biology. American Society for Microbiology, Washington, DC, pp. 1553–1569.

Brockman, I. M., Prather, K. L., 2015. Dynamic knockdown of E. coli central metabolism for redirecting fluxes of primary metabolites. Metab Eng. 28, 104-13.

Callura, J. M., Cantor, C. R., Collins, J. J., 2012. Genetic switchboard for synthetic biology applications. Proceedings of the National Academy of Sciences of the United States of America. 109, 5850-5.

Cameron, D. E., Collins, J. J., 2014. Tunable protein degradation in bacteria. Nat Biotech. 32, 1276-1281.

Canonaco, F., Hess, T. A., Heri, S., Wang, T., Szyperski, T., Sauer, U., 2001. Metabolic flux response to phosphoglucose isomerase knock-out in Escherichia coli and impact of overexpression of the soluble transhydrogenase UdhA. FEMS Microbiol Lett. 204, 247-52.

Cardinale, S., Arkin, A. P., 2012. Contextualizing context for synthetic biology – identifying causes of failure of synthetic biological systems. Biotechnology Journal. 7, 856-866.

Chassagnole, C., Noisommit-Rizzi, N., Schmid, J. W., Mauch, K., Reuss, M., 2002. Dynamic modeling of the central carbon metabolism of Escherichia coli. Biotechnol Bioeng. 79, 53-73.

Chen, Z., Zeng, A.-P., 2013. Protein design in systems metabolic engineering for industrial strain development. Biotechnology Journal. 8, 523-533.

Collins, C. H., Arnold, F. H., Leadbetter, J. R., 2005. Directed evolution of Vibrio fischeri LuxR for increased sensitivity to a broad spectrum of acyl-homoserine lactones. Molecular Microbiology. 55, 712-723.

Dahl, R. H., Zhang, F., Alonso-Gutierrez, J., Baidoo, E., Batth, T. S., Redding-Johanson, A. M., Petzold, C. J., Mukhopadhyay, A., Lee, T. S., Adams, P. D., Keasling, J. D., 2013. Engineering dynamic pathway regulation using stress-response promoters. Nat Biotech. 31, 1039-1046.

Datsenko, K. A., Wanner, B. L., 2000. One-step inactivation of chromosomal genes in Escherichia coli K-12 using PCR products. Proceedings of the National Academy of Sciences of the United States of America. 97, 6640-5.

Davis, J. H., Baker, T. A., Sauer, R. T., 2011. Small-molecule control of protein degradation using split adaptors. ACS Chem Biol. 6, 1205-13.

De Anda, R., Lara, A. R., Hernández, V., Hernández-Montalvo, V., Gosset, G., Bolívar, F., Ramírez, O. T., 2006. Replacement of the glucose phosphotransferase transport system by galactose permease reduces acetate accumulation and improves process performance of Escherichia coli for recombinant protein production without impairment of growth rate. Metabolic Engineering. 8, 281-290.

Delgado, J., Meruane, J., Liao, J. C., 1993. Experimental determination of flux control distribution in biochemical systems: in vitro model to analyze transient metabolite concentrations. Biotechnol Bioeng. 41, 1121-8.

Edwards, W. R., Williams, A. J., Morris, J. L., Baldwin, A. J., Allemann, R. K., Jones, D. D., 2010. Regulation of beta-lactamase activity by remote binding of heme: functional coupling of unrelated proteins through domain insertion. Biochemistry. 49, 6541-9.

Ellington, A. D., Szostak, J. W., 1990. In vitro selection of RNA molecules that bind specific ligands. Nature. 346, 818-822.

Farmer, W. R., Liao, J. C., 2000. Improving lycopene production in Escherichia coli by engineering metabolic control. Nat Biotechnol. 18, 533-7.

Fischer, E., Sauer, U., 2003. Metabolic flux profiling of Escherichia coli mutants in central carbon metabolism using GC-MS. European Journal of Biochemistry. 270, 880-891.

Franchini, A. G., Egli, T., 2006. Global gene expression in Escherichia coli K-12 during short-term and long-term adaptation to glucose-limited continuous culture conditions. Microbiology. 152, 2111-2127.

Gadkar, K. G., Doyle Iii, F. J., Edwards, J. S., Mahadevan, R., 2005. Estimating optimal profiles of genetic alterations using constraint-based models. Biotechnology and Bioengineering. 89, 243-251.

Gardner, T. S., Cantor, C. R., Collins, J. J., 2000. Construction of a genetic toggle switch in Escherichia coli. Nature. 403, 339-342.

Gonzalez, B., François, J., Renaud, M., 1997. A rapid and reliable method for metabolite extraction in yeast using boiling buffered ethanol. Yeast. 13, 1347-1355.

Guzman, L. M., Belin, D., Carson, M. J., Beckwith, J., 1995. Tight regulation, modulation, and high-level expression by vectors containing the arabinose PBAD promoter. Journal of Bacteriology. 177, 4121-30.

Hansen, C. A., Dean, A. B., Draths, K. M., Frost, J. W., 1999. Synthesis of 1,2,3,4-Tetrahydroxybenzene from d-Glucose:â€‰ Exploiting myo-Inositol as a Precursor to Aromatic Chemicals. Journal of the American Chemical Society. 121, 3799-3800.

Hanson, S., Berthelot, K., Fink, B., McCarthy, J. E. G., Suess, B., 2003. Tetracycline-aptamer-mediated translational regulation in yeast. Molecular Microbiology. 49, 1627-1637.

Haverkorn Van Rijsewijk, B. R. B., Nanchen, A., Nallet, S., Kleijn, R. J., Sauer, U., 2011. Large-scale 13C-flux analysis reveals distinct transcriptional control of respiratory and fermentative metabolism in Escherichia coli. Molecular Systems Biology. 7.

Hiller, J., Franco-Lara, E., Weuster-Botz, D., 2007. Metabolic profiling of Escherichia coli cultivations: evaluation of extraction and metabolite analysis procedures. Biotechnol Lett. 29, 1169-1178.

Holms, H., 1996. Flux analysis and control of the central metabolic pathways in Escherichia coli. FEMS Microbiology Reviews. 19, 85-116.

Holtz, W. J., Keasling, J. D., 2010. Engineering Static and Dynamic Control of Synthetic Pathways. Cell. 140, 19-23.

http://partsregistry.org, Registry of Standard Biological Parts. Vol. 2011.

Hua, Q., Yang, C., Baba, T., Mori, H., Shimizu, K., 2003. Responses of the central metabolism in Escherichia coli to phosphoglucose isomerase and glucose-6-phosphate dehydrogenase knockouts. J Bacteriol. 185, 7053-67.

Ishii, N., Nakahigashi, K., Baba, T., Robert, M., Soga, T., Kanai, A., Hirasawa, T., Naba, M., Hirai, K., Hoque, A., Ho, P. Y., Kakazu, Y., Sugawara, K., Igarashi, S., Harada, S., Masuda, T., Sugiyama, N., Togashi, T., Hasegawa, M., Takai, Y., Yugi, K., Arakawa, K., Iwata, N., Toya, Y., Nakayama, Y., Nishioka, T., Shimizu, K., Mori, H., Tomita, M., 2007. Multiple High-Throughput Analyses Monitor the Response of E. coli to Perturbations. Science. 316, 593-597.

Johansson, L., Lindskog, A., Silfversparre, G., Cimander, C., Nielsen, K. F., Lidén, G., 2005. Shikimic acid production by a modified strain of E. coli (W3110.shik1) under phosphate-limited and carbon-limited conditions. Biotechnology and Bioengineering. 92, 541-552.

Jungbluth, M., Renicke, C., Taxis, C., 2010. Targeted protein depletion in Saccharomyces cerevisiae by activation of a bidirectional degron. BMC Syst Biol. 4, 176.

Kamionka, A., Bogdanska-Urbaniak, J., Scholz, O., Hillen, W., 2004. Two mutations in the tetracycline repressor change the inducer anhydrotetracycline to a corepressor. Nucleic Acids Research. 32, 842-847.

Karig, D., Weiss, R., 2005. Signal-amplifying genetic circuit enables in vivo observation of weak promoter activation in the Rhl quorum sensing system. Biotechnology and Bioengineering. 89, 709-718.

Keseler, I. M., Collado-Vides, J., Santos-Zavaleta, A., Peralta-Gil, M., Gama-Castro, S., Muñiz-Rascado, L., Bonavides-Martinez, C., Paley, S., Krummenacker, M., Altman, T., Kaipa, P., Spaulding, A., Pacheco, J., Latendresse, M., Fulcher, C., Sarker, M., Shearer, A. G., Mackie, A., Paulsen, I., Gunsalus, R. P., Karp, P. D., 2011. EcoCyc: a comprehensive database of Escherichia coli biology. Nucleic Acids Research. 39, D583-D590.

Kiely, D. E., Chen, L., Glucaric acid monoamides and their use to prepare poly(glucaramides). Google Patents, 1994.

Kim, J. Y. H., Cha, H. J., 2003. Down-regulation of acetate pathway through antisense strategy in Escherichia coli: Improved foreign protein production. Biotechnology and Bioengineering. 83, 841-853.

Klipp, E., Heinrich, R., Holzhütter, H.-G., 2002. Prediction of temporal gene expression. European Journal of Biochemistry. 269, 5406-5413.

Kobayashi, H., Kærn, M., Araki, M., Chung, K., Gardner, T. S., Cantor, C. R., Collins, J. J., 2004. Programmable cells: Interfacing natural and engineered gene networks. Proceedings of the National Academy of Sciences of the United States of America. 101, 8414-8419.

Kotlarz, D., Buc, H., 1982. [11] Phosphofructokinases from Escherichia coli. In: Willis, A. W., (Ed.), Methods in Enzymology. vol. Volume 90. Academic Press, pp. 60-70.

Kotlarz, D., Garreau, H., Buc, H., 1975. Regulation of the amount and of the activity of phosphofructokinases and pyruvate kinases in Escherichia coli. Biochimica et Biophysica Acta (BBA) - General Subjects. 381, 257-268.

Kuhlman, T. E., Cox, E. C., 2010. Site-specific chromosomal integration of large synthetic constructs. Nucleic Acids Res. 38, e92.

Laird, M. W., Sampey, G. C., Johnson, K., Zukauskas, D., Pierre, J., Hong, J. S., Cooksey, B. A., Li, Y., Galperina, O., Karwoski, J. D., Burke, R. N., 2005. Optimization of BLyS production and purification from Escherichia coli. Protein Expression and Purification. 39, 237-246.

Lee, J., Natarajan, M., Nashine, V. C., Socolich, M., Vo, T., Russ, W. P., Benkovic, S. J., Ranganathan, R., 2008. Surface sites for engineering allosteric control in proteins. Science. 322, 438-42.

Lee, J. W., Kim, H. U., Choi, S., Yi, J., Lee, S. Y., 2011. Microbial production of building block chemicals and polymers. Curr Opin Biotechnol.

Lee, J. W., Na, D., Park, J. M., Lee, J., Choi, S., Lee, S. Y., 2012. Systems metabolic engineering of microorganisms for natural and non-natural chemicals. Nat Chem Biol. 8, 536-546.

Liu, H., Lu, T., 2015. Autonomous production of 1,4-butanediol via a de novo biosynthesis pathway in engineered Escherichia coli. Metab Eng.

Lucks, J. B., Qi, L., Mutalik, V. K., Wang, D., Arkin, A. P., 2011. Versatile RNA-sensing transcriptional regulators for engineering genetic networks. Proceedings of the National Academy of Sciences. 108, 8617-8622.

Lutz, R., Bujard, H., 1997. Independent and tight regulation of transcriptional units in Escherichia coli via the LacR/O, the TetR/O and AraC/I1-I2 regulatory elements. Nucleic Acids Res. 25, 1203-10.

Lynch, S. A., Gallivan, J. P., 2009. A flow cytometry-based screen for synthetic riboswitches. Nucleic Acids Research. 37, 184-192.

Majumder, A. L., Johnson, M. D., Henry, S. A., 1997. 1-myo-Inositol-1-phosphate synthase. Biochimica et Biophysica Acta (BBA) - Lipids and Lipid Metabolism. 1348, 245-256.

McGinness, K. E., Baker, T. A., Sauer, R. T., 2006. Engineering controllable protein degradation. Mol Cell. 22, 701-7.

Mehltretter, C. L., Rist, C. E., 1953. Sugar Oxidation, Saccharic and Oxalic Acids by the Nitric Acid Oxidation of Dextrose. Journal of Agricultural and Food Chemistry. 1, 779-783.

Michener, J. K., Thodey, K., Liang, J. C., Smolke, C. D., 2012. Applications of genetically-encoded biosensors for the construction and control of biosynthetic pathways. Metabolic Engineering. 14, 212-222.

Miksch, G., Bettenworth, F., Friehs, K., Flaschel, E., Saalbach, A., Twellmann, T., Nattkemper, T. W., 2005. Libraries of synthetic stationary-phase and stress promoters as a tool for fine-tuning of expression of recombinant proteins in Escherichia coli. Journal of Biotechnology. 120, 25-37.

Milias-Argeitis, A., Summers, S., Stewart-Ornstein, J., Zuleta, I., Pincus, D., El-Samad, H., Khammash, M., Lygeros, J., 2011. In silico feedback for in vivo regulation of a gene expression circuit. Nat Biotech. 29, 1114-1116.

Minogue, T. D., Trebra, M. W.-v., Bernhard, F., Bodman, S. B. v., 2002. The autoregulatory role of EsaR, a quorum-sensing regulator in Pantoea stewartii ssp. stewartii: evidence for a repressor function. Molecular Microbiology. 44, 1625-1635.

Moon, T. S., Dueber, J. E., Shiue, E., Prather, K. L., 2010. Use of modular, synthetic scaffolds for improved production of glucaric acid in engineered E. coli. Metab Eng. 12, 298-305.

Moon, T. S., Yoon, S. H., Lanza, A. M., Roy-Mayhew, J. D., Prather, K. L., 2009. Production of glucaric acid from a synthetic pathway in recombinant Escherichia coli. Appl Environ Microbiol. 75, 589-95.

Morales, V. M., Bäckman, A., Bagdasarian, M., 1991. A series of wide-host-range low-copy-number vectors that allow direct screening for recombinants. Gene. 97, 39-47.

Morita, T., El-Kazzaz, W., Tanaka, Y., Inada, T., Aiba, H., 2003. Accumulation of glucose 6-phosphate or fructose 6-phosphate is responsible for destabilization of glucose transporter mRNA in Escherichia coli. The Journal of biological chemistry. 278, 15608-14.

Moser, F., Broers, N. J., Hartmans, S., Tamsir, A., Kerkman, R., Roubos, J. A., Bovenberg, R., Voigt, C. A., 2012. Genetic Circuit Performance under Conditions Relevant for Industrial Bioreactors. ACS Synthetic Biology. 1, 555-564.

Mutalik, V. K., Guimaraes, J. C., Cambray, G., Lam, C., Christoffersen, M. J., Mai, Q.-A., Tran, A. B., Paull, M., Keasling, J. D., Arkin, A. P., Endy, D., 2013. Precise and reliable gene expression via standard transcription and translation initiation elements. Nat Meth. 10, 354-360.

Nakajima, M., Imai, K., Ito, H., Nishiwaki, T., Murayama, Y., Iwasaki, H., Oyama, T., Kondo, T., 2005. Reconstitution of Circadian Oscillation of Cyanobacterial KaiC Phosphorylation in Vitro. Science. 308, 414-415.

Nakamura, C. E., Whited, G. M., 2003. Metabolic engineering for the microbial production of 1,3-propanediol. Current Opinion in Biotechnology. 14, 454-459.

Neubauer, P., Junne, S., 2010. Scale-down simulators for metabolic analysis of large-scale bioprocesses. Current Opinion in Biotechnology. 21, 114-121.

Ogawa, T., Mori, H., Tomita, M., Yoshino, M., 2007. Inhibitory effect of phosphoenolpyruvate on glycolytic enzymes in Escherichia coli. Res Microbiol. 158, 159-63.

Ostermeier, M., 2005. Engineering allosteric protein switches by domain insertion. Protein engineering, design & selection : PEDS. 18, 359-64.

Patrick, W. M., Quandt, E. M., Swartzlander, D. B., Matsumura, I., 2007. Multicopy Suppression Underpins Metabolic Evolvability. Molecular Biology and Evolution. 24, 2716-2722.

Peti, W., Page, R., 2007. Strategies to maximize heterologous protein expression in Escherichia coli with minimal cost. Protein Expression and Purification. 51, 1-10.

Pósfai, G., Plunkett, G., Fehér, T., Frisch, D., Keil, G. M., Umenhoffer, K., Kolisnychenko, V., Stahl, B., Sharma, S. S., de Arruda, M., Burland, V., Harcum, S. W., Blattner, F. R., 2006. Emergent Properties of Reduced-Genome Escherichia coli. Science. 312, 1044-1046.

Quan, J., Tian, J., 2009. Circular Polymerase Extension Cloning of Complex Gene Libraries and Pathways. PLoS ONE. 4, e6441.

Raman, B., Nandakumar, M. P., Muthuvijayan, V., Marten, M. R., 2005. Proteome analysis to assess physiological changes in Escherichia coli grown under glucose-limited fed-batch conditions. Biotechnology and Bioengineering. 92, 384-392.

Raman, S., Rogers, J. K., Taylor, N. D., Church, G. M., 2014. Evolution-guided optimization of biosynthetic pathways. Proceedings of the National Academy of Sciences. 111, 17803-17808.

Reisch, C. R., Prather, K. L. J., in preparation. Cas9 Endonuclease as Counter-Selectable Marker for Scarless Genome Editing in E. coli.

Ro, D.-K., Paradise, E. M., Ouellet, M., Fisher, K. J., Newman, K. L., Ndungu, J. M., Ho, K. A., Eachus, R. A., Ham, T. S., Kirby, J., Chang, M. C. Y., Withers, S. T., Shiba, Y., Sarpong, R., Keasling, J. D., 2006. Production of the antimalarial drug precursor artemisinic acid in engineered yeast. Nature. 440, 940-943.

Ryu, M.-H., Gomelsky, M., 2014. Near-infrared Light Responsive Synthetic c-di-GMP Module for Optogenetic Applications. ACS Synthetic Biology. 3, 802-810.

Saeidi, N., Wong, C. K., Lo, T.-M., Nguyen, H. X., Ling, H., Leong, S. S. J., Poh, C. L., Chang, M. W., 2011. Engineering microbes to sense and eradicate Pseudomonas aeruginosa, a human pathogen. Mol Syst Biol. 7.

Salis, H. M., 2011. Chapter two - The Ribosome Binding Site Calculator. In: Christopher, V., (Ed.), Methods in Enzymology. vol. Volume 498. Academic Press, pp. 19-42.

Santos, C. N. S., Stephanopoulos, G., 2008. Combinatorial engineering of microbes for optimizing cellular phenotype. Current Opinion in Chemical Biology. 12, 168-176.

Sanwal, B. D., 1970. Regulatory Mechanisms Involving Nicotinamide Adenine Nucleotides as Allosteric Effectors .3. Control of Glucose 6-Phosphate Dehydrogenase. Journal of Biological Chemistry. 245, 1626-&.

Scalcinati, G., Knuf, C., Partow, S., Chen, Y., Maury, J., Schalk, M., Daviet, L., Nielsen, J., Siewers, V., 2012. Dynamic control of gene expression in Saccharomyces cerevisiae engineered for the production of plant sesquitepene alpha-santalene in a fed-batch mode. Metab Eng. 14, 91-103.

Schallmey, M., Frunzke, J., Eggeling, L., Marienhagen, J., 2014. Looking for the pick of the bunch: high-throughput screening of producing microorganisms with biosensors. Current Opinion in Biotechnology. 26, 148-154.

Schu, D. J., Carlier, A. L., Jamison, K. P., von Bodman, S., Stevens, A. M., 2009. Structure/Function Analysis of the Pantoea stewartii Quorum-Sensing Regulator EsaR as an Activator of Transcription. Journal of Bacteriology. 191, 7402-7409.

Serganov, A., Patel, D. J., 2012. Metabolite Recognition Principles and Molecular Mechanisms Underlying Riboswitch Function. Annual Review of Biophysics. 41, 343-370.

Sharma, V., Nomura, Y., Yokobayashi, Y., 2008. Engineering Complex Riboswitch Regulation by Dual Genetic Selection. Journal of the American Chemical Society. 130, 16310-16315.

Shetty, R. P., Endy, D., Knight, T. F., Jr., 2008. Engineering BioBrick vectors from BioBrick parts. J Biol Eng. 2, 5.

Shin, P. K., Seo, J.-H., 1990. Analysis of E. coli phoA-lacZ fusion gene expression inserted into a multicopy plasmid and host cell's chromosome. Biotechnology and Bioengineering. 36, 1097-1104.

Shiue, E., Brockman, I. M., Prather, K. L., 2015. Improving product yields on D-glucose in Escherichia coli via knockout of pgi and zwf and feeding of supplemental carbon sources. Biotechnol Bioeng. 112, 579-87.

Shiue, E., Prather, K. L., 2014. Improving D-glucaric acid production from myo-inositol in E. coli by increasing MIOX stability and myo-inositol transport. Metab Eng. 22, 22-31.

Shiue, E., Prather, K. L. J., 2012. Synthetic biology devices as tools for metabolic engineering. Biochemical Engineering Journal. 65, 82-89.

Shong, J., Collins, C. H., 2013. Engineering the esaR Promoter for Tunable Quorum Sensing-Dependent Gene Expression. ACS Synthetic Biology. 2, 568-575.

Shong, J., Huang, Y.-M., Bystroff, C., Collins, C. H., 2013. Directed Evolution of the Quorum-Sensing Regulator EsaR for Increased Signal Sensitivity. ACS Chemical Biology. 8, 789-795.

Smanski, M. J., Bhatia, S., Zhao, D., Park, Y., B A Woodruff, L., Giannoukos, G., Ciulla, D., Busby, M., Calderon, J., Nicol, R., Gordon, D. B., Densmore, D., Voigt, C. A., 2014. Functional optimization of gene clusters by combinatorial design and assembly. Nat Biotech. 32, 1241-1249.

Smith, T. N., Kiely, D. E., Kramer-Presta, K., Corrosion inhibiting composition. Google Patents, 2012.

Solomon, K. V., Moon, T. S., Ma, B., Sanders, T. M., Prather, K. L. J., 2012a. Tuning Primary Metabolism for Heterologous Pathway Productivity. ACS Synthetic Biology.

Solomon, K. V., Sanders, T. M., Prather, K. L., 2012b. A dynamic metabolite valve for the control of central carbon metabolism. Metab Eng. 14, 661-71.

Soma, Y., Tsuruno, K., Wada, M., Yokota, A., Hanai, T., 2014. Metabolic flux redirection from a central metabolic pathway toward a synthetic pathway using a metabolic toggle switch. Metab Eng. 23, 175-84.

Soukup, G. A., Breaker, R. R., 1999. Engineering precision RNA molecular switches. Proceedings of the National Academy of Sciences. 96, 3584-3589.

Sowa, S. W., Baldea, M., Contreras, L. M., 2014. Optimizing Metabolite Production Using Periodic Oscillations. PLoS Comput Biol. 10, e1003658.

St-Pierre, F., Cui, L., Priest, D. G., Endy, D., Dodd, I. B., Shearwin, K. E., 2013. One-step cloning and chromosomal integration of DNA. ACS Synth Biol. 2, 537-41.

Stephanopoulos, G., Aristidou, A. A., Nielsen, J. H., 1998. Metabolic engineering : principles and methodologies. Academic Press, San Diego.

Stevens, J. T., Carothers, J. M., 2015. Designing RNA-Based Genetic Control Systems for Efficient Production from Engineered Metabolic Pathways. ACS Synth Biol. 4, 107-15.

Swartz, J. R., 2001. Advances in Escherichia coli production of therapeutic proteins. Current Opinion in Biotechnology. 12, 195-201.

Torella, J. P., Ford, T. J., Kim, S. N., Chen, A. M., Way, J. C., Silver, P. A., 2013. Tailored fatty acid synthesis via dynamic control of fatty acid elongation. Proceedings of the National Academy of Sciences. 110, 11290-11295.

Tsao, C.-Y., Hooshangi, S., Wu, H.-C., Valdes, J. J., Bentley, W. E., 2010. Autonomous induction of recombinant proteins by minimally rewiring native quorum sensing regulon of E. coli. Metabolic Engineering. 12, 291-297.

Tseng, H.-C., Martin, C. H., Nielsen, D. R., Prather, K. L. J., 2009. Metabolic Engineering of Escherichia coli for Enhanced Production of (R)- and (S)-3-Hydroxybutyrate. Applied and Environmental Microbiology. 75, 3137-3145.

Tyo, K. E. J., Kocharin, K., Nielsen, J., 2010. Toward design-based engineering of industrial microbes. Current Opinion in Microbiology. 13, 255-262.

Walaszek, Z., 1990. Potential use of d-glucaric acid derivatives in cancer prevention. Cancer Letters. 54, 1-8.

Wang, H. H., Kim, H., Cong, L., Jeong, J., Bang, D., Church, G. M., 2012. Genome-scale promoter engineering by coselection MAGE. Nat Meth. 9, 591-593.

Werpy, T., Petersen, G., Top value added chemical from biomass, volume 1 - results of screening for potential candidates from sugars and synthetic gas. U.S. Department of Energy, Washington, D.C., 2004.

Wessely, F., Bartl, M., Guthke, R., Li, P., Schuster, S., Kaleta, C., 2011. Optimal regulatory strategies for metabolic pathways in Escherichia coli depending on protein costs. Mol Syst Biol. 7, 515.

Woolston, B. M., Edgar, S., Stephanopoulos, G., 2013. Metabolic Engineering: Past and Future. Annual Review of Chemical and Biomolecular Engineering. 4, 259-288.

Xie, W., Ye, L., Lv, X., Xu, H., Yu, H., 2015. Sequential control of biosynthetic pathways for balanced utilization of metabolic intermediates in Saccharomyces cerevisiae. Metabolic Engineering. 28, 8-18.

Xu, B., Jahic, M., Blomsten, G., Enfors, S. O., 1999. Glucose overflow metabolism and mixed-acid fermentation in aerobic large-scale fed-batch processes with Escherichia coli. Applied Microbiology and Biotechnology. 51, 564-571.

Xu, P., Li, L., Zhang, F., Stephanopoulos, G., Koffas, M., 2014. Improving fatty acids production by engineering dynamic pathway regulation and metabolic control. Proceedings of the National Academy of Sciences. 111, 11299-11304.

Xu, P., Wang, W., Li, L., Bhan, N., Zhang, F., Koffas, M. A. G., 2013. Design and Kinetic Analysis of a Hybrid Promoter–Regulator System for Malonyl-CoA Sensing in Escherichia coli. ACS Chemical Biology. 9, 451-458.

Yamaoka, M., Osawa, S., Morinaga, T., Takenaka, S., Yoshida, K.-i., 2011. A cell factory of Bacillus subtilis engineered for the simple bioconversion of myo-inositol to scyllo-inositol, a potential therapeutic agent for Alzheimer's disease. Microbial Cell Factories. 10, 1-6.

Ye, H., Baba, M. D.-E., Peng, R.-W., Fussenegger, M., 2011. A Synthetic Optogenetic Transcription Device Enhances Blood-Glucose Homeostasis in Mice. Science. 332, 1565-1568.

Yokobayashi, Y., Weiss, R., Arnold, F. H., 2002. Directed evolution of a genetic circuit. Proceedings of the National Academy of Sciences. 99, 16587-16591.

Yoo, S. M., Na, D., Lee, S. Y., 2013. Design and use of synthetic regulatory small RNAs to control gene expression in Escherichia coli. Nat. Protocols. 8, 1694-1707.

Yoon, S.-H., Moon, T. S., Iranpour, P., Lanza, A. M., Prather, K. J., 2009. Cloning and Characterization of Uronate Dehydrogenases from Two Pseudomonads and Agrobacterium tumefaciens Strain C58. Journal of Bacteriology. 191, 1565-1573.

Yoon, S. K., Kang, W. K., Park, T. H., 1996. Regulation of trp promoter for production of bovine somatotropin in recombinant Escherichia coli fed-batch fermentation. Journal of Fermentation and Bioengineering. 81, 153-157.

Youngquist, J. T., Rose, J., Pfleger, B., 2013. Free fatty acid production in Escherichia coli under phosphate-limited conditions. Applied Microbiology and Biotechnology. 97, 5149-5159.

Zaslaver, A., Bren, A., Ronen, M., Itzkovitz, S., Kikoin, I., Shavit, S., Liebermeister, W., Surette, M. G., Alon, U., 2006. A comprehensive library of fluorescent transcriptional reporters for Escherichia coli. Nat Meth. 3, 623-628.

Zaslaver, A., Mayo, A. E., Rosenberg, R., Bashkin, P., Sberro, H., Tsalyuk, M., Surette, M. G., Alon, U., 2004. Just-in-time transcription program in metabolic pathways. Nat Genet. 36, 486-491.

Zhang, F., Carothers, J. M., Keasling, J. D., 2012. Design of a dynamic sensor-regulator system for production of chemicals and fuels derived from fatty acids. Nat Biotech. 30, 354-359.

Zhang, F., Keasling, J., 2011. Biosensors and their applications in microbial metabolic engineering. Trends in Microbiology. 19, 323-329.

Zhao, J., Baba, T., Mori, H., Shimizu, K., 2004. Effect of zwf gene knockout on the metabolism of Escherichia coli grown on glucose or acetate. Metabolic Engineering. 6, 164-174.

Zhu, Y., Eiteman, M. A., Altman, R., Altman, E., 2008. High Glycolytic Flux Improves Pyruvate Production by a Metabolically Engineered Escherichia coli Strain. Applied and Environmental Microbiology. 74, 6649-6655.

Zor, T., Selinger, Z., 1996. Linearization of the Bradford Protein Assay Increases Its Sensitivity: Theoretical and Experimental Studies. Analytical Biochemistry. 236, 302-308.

Appendix A: Modeling of glucose-6-phosphate pools in response to changes in enzyme level

A.1 Modeling of upper glycolysis for prediction of increases in flux through INO1

Kinetic parameters for enzymes included in the model are given in Table A.1, as are the kinetic equations utilized. The general forms of the kinetic equations are as follows:

Irreversible two-substrate Michaelis-Menten:

$$v = v_{max}E \frac{S_1 S_2}{K_{iS_1}K_{MS_2} + K_{MS_1}S_2 + K_{MS_2}S_1 + S_1 S_2}$$

Reversible Michaelis-Menten:

$$v = v_{max}E \frac{S_1 - \dfrac{S_2}{K_{eq}}}{S_1 + K_{MS_1}\left(1 + \dfrac{S_2}{K_{MS_2}}\right)}$$

where S_1 and S_2 are the respective substrates and E is the enzyme level (scaled to one for wild-type levels of enzyme). K_{iS_1} is the equilibrium dissociation constant of S_1, but was set equal to K_{MS_1}, as in the irreversible two-substrate Michaelis-Menten equations used in Chassagnole et. al. (Chassagnole et al., 2002). To calculate v_{max} for each enzyme, values for the glucose-6-phosphate level (G6P), fructose-6-phosphate level (F6P), cofactor levels, and glucose uptake rate were also taken as the values measured by Chassagnole et. al. (2002). The value of v_{max} for INO1 was calculated based on activity measurements in crude lysates and estimates of cellular protein content and volume (Bremer and Dennis, 1996; Moon et al., 2009). Simplifying assumptions used in this calculation of v_{max} values are listed in Table A.2.

After values of v_{max} were calculated, the resulting equations were used to set up a system of ODEs for calculation of G6P and F6P levels in the cells.

$$\frac{dG6P}{dt} = v_{PTS} - v_{Pgi} - v_{Zwf} - v_{INO1} - \mu(G6P)$$

$$\frac{dF6P}{dt} = v_{Pgi} + 0.5(v_{Zwf}) - v_{Pfk} - \mu(F6P)$$

These equations reflect the assumptions listed in Table A.2: constant glucose uptake rate (constant v_{PTS}) and 50% of the carbon flux entering the pentose phosphate pathway returns to glycolysis at fructose-6-phosphate. The starting values for G6P and F6P were set as the previously used wild-type values. After calculating the new steady state values of G6P and F6P, as affected by expression of INO1, the predicted rate of G6P conversion to myo-inositol-1-phosphate by INO1 was calculated. This was repeated with various values of enzyme level (E) for Pgi, Zwf, and Pfk to generate predictions as a function of enzyme knockdown from wild-type.

Table A.1 | Kinetic parameters for glucose-6-phosphate utilization model.

Enzyme	Kinetic equation	Parameters	Value	Source
Pgi	Reversible Michaelis-Menten	$K_{M,Pgi,G6P}$	1.01	(Ogawa et al., 2007)
		$K_{M,Pgi,F6P}$	0.078	(Ogawa et al., 2007)
		K_{eq}	0.3	(Ishii et al., 2007)
Zwf	Irreversible two substrate Michaelis-Menten	$K_{M,Zwf,G6P}$	0.07	(Sanwal, 1970)
		$K_{M,Zwf,NADP}$	0.015	(Sanwal, 1970)
INO1	Irreversible two substrate Michaelis-Menten	$K_{M,Ino1,G6P}$	1.18	(Majumder et al., 1997)
		$K_{M,Ino1,NAD}$	0.008	(Balleza et al., 2009)
Pfk-I	Irreversible two substrate Michaelis-Menten	$K_{M,PfkA,F6P}$	0.03	(Berger and Evans, 1991)
		$K_{M,PfkA,ATP}$	0.06	(Blangy et al., 1968)

Table A.2 | Additional simplifying assumptions in glucose-6-phosphate utilization model.
Some assumptions about flux distributions between glycolysis and the pentose phosphate pathways were required in order to solve for steady state values of v_{max} for the enzymes in the model.

	Comments
1) Carbon flux is split 80% to glycolysis and 20% to the pentose phosphate pathway	Values in this range were measured in several studies of growth on glucose (Hua et al., 2003; Zhao et al., 2004). Flux partitioning between glycolysis and the pentose phosphate pathway was shown to be fairly rigid over a range of substrate uptake rates (Haverkorn Van Rijsewijk et al., 2011).
2) 50% of the carbon flux entering the pentose phosphate pathway returns to glycolysis at fructose-6-phosphate	
3) Glucose uptake rate is constant	Accumulation of glucose-6-phosphate and fructose-6-phosphate will likely affect the glucose uptake rate via the PTS system (Morita et al., 2003). Experimental work also confirms this, but alternative PTS-independent glucose uptake schemes could be envisioned.
4) Levels of cofactors and ATP are constant	The pathway itself does not place an extreme cofactor demand on the cell. However, reducing the level of Pfk-I will reduce flux into the TCA cycle and effect production of reducing equivalents and energy.
5) Enzymes with minor substrate consumption (Pgm and Pfk-II) were ignored	The contribution of these enzymes to overall fluxes is known to be minor compared with the other enzymes in the model (Chassagnole et al., 2002).

A.2 MATLAB code for generating Figure 2.1

```
function G6P_Model_7Nov
%%%%%%%%%%%%%%%%%%%%%%%%%%%%%%%%%%%%%%%%%%%%%%%%%%%%%%%%%%%%%%%%%%%%%%%%%%
%    This function is used to model a portion of the central
%    metabolism of E. coli, centered around the consumption of G6P
%    for both primary metabolism and glucaric acid production
%%%%%%%%%%%%%%%%%%%%%%%%%%%%%%%%%%%%%%%%%%%%%%%%%%%%%%%%%%%%%%%%%%%%%%%%%%


%Steady state intracellular metabolite concentrations
%Values from Chassagnole 2002, Dynamic modeling of the central carbon
metabolism of E. coli
%All metabolite concentrations given in mM
glu_ext=0.0556;       %extracellular glucose
g6p=3.48;             %glucose-6-phosphate
f6p=0.60;             %fructose-6-phosphate
g1p=0.653;            %glucose-1-phosphate
nadp=0.195;           %NADP+
nadph=0.062;          %NADPH
nad=1.47;             %NAD+
nadh=0.1;             %NADH
atp=4.27;             %ATP


meta=[glu_ext;g6p;f6p;g1p;nadp;nadph;nad;nadh;atp];


%Rate of growth for above steady state metabolite concentrations, Chassagnole
2002
mu=0.278E-4; %(1/s)


%Constants for enzyme kinetic equations (mM)
%Pgi
%Reversable M-M: rate = vmax*(g6p-f6p/Keq)/(Kmg6p*(1+f6p/Kmf6p)+g6p)
%6PG inhibition dropped for simplicity
%Ogawa 2007 (Ecocyc)
km_pgi_g6p=1.01;
km_pgi_f6p=0.078;
%Ishii 2007 (Ecocyc)
keq_pgi=0.30;


%Zwf
%Km values from Sanwal 1970
%Two substrate irreversible M-M: rate =
vmax*g6p*nadp/(Kig6p*Kmnadp+Kmnapd*g6p+Kmg6p*nadp+g6p*nadp)
%NADPH inhibition has been dropped
km_zwf_g6p=0.07;
km_zwf_nadp=0.015;
ki_zwf_g6p=0.07; %arbitrarily set to km_zwf_g6p


%Ino1
%Km values for Ino1 from S. cerevisiae Majumder (1997)
%Two substrate irreversible M-M
km_ino1_g6p=1.18;
km_ino1_nad=0.008;
```

```
ki_ino1_g6p=1.18; %arbitrarily set to km_ino1_g6p

%PfkA
%Two substrate irreversible M-M
%PfkB isozyme was dropped
%Berger 1991 (Ecocyc)
km_pfk_f6p=0.03;
%Blangy 1968 (Ecocyc)
km_pfk_atp=0.06;

%All kinetic parameters
k=[km_pgi_g6p;km_pgi_f6p; keq_pgi;km_zwf_g6p;km_zwf_nadp;ki_zwf_g6p;...
    km_ino1_g6p;km_ino1_nad;ki_ino1_g6p;km_pfk_f6p;km_pfk_atp];

%Fractional enzyme concentration, where steady state concentration is defined
as 1
Epgi=1;
Ezwf=1;
Eino1=1;
Epfk=1;
E=[Epgi;Ezwf;Eino1;Epfk];

%Glucose uptake rate
%Chassagnole 2002, D = 0.1 hr^-1
glu_cons=1.057; %mmol/(g cell DW * hr)
%Hua 2003 reports a similar value of 1.4 mmmol/(g*hr)
cellwv=564; %g cell DW / L cell internal volume
rpts=glu_cons*1/3600*cellwv;

%Solve for steady state values of vmax for each enzyme using the metabolite
%concentrations, enzyme parameters, and glucose uptake rates given.
vmax0=[1;1;1;1];
%initial guess for vmax=[vmaxpgi;vmaxzwf;vmaxino1;vmaxpfk];
[vmax,fval]=fsolve(@(vmax)ssvmax(meta,k,vmax,rpts,mu),vmax0);

%Using calculated values of vmax, predict flux through each pathway
%when Ino1 is "induced"
y0=[g6p;f6p];
tspan=[0 1000];
[t,y]=ode45(@(t,y)diffsystem2(t,y,meta,k,E,vmax,rpts,mu),tspan,y0);
rates=getrates(y,meta,k,E,vmax);

%%%%%%%%%%%%%%%%%%%%%%%%%%%%%%%%%%%%%%%%%%%%%%%%%%%%%%%%%%%%%%%%%%%%%%
%    Plots
%%%%%%%%%%%%%%%%%%%%%%%%%%%%%%%%%%%%%%%%%%%%%%%%%%%%%%%%%%%%%%%%%%%%%%

%Metabolite concentrations as a function of time
figure(1)
plot(t,y(:,1),'-',t,y(:,2),'-.')
title('Internal metabolite concentrations')
legend('G6P','F6P')
xlabel('time after Ino1 "induction" (s)')
ylabel('concentration (mM)')

%Relative rates of G6P consumption
```

```matlab
figure(2)
%pgi
plot(t,rates(:,1),'r')
hold on
%zwf
plot(t,rates(:,2),'b','LineStyle','--')
%ino1
plot(t,rates(:,3),'g')
%pfkA
plot(t,rates(:,4),'LineStyle','-.','Color',[0.85 0.16 0])

title('Relative rates of substrate consumption')
xlabel('time after Ino1 "induction" (s)')
ylabel('rate of substrate consumption (mM/s)')
legend('Pgi','Zwf','INO1','Pfk')
hold off


%Plot steady state rate of flux through Ino1 as function of Epfk and
%km_ino1_gp6
k=[km_pgi_g6p;km_pgi_f6p; keq_pgi;km_zwf_g6p;km_zwf_nadp;ki_zwf_g6p;...
   km_ino1_g6p;km_ino1_nad;ki_ino1_g6p;km_pfk_f6p;km_pfk_atp];
i=1;
j=1;
%for km_ino1_g6p=2:-0.04:0.25
%    k=[km_pgi_g6p;km_pgi_f6p; keq_pgi;km_zwf_g6p;km_zwf_nadp;ki_zwf_g6p;...
%        km_ino1_g6p;km_ino1_nad;km_ino1_g6p;km_pfk_f6p;km_pfk_atp];
    for Epfk=1:-0.01:0
        E=[Epgi;Ezwf;Eino1;Epfk];
        [t,y]=ode45(@(t,y)diffsystem2(t,y,meta,k,E,vmax,rpts,mu),tspan,y0);
        rates=getrates(y,meta,k,E,vmax);
        ino1res=rates(:,3);
        out(i,j)=ino1res(end);
        i=i+1;
    end
%    i=1;
%    j=j+1;
%end
i=1;
Epfk=1;
j=2;
    for Ezwf=1:-0.01:0
        E=[Epgi;Ezwf;Eino1;Epfk];
        [t,y]=ode45(@(t,y)diffsystem2(t,y,meta,k,E,vmax,rpts,mu),tspan,y0);
        rates=getrates(y,meta,k,E,vmax);
        ino1res=rates(:,3);
        out(i,j)=ino1res(end);
        i=i+1;
    end
i=1;
j=3;
Ezwf=1;
    for Epgi=1:-0.01:0
        E=[Epgi;Ezwf;Eino1;Epfk];
        [t,y]=ode45(@(t,y)diffsystem2(t,y,meta,k,E,vmax,rpts,mu),tspan,y0);
        rates=getrates(y,meta,k,E,vmax);
```

```matlab
        ino1res=rates(:,3);
        out(i,j)=ino1res(end);
        i=i+1;
    end


%Plot flux through Ino1 as a function of various enzyme levels
figure(3)
plot(1:-0.01:0,out(:,1),'LineStyle','-.','Color',[0.85 0.16 0])
axis([0 1 0 0.025])
set(gca,'XDir','reverse')
xlabel('Enzyme level (fraction of wild type)');
ylabel('Predicted flux through INO1 (mM/s)');
hold on
plot(1:-0.01:0,out(:,2),'b','LineStyle','--')
plot(1:-0.01:0,out(:,3),'r')
legend('Pfk','Zwf','Pgi')
hold off

end


function bal=ssvmax(meta,k,vmax,rpts,mu)
%To be used with fmincon to solve for vmax at steady state concentrations
%or known turnover rates (Ino1).
%Output:
    %bal = metabolic constraints [rate of accumlation of G6P;balance between
Pgi and Zwf flux;
    %       balance of Ino1 flux; balance of PfkA flux]
%Inputs:
    %meta = steady state metabolite pools
[glu_ext;g6p;f6p;g1p;nadp;nadph;nad;nadh;atp];
    %k = kinetic parameters
    %   [km_pgi_g6p;km_pgi_f6p; keq_pgi;km_zwf_g6p;km_zwf_nadp;ki_zwf_g6p;...
    %    km_ino1_g6p;km_ino1_nad;ki_ino1_g6p;km_pfk_f6p;km_pfk_atp];
    %vmax = maximum reaction rates [vmaxpgi;vmaxzwf;vmaxino1;vmaxpfk];
    %rpts = glucose uptake rate
    %mu = growth rate (1/s)

%Rate of G6P consumption by Pgi
rpgi=vmax(1)*(meta(2)-meta(3)/k(3))/(k(1)*(1+meta(3)/k(2))+meta(2));

%Rate of G6P consumption by Zwf
rzwf=vmax(2)*meta(2)*meta(5)/(meta(2)*meta(5)+k(4)*meta(5)+...
    k(5)*meta(2)+k(5)*k(6));

%Rate of G6P consumption by Ino1
rino1=vmax(3)*1; %All substrates in excess during in vitro assay

%Rate of F6P consumption by PfkA
rpfk=vmax(4)*meta(3)*meta(9)/(k(10)*k(11)+meta(3)*k(11)+meta(9)*k(10)+meta(3)
*meta(9));

%At steady state, dg6p/dt=0
%Ino1 is not included in this balance, as it was not present when the
%origianl data was collected
```

```
    dg6pdt=rpts-rpgi-rzwf-mu*meta(2);

    %Several sources (Hua, Zhao) indicate a split of ~80% flux through Pgi and
    %~20% flux through Zwf, so I have assumed that the following constraint
    %is satisfied: ratepgi=4*ratezwf
    pgibal=rpgi-4*rzwf;

    %Moon (2008) reports in vitro activity of 344 nmol/(hr*mg total protein)
    %for Ino1 expressed from pTrcIno1
    %For conversion to mM/s, assumptions are
    %200E-15 g protein/cell (Bremmer, Dennis 1987)
    %Cell volume = 1E-15 L
    ino1_turnover=0.019; %mM/s

    %Ino1 production must match the turnover
    ino1bal=ino1_turnover-rino1;

    %Hua 2003 indicates that 50% of flux entereing PPP returns to glycoylysis
    %at F6P. Rate away from F6P = rate into F6P steady state
    %Known rate in = rpgi+0.5*rzwf, so steady state rate of Pfk is
    pfkbal=rpfk-(rpgi+0.5*rzwf);

    bal=[dg6pdt;pgibal;ino1bal;pfkbal];
    end


function dy=diffsystem2(t,y,meta,k,E,vmax,rpts,mu)
%To be used with ODE solvers to track change in G6P and F6P concentration
%with time.
%Output:
    %dy = [rate of G6P consumption; rate of F6P consumption]
%Inputs:
    %t = time (s)
    %y = variable metabolite pools [g6p;f6p]
    %meta = steady state metabolite pools
[glu_ext;g6p;f6p;g1p;nadp;nadph;nad;nadh;atp];
    %k = kinetic parameters
    %  [km_pgi_g6p;km_pgi_f6p; keq_pgi;km_zwf_g6p;km_zwf_nadp;ki_zwf_g6p;...
    %   km_ino1_g6p;km_ino1_nad;ki_ino1_g6p;km_pfk_f6p;km_pfk_atp];
    %vmax = maximum reaction rates [vmaxpgi;vmaxzwf;vmaxino1;vmaxpfk];
    %rpts = glucose uptake rate
    %E = [Epgi;Ezwf;Eino1;Epfk];
    %mu = growth rate (1/s)

%Rate of G6P consumption by Pgi
rpgi=vmax(1)*E(1)*(y(1)-y(2)/k(3))/(k(1)*(1+y(2)/k(2))+y(1));

%Rate of G6P consumption by Zwf
rzwf=vmax(2)*E(2)*y(1)*meta(5)/(y(1)*meta(5)+k(4)*meta(5)+...
    k(5)*y(1)+k(5)*k(6));

%Rate of G6P consumption by Ino1
rino1=vmax(3)*E(3)*y(1)*meta(7)/(y(1)*meta(7)+k(7)*meta(7)+...
    k(8)*y(1)+k(8)*k(9));
```

```matlab
%Rate of F6P consumption by PfkA
rpfk=E(4)*vmax(4)*y(2)*meta(9)/(k(10)*k(11)+...
    k(11)*y(2)+k(10)*meta(9)+meta(9)*y(2));

%Rate of change in G6P concentration
dg6p=rpts-rpgi-rzwf-rino1-mu*y(1);

%Rate of change in F6P concentration
df6p=rpgi+0.5*rzwf-rpfk-mu*y(2);

dy=[dg6p;df6p];
end


function rates=getrates(y,meta,k,E,vmax)
%Output:
    %rates = [rate of G6P consumption by Pgi; Zwf; Ino1];
%Inputs:
    %y = variable metabolite pools [g6p;f6p]
    %meta = steady state metabolite pools
[glu_ext;g6p;f6p;g1p;nadp;nadph;nad;nadh;atp];
    %k = kinetic parameters
    %  [km_pgi_g6p;km_pgi_f6p; keq_pgi;km_zwf_g6p;km_zwf_nadp;ki_zwf_g6p;...
    %   km_ino1_g6p;km_ino1_nad;ki_ino1_g6p;km_pfk_f6p;km_pfk_atp];
    %vmax = maximum reaction rates [vmaxpgi;vmaxzwf;vmaxino1;vmaxpfk];
    %E = [Epgi;Ezwf;Eino1;Epfk];

for i=1:size(y,1)
%Rate of G6P consumption by Pgi
rates(i,1)=vmax(1)*E(1)*(y(i,1)-y(i,2)/k(3))/(k(1)*(1+y(i,2)/k(2))+y(i,1));

%Rate of G6P consumption by Zwf
rates(i,2)=vmax(2)*E(2)*y(i,1)*meta(5)/(y(i,1)*meta(5)+k(4)*meta(5)+...
    k(5)*y(i,1)+k(5)*k(6));

%Rate of G6P consumption by Ino1
rates(i,3)=vmax(3)*E(3)*y(i,1)*meta(7)/(y(i,1)*meta(7)+k(7)*meta(7)+...
    k(8)*y(i,1)+k(8)*k(9));

%Rate of F6P consumption by PfkA
rates(i,4)=vmax(4)*E(4)*y(i,2)*meta(9)/(k(10)*k(11)+...
    k(11)*y(i,2)+k(10)*meta(9)+meta(9)*y(i,2));

end

end
```

Appendix B: *In vitro* degradation of tagged Pfk-I

B.1 Materials and Methods

An *in vitro* assay of Pfk-I degradation was carried out to confirm that the expected degradation of the protein occurred in the presence of ClpXP and ATP. This would alleviate concerns that the structure of Pfk-I limited accessibility of the degradation tag or promoted cleavage of the tag without unfolding and degradation of the remaining protein.

B.1.1 Purification of degradation tagged Pfk-I

N-terminal 6x-His-tagged versions of Pfk-I (with and without C terminal degradation tags) were overexpressed in DH10B in LB from pMMB206-based plasmids. Protein was purified from each culture using QIAGEN Ni-NTA spin columns and following the standard protocol recommended in the kit handbook for protein purification under native conditions. Eluted protein samples were dialyzed overnight at 4° C into a buffer containing 20 mM HEPES, 400 mM NaCl, 100 mM KCl, and 10% glycerol (pH 7.6). Protein concentrations were measured by Bradford assay.

B.1.2 *In vitro* assay of Pfk-I degradation

The *in vitro* degradation assay was carried out via a protocol developed by the Sauer Lab at MIT (Department of Biology). Each reaction contained 0.3 µM ClpX$_6$ and 0.9 µM ClpP$_{14}$ and 10 µM of the Pfk-I variant of interest in PD buffer (25 mM HEPES, 100 mM KCl, 10 mM MgCl$_2$, 10% glycerol). The reaction mixture also contained an ATP regeneration system consisting of 5 mM ATP, 0.032 mg/ml creatine kinase, and 16 mM phosphocreatine. Reactions were sampled at 0, 2, 5, 10, 20, 30, 45, and 60 minutes and quenched by dilution into an equal volume of SDS-PAGE buffer (65.8 mM Tris-HCl, pH 6.8, 2.1% SDS, 26.3% (w/v) glycerol, 0.01% bromophenol blue, 5% β-mercaptoethanol) followed by heating at 95° C for 5 minutes. Samples were resolved by SDS-PAGE.

B.2 Results

Untagged Pfk-I (Fig. B.1) does not show significant degradation during the 60 minute incubation with ClpXP. In contrast, Pfk-I with the native ssrA tag (LAA) appended to the C terminus shows almost complete disappearance by 20 minutes (Fig. B.2), indicating strong degradation of the tagged protein. With the modified DAS+4 tag, no significant degradation was observed over the 60 minute period (Fig. B.3), which was the expected outcome in the absence of SspB. These results indicated that degradation strategies based on addition of a C-terminal ssrA tag to Pfk-I should be feasible.

In all figures below, the lanes are as follows:
1) ladder
2) purified Pfk-I variant
3) – 10) Reaction samples at 0, 2, 5, 10, 20, 30, 45, and 60 minutes, respectively
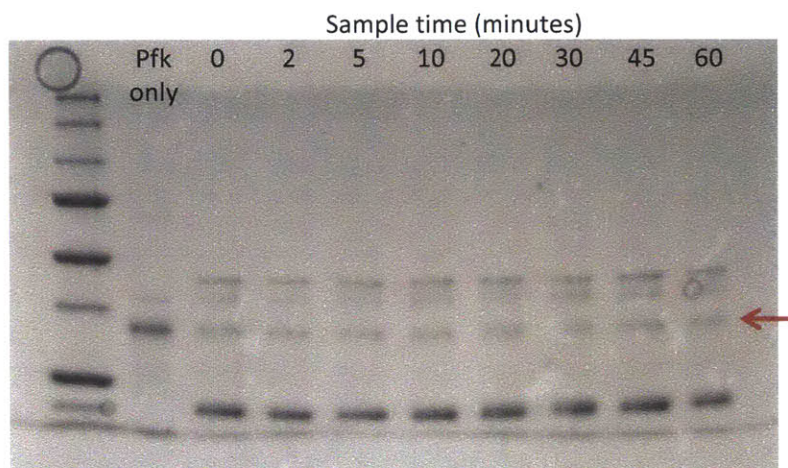The Pfk-I band is noted with an arrow. The other bands are ClpX, ClpP, and creatine kinase.
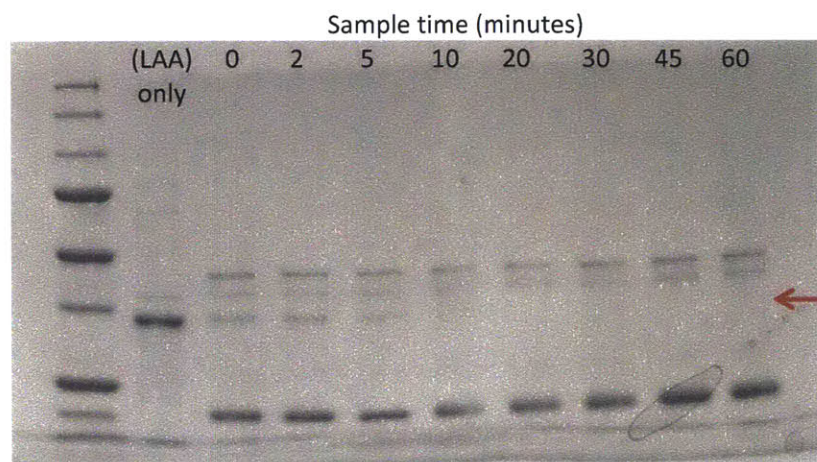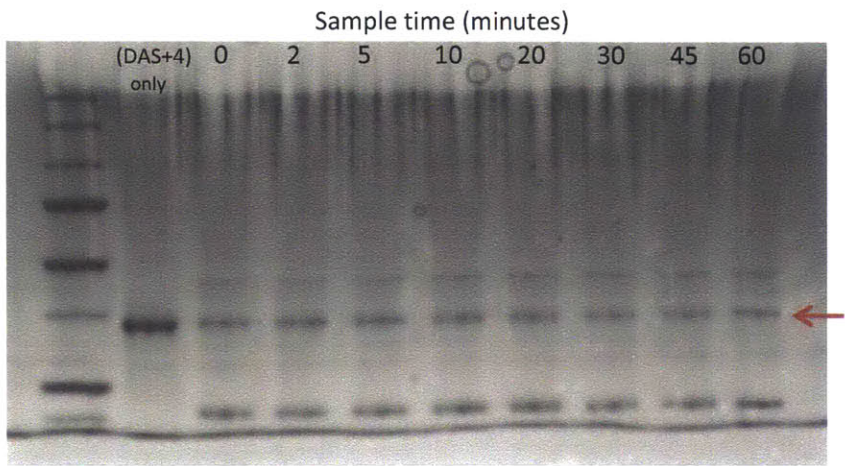

Fig B.1 | Degradation of Pfk-I (untagged)

Fig. B.2 | Degradation of Pfk-I (LAA)

Fig. B.3 | Degradation of Pfk-I (DAS+4)